

Technische Universität München

Department of Mathematics

Directed Percolation: A Mathematical Framework

Bachelor's Thesis

by

Sara-Viola Kuntz

Supervisor:	Prof. Dr. Christian Kühn
Advisor:	Dr. Maximilian Engel
Submission Date:	28$^{\text{th}}$ of August, 2019

I assure the single handed composition of this bachelor's thesis only supported by declared resources.

Garching, 28^{th} of August, 2019

Abstract

This bachelor thesis illuminates the spreading process called directed percolation as well as related models. In the first Chapter, application fields of models introduced in this bachelor thesis are presented. The second Chapter is about the geometrically defined models ordinary and oriented bond percolation. The percolation probability is defined and the critical phenomenon is analysed. As oriented bond percolation in two dimensions is equivalent to directed percolation in $1+1$ dimensions, the results of the second Chapter provide a basis for the dynamic percolation processes of the third Chapter and some results follow immediately. The third Chapter deals with three dynamic percolation processes: the 1+1 dimensional Domany-Kinzel automaton, $d+1$ dimensional directed percolation and the $d+1$ dimensional contact process. Directed percolation is a discrete time process and the contact process is a continuous time adaption of it. They all have the same critical behaviour and belong therefore to the same universality class. In the fourth Chapter, first the scaling theory to analyse the critical behaviour of spreading processes is introduced and afterwards the critical exponents of the directed percolation universality class are approximated numerically and with mean-field theory. The last Chapter gives an outlook on percolation models used in fluid dynamics.

Zusammenfassung

In dieser Bachelorarbeit werden der Ausbreitungsprozess der gerichteten Perkolation, sowie verwandte Modelle beleuchtet. Das erste Kapitel stellt Anwendungsgebiete der in dieser Arbeit betrachteten Modelle dar. Die geometrisch definierten Modelle der gewöhnlichen Kantenperkolation und der orientierten Kantenperkolation werden im zweiten Kapitel vorgestellt, ihre Perkolationswahrscheinlichkeit definiert and das kritische Verhalten analysiert. Da zweidimensionale, orientierte Kantenperkolation äquivalent zu gerichteter Perkolation in $1+1$ Dimensionen ist, bilden die Ergebnisse des zweiten Kapitels eine gute Grundlage für die dynamischen Perkolationsmodelle des dritten Kapitels und einige Resultate können sofort übernommen werden. Das dritte Kapitel behandelt die folgenden drei dynamischen Perkolationsprozesse: Den zellulären Automaten von Domany und Kinzel in $1+1$ Dimensionen, $d+1$ dimensionale gerichtete Perkolation, sowie den $d+1$ dimensionalen Kontaktprozess. Gerichtete Perkolation ist ein Prozess mit einer diskreten Zeitkomponente, der Kontaktprozess ist eine Adaption in kontinuierlicher Zeit hiervon. Die aufgezählten Modelle haben das gleiche kritische Verhalten und gehören somit zur gleichen Universalitätsklasse. Um diese zu bestimmen, wird im vierten Kapitel die hierfür notwendige Skalierungstheorie eingeführt, sowie die kritischen Exponenten numerisch und mit Hilfe der Molekularfeldtheorie angenähert. Das letzte Kapitel gibt einen Ausblick auf die Anwendung von Perkolationsprozessen in der Strömungsdynamik.

Contents

1. Modelling of Spreading Processes **1**

2. Bond Percolation on $\mathbb{Z}^d$ **2**
2.1. Definition of Ordinary and Oriented Bond Percolation on $\mathbb{Z}^d$ 2
2.2. The Existence of an Infinite Open Cluster 4
2.3. The Critical Phenomenon 6

3. Dynamic Percolation Processes **11**
3.1. Domany-Kinzel Cellular Automaton on $\mathbb{Z} \times \mathbb{N}_0$ 11
3.2. Directed Percolation on $\mathbb{Z}^d \times \mathbb{N}_0$ 14
3.2.1. Definition of Directed Percolation in $d+1$ dimensions 14
3.2.2. The Critical Phenomenon 15
3.2.3. Equivalence of Directed and Oriented Bond Percolation 15
3.3. The Contact Process on $\mathbb{Z}^d \times \mathbb{R}_{\geq 0}$ 18
3.3.1. Definition of the Contact Process in $d+1$ dimensions 18
3.3.2. Master Equation of the $1+1$ dimensional Contact Process 19
3.3.3. Generator Matrix Q of the $1+1$ dimensional Contact Process 21
3.3.4. The Critical Phenomenon 22

4. Critical Exponents of Dynamic Percolation **25**
4.1. Phenomenological Scaling Theory 25
4.1.1. The Critical Exponents β, β', $\nu_\perp$, $\nu_\parallel$ and the Dynamic Exponent z 25
4.1.2. Universal Scaling Functions and the Hyperscaling Relation 27
4.2. Mean-Field Approximation of the Contact Process 29
4.3. Numerical Analysis of Directed Percolation 31

5. Directed Percolation in Fluid Dynamics **35**

Appendix A. Basics Probability Theory **38**

Appendix B. Basics Analysis and Algebra **42**

Appendix C. Numerical Code and Computations **48**
C.1. Directed Percolation in $d+1$ dimensions, $d \in \{1,2,3\}$ 48
C.2. Approximation of the Critical Probabilities 55
C.3. Approximation of the Critical Exponents 57
C.4. Eigenvalues of the Q-matrix of the Contact Process 59

Bibliography **61**

1. Modelling of Spreading Processes

In physics and biology, growth and decay of populations or particles is often modelled by spreading processes. One mathematical class of models including all these properties is dynamic percolation, which describes the time evolution of particles located on vertices, also called sites of a lattice. These particles can either be active or inactive and, depending on their state, they can stochastically interact with their neighbours. All dynamic percolation models are built up with the same reaction diffusion scheme: particles can produce offspring, self-destruct, merge with other particles or diffuse [15]. Models with these properties are for example the Domany-Kinzel cellular automaton, the contact processes and directed percolation, which is the main model of this thesis. They are introduced in Chapter 3 and further analysis is done in Chapter 4.

There are various deployments in different application fields, which can be modelled with dynamic percolation processes. In the following, three of them will be presented:

Firstly, when modelling a disease, we represent infected individuals as active and healthy individuals as inactive sites. Infected individuals can pass the disease to their neighbours or cure themselves, with given respective rates. The main question of such a process is whether it is possible to eradicate the disease depending on given probabilities. If all individuals are cured, it is not possible to get infected again, since the system is modelled without external pathogens. If the infection probability is above a critical value, there will be a balance of infected and cured individuals and on average the fraction of infected individuals will stay constant [15].

Secondly, it is possible to model the oxidation of carbon monoxide, whose chemical equation is given by $CO + O \to CO_2$. A gas composed of carbon monoxide CO and oxygen molecules O_2 is brought onto a catalytic material, which is represented by the square lattice $\mathbb{Z}^2$. Each vertex of the lattice can be empty or filled by a CO molecule or an O atom. With given rates, CO molecules can occupy empty sites, O_2 molecules can split into O atoms and fill neighbouring sites, and neighbouring CO molecules and O atoms can recombine to form CO_2 molecules, which dissolve from the lattice and leave two empty sites. The process ends in an absorbing or in a fluctuating steady state. In the former case, all vertices are filled either only with CO molecules or only with O atoms, such that no reaction is possible. In the latter case, the average concentration of gases stays constant [15].

Finally, dynamic percolation processes can be used to model turbulence of flows in a pipe. The fluid mechanical behaviour is strongly simplified, nevertheless good results are obtained [1], [24]. In Chapter 5 a one- as well as a three-dimensional percolation model of fluid dynamics will be presented.

Initially, percolation systems were not defined to model the time evolution of spreading processes. Rather, they are applied geometrically to analyse the connectivity of particles in arbitrary media [18]. In Chapter 2, ordinary and oriented bond percolation models are introduced, analysed and shortly connected to an ordinary site percolation model.

An example for bond percolation is the analysis of water channel arrangement in porous rocks. The passageways of the rocks are modelled by edges between vertices of a lattice, which are open or closed with a given probability. Considering a rock under the influence of gravity, the passageways are modelled by directed edges, such that the water can only spread through channels directed towards Earth's centre. The major interest of this percolation model is the situation of open edges building an infinite cluster, such that the water can pass arbitrarily far and the rock gets drenched [15].

There are many similarities between dynamic percolation processes and oriented bond percolation. In Chapter 3, the equivalence of directed percolation in $1 + 1$ dimensions and oriented bond percolation in two dimensions is shown.

2. Bond Percolation on $\mathbb{Z}^d$

In the literature various models for spreading processes exist, whose applications were already mentioned in Chapter 1. Percolation models simplify the behaviour of objects like particles, as they are considered to be located on vertices or move along edges of discrete, regular lattices. Additionally, the particles are restricted to two different states: active or inactive. Even if it is not complicated to define percolation models, they have a non-trivial dynamical behaviour and can help to understand more complicated models describing real-life phenomena [8], [15].

There are mainly three different types of percolation models: firstly, the model of different states of edges of the lattice (bond percolation), secondly the model of different states of vertices of the lattice (site percolation) and lastly, the model of interaction of vertices with their nearest neighbours depending on their states (dynamic percolation). Therefore an additional time component is added to model the growth and decay of particle clusters and analyse stationary states and survival probabilities, see Chapter 3 and 4. In the geometrically defined bond percolation models, ordinary or directed edges are open or closed with a given probability. The main question is to find the critical probability, such that an infinite cluster of open edges exists [15].

In this Section, firstly, the concepts of ordinary and oriented bond percolation are introduced and shortly connected to an ordinary site percolation model. Then, two properties called percolation probability and critical probability are defined and the critical phenomenon is analysed. This is achieved by joining and expanding the definitions and results given in [8] and [18] for ordinary bond percolation and applying them to oriented bond percolation. The probabilistic definitions, lemmas and theorems used in this Chapter can be found in Appendix A.

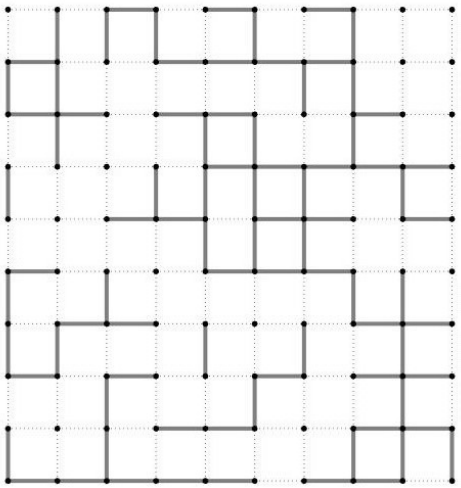
2.1. Definition of Ordinary and Oriented Bond Percolation on $\mathbb{Z}^d$

Ordinary and oriented bond percolation are usually defined on d-dimensional square lattices whose vertices are $\mathbb{Z}^d$ with $d \in \mathbb{N} := \{1, 2, 3, ...\}$. For two vertices $x = (x_1, x_2, ..., x_d)$, $y = (y_1, y_2, ..., y_d) \in \mathbb{Z}^d$ we denote the graph theoretic distance by $\delta(x, y) := \sum_{i=1}^{d} |x_i - y_i|$. It describes the least number of steps to be taken to get from x to y. The edges related to the vertices $\mathbb{Z}^d$ are given by

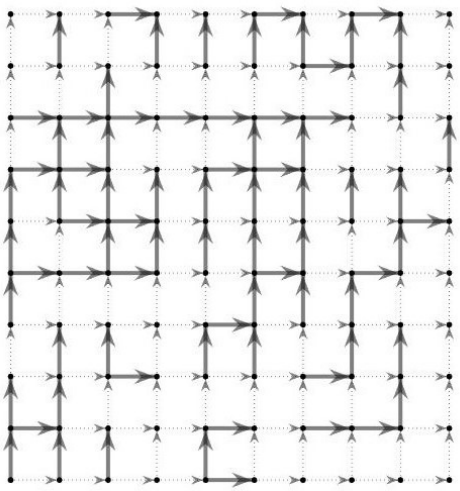
$$\begin{aligned} \mathbb{E}^d &:= \{e = \{x, y\} : x, y \in \mathbb{Z}^d \wedge \delta(x, y) = 1\}, \\ \vec{\mathbb{E}}^d &:= \{e = \langle x, y\rangle : x, y \in \mathbb{Z}^d \wedge x_i \leq y_i \; \forall i \in \{1, ..., d\} \wedge \delta(x, y) = 1\}, \end{aligned} \tag{2.1}$$

where $\{x, y\}$ denotes an undirected edge between x and y and $\langle x, y\rangle$ a directed edge from x to y. Since most oriented models require a prescribed direction because of influences like gravity, the common definition of oriented bond percolation only considers edges directed from a vertex x towards a vertex y, where each component of y is larger or equal to the corresponding component of x. For oriented bond percolation without a prescribed direction of the edges, fewer results are known and they are more difficult to prove [9]. The hypercubic lattices considered here are $\mathbb{L}^d := (\mathbb{Z}^d, \mathbb{E}^d)$ for ordinary bond percolation and $\vec{\mathbb{L}}^d := (\mathbb{Z}^d, \vec{\mathbb{E}}^d)$ for oriented bond percolation. Figure 2.1(a) shows the lattice of ordinary bond percolation in two dimensions, Figure 2.1(b) the 'north-east'-lattice of oriented bond percolation in two dimensions.

For a probabilistic definition of ordinary or oriented bond percolation we consider the probability spaces $(\Omega, \mathcal{F}, \mathbb{P}_p)$ or $(\vec{\Omega}, \vec{\mathcal{F}}, \vec{\mathbb{P}}_p)$ with sample spaces $\Omega := \prod_{e \in \mathbb{E}^d} \{0, 1\}$ or $\vec{\Omega} := \prod_{e \in \vec{\mathbb{E}}^d} \{0, 1\}$ and σ-algebras $\mathcal{F}$ or $\vec{\mathcal{F}}$ generated by the finite-dimensional cylinder sets (A.14) of events which can occur in the percolation processes respectively. The related probability measures are defined as product measures of Bernoulli-distributions $\mathbb{P}_p := \prod_{e \in \mathbb{E}^d} \mathrm{Ber}_p$ or $\vec{\mathbb{P}}_p := \prod_{e \in \vec{\mathbb{E}}^d} \mathrm{Ber}_p$ with the



(a) Excerpt of the lattice $\mathbb{L}^2$ and a realisation $(\mathbb{Z}^2, \mathbb{E}^2_{0.5}(\omega))$ of ordinary bond percolation.



(b) Excerpt of the lattice $\vec{\mathbb{L}}^2$ and a realisation $(\vec{\mathbb{Z}}^2, \vec{\mathbb{E}}^2_{0.5}(\omega))$ of oriented bond percolation.

Figure 2.1.: Excerpt of realisations of ordinary and oriented bond percolation. Solid lines represent open edges and the dotted lines closed edges.

corresponding expectation operators E_p and $\vec{E}_p$. Every vector $\omega \in \Omega$ or $\vec{\omega} \in \vec{\Omega}$ is called a configuration of the corresponding percolation model. The values 0 and 1 of the components of these vectors have the following interpretation: each edge is supposed to be open (existing) with probability $p \in [0,1]$ or otherwise closed (not existing) and each are independent from the other edges. To model this, we consider a vector of independent and Bernoulli distributed random variables on $(\Omega, \mathcal{F}, \mathbb{P}_p)$ and $(\vec{\Omega}, \vec{\mathcal{F}}, \vec{\mathbb{P}}_p)$ respectively:

$$X^p = (X^p_e : e \in \mathbb{E}^d) : \Omega \to \{0,1\}, \qquad \vec{X}^p = (\vec{X}^p_e : e \in \vec{\mathbb{E}}^d) : \vec{\Omega} \to \{0,1\}, \tag{2.2}$$

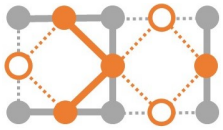
where X^p_e denotes the projection to the component with index $e \in \mathbb{E}^d$ and $\vec{X}^p_e$ the projection to the component with index $e \in \vec{\mathbb{E}}^d$. This means $\mathbb{P}(X^p_e = 1) = 1 - \mathbb{P}(X^p_e = 0) = p$ for all $e \in \mathbb{E}^d$ and $\mathbb{P}(\vec{X}^p_e = 1) = 1 - \mathbb{P}(\vec{X}^p_e = 0) = p$ for all $e \in \vec{\mathbb{E}}^d$. The sets of open edges are for a given probability $p \in [0,1]$ and a given configuration ω or $\vec{\omega}$ defined as

$$\mathbb{E}^d_p(\omega) \coloneqq \{e \in \mathbb{E}^d : X^p_e(\omega) = 1\}, \qquad \vec{\mathbb{E}}^d_p(\vec{\omega}) \coloneqq \{e \in \vec{\mathbb{E}}^d : X^p_e(\vec{\omega}) = 1\}. \tag{2.3}$$

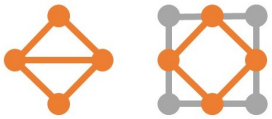
The sets of closed edges are consequently given by $\mathbb{E}^d \backslash \mathbb{E}^d_p(\omega)$ and $\vec{\mathbb{E}}^d \backslash \vec{\mathbb{E}}^d_p(\omega)$. By regarding only the remaining subgraphs $(\mathbb{Z}^d, \mathbb{E}^d_p(\omega))$ and $(\vec{\mathbb{Z}}^d, \vec{\mathbb{E}}^d_p(\omega))$, which arise from removing the closed edges, a realisation of ordinary or oriented bond percolation is obtained, see Figure 2.1.

In contrast to ordinary bond percolation, in ordinary site percolation vertices are open or exist with probability $p \in [0,1]$ and are closed otherwise. The following results for ordinary bond percolation are often similar to the ones for ordinary site percolation, but the values of the critical probabilities differ. Most arguments from bond percolation models can be applied or modified to different lattice models. Given an ordinary bond percolation model, an ordinary site percolation model is obtained by replacing every open (closed) edge e by an active (inactive) vertex e' on a new lattice and by joining each two new vertices e' and f' by a new open edge if and only if the two corresponding edges e and f on the old lattice are adjacent. This edge between e' and f' is open if and only if both vertices are active, see Figure 2.2(a) [12], [15].

Ordinary site percolation is more general, as there exist ordinary site percolation models, which cannot be transformed into an ordinary bond percolation model, see Figure 2.2(b): every orange active vertex of the ordinary site percolation configuration has to be replaced by an open grey edge of ordinary bond percolation. In the ordinary site percolation model the left and right vertex are joined, but it is not possible that the left and the right edge of ordinary bond percolation are adjacent.



(a) Transformation from bond percolation in grey to site percolation in orange.



(b) Site percolation configuration which cannot be obtained from a bond percolation model.

Figure 2.2.: Bond percolation in grey and site percolation in orange. Solid lines represent open bonds and dotted lines closed bonds; filled cycles represent active sites and hollow cycles inactive sites.

2.2. The Existence of an Infinite Open Cluster

To analyse an obtained realisation $(\mathbb{Z}^d, \mathbb{E}_p^d(\omega))$ or $(\vec{\mathbb{Z}}^d, \vec{\mathbb{E}}_p^d(\omega))$ of ordinary or oriented bond percolation, we introduce the following notation for ordinary bond percolation: for $x, y \in \mathbb{Z}^d$ we write $x \leftrightarrow y$ for an open path through x and y and then call x and y connected if there exists a sequence $\pi = (x^0, x^1, ..., x^n), n \geq 0$ of points $x^0, x^1, ..., x^n \in \mathbb{Z}^d$ with $\{x^{i-1}, x^i\} \in \mathbb{E}_p^d$ $\forall i \in \{1, ..., n\}$ and $x = x^0$ and $y = x^n$. Analogously we write for oriented bond percolation $x \to y$ if a sequence $\pi = (x^0, x^1, ..., x^n), n \geq 0$ of points $x^0, x^1, ..., x^n \in \mathbb{Z}^d$ with $\langle x^{i-1}, x^i \rangle \in \vec{\mathbb{E}}_p^d$ $\forall i \in \{1, ..., n\}$ and $x = x^0$ and $y = x^n$ exists. The open cluster or connected component of x is defined as

$$C_p(x) := \{y \in \mathbb{Z}^d : x \leftrightarrow y\}, \quad \vec{C}_p(x) := \{y \in \mathbb{Z}^d : x \to y\}. \tag{2.4}$$

For the origin we set $C_p := C_p(0)$ and $\vec{C}_p := \vec{C}_p(0)$. In the case of ordinary bond percolation the operator $\leftrightarrow$ is an equivalence relation on $\mathbb{E}_p^d$ since it is reflexive ($x \leftrightarrow x$), symmetric ($x \leftrightarrow y \Rightarrow y \leftrightarrow x$) and transitive ($x \leftrightarrow y \wedge y \leftrightarrow z \Rightarrow x \leftrightarrow z$) $\forall x, y, z \in \mathbb{E}_p^d$. For oriented bond percolation the operator $\to$ is reflexive and transitive, but symmetry is not fulfilled.

In the following, some probabilistic results of bond percolation are proved for ordinary bond percolation similarly to [18]. Since the proofs do not use that the edges are undirected, they hold analogously for oriented bond percolation and can be obtained by replacing every variable or set by the corresponding one from oriented bond percolation.

Lemma 2.1 [18]. *Let $x, y \in \mathbb{Z}^d$. Then the indicator functions*

$$\mathbb{1}_{\{x \leftrightarrow y\}}(\omega) := \begin{cases} 1, & \text{if } x \leftrightarrow y, \\ 0, & \text{otherwise.} \end{cases} \qquad \mathbb{1}_{\{x \to y\}}(\vec{\omega}) := \begin{cases} 1, & \text{if } x \to y, \\ 0, & \text{otherwise,} \end{cases}$$

as well as the cardinality of the open clusters $|C_p(x)(\omega)|$ and $|\vec{C}_p(x)(\vec{\omega})|$ are random variables with respect to the probability spaces $(\Omega, \mathcal{F}, \mathbb{P}_p)$ and $(\vec{\Omega}, \vec{\mathcal{F}}, \vec{\mathbb{P}}_p)$, where $\omega \in \Omega$ and $\vec{\omega} \in \vec{\Omega}$.

Proof. (Only for ordinary bond percolation). Since the lattice $\mathbb{Z}^d$ is invariant under translation we can suppose x = 0. For given $y \in \mathbb{Z}^d$ we define for $n \in \mathbb{N}$ the functions

$$f_n^y : \Omega \to \{0, 1\}, \quad f_n^y(\omega) := \begin{cases} 1, & \text{if there exists an open path of length} \leq n \\ & \text{from 0 to y,} \\ 0, & \text{otherwise.} \end{cases}$$

Every path of length $\leq n$ is also an path of length $\leq n + 1$ and therefore f_n is monotone: $f_n^y(\omega) \leq f_{n+1}^y(\omega)$ $\forall \omega \in \Omega$. As $\mathbb{1}_{\{x \leftrightarrow y\}}(\omega)$ is 1 if and only if there exists a path of arbitrary length from 0 to y it holds $\mathbb{1}_{\{x \leftrightarrow y\}}(\omega) = \lim_{n \to \infty} f_n^y(\omega) = \sup_{n \in \mathbb{N}} f_n^y(\omega)$ $\forall \omega \in \Omega$, where the last equation follows from the monotony of f_n^y in n. Since the supremum of measurable maps is measurable it is sufficient to show that f_n is measurable for all $y \in \mathbb{Z}^d$.

Let $Q_n := \{x = (x_1, ..., x_d) \in \mathbb{Z}^d : \|x\|_\infty := \max_{i \in d} x_i \leq n\}$ and $\mathbb{F}_n^d := \{e = \{x_1, x_2\} \in \mathbb{E}^d : x_1, x_2 \in Q_n\}$ be the set of edges between points of the cube Q_n. As every component X_e^p

with $e \in \mathbb{E}^d$ of the random variable $X^p : \Omega \to \{0,1\}$ (cf. equation (2.2)) is measurable, also $h_n \coloneqq (X_e^p : e \in \mathbb{F}_n^d) : \Omega \to \prod_{e\in\mathbb{F}_n^d}\{0,1\}$, which is the projection from X^p to its components indexed by $e \in \mathbb{F}_n^d$, is measurable. f_n is a function of h_n because all edges of paths of length $\leq n$ starting at 0 are contained in $\mathbb{F}_n^d$. Hence, we can write $f_n(\omega) = g_n \circ h_n(\omega)$ for some suitable measurable map $g_n : \prod_{e\in\mathbb{F}_n^d}\{0,1\} \to \{0,1\}$. It is measurable, since the preimage of 1 is an open path of length $\leq n$, which is a finite dimensional cylinder set (cf. A.14) of Ω and so contained in the σ-algebra of the underlying probability space $(\Omega, \mathcal{F}, \mathbb{P}_p)$ (cf. definition is Section 2.1). The preimage of 0 is the counter event of the preimage of 1 and so also measurable. It follows that f_n is measurable as a composition of the measurable maps g_n and h_n and so the indicator function $\mathbb{1}_{\{x\leftrightarrow y\}}(\omega)$ is a random variable.

As $|C_p(x)| = \sum_{y\in\mathbb{Z}^d} \mathbb{1}_{\{x\leftrightarrow y\}}$, the cardinality of the open cluster $|C_p(x)|$ is a random variable as a sum of random variables. □

Since we have shown that $|C_p(x)|$ and $|\vec{C}_p(x)|$ are random variables, the percolation probabilities $\theta(p)$ and $\vec{\theta}(p)$ can be defined as the probability of the origin belonging to an infinite cluster of open edges:

$$\theta(p) \coloneqq \mathbb{P}_p(|C_p| = \infty), \qquad \vec{\theta}(p) \coloneqq \vec{\mathbb{P}}_p(|\vec{C}_p| = \infty). \tag{2.5}$$

Because of the invariance of the lattice $\mathbb{Z}^d$ under translation, it holds

$$\theta(p) = \mathbb{P}_p(|C_p(y)| = \infty) \quad \text{and} \quad \vec{\theta}(p) = \vec{\mathbb{P}}_p(|\vec{C}_p(y)| = \infty) \qquad \forall y \in \mathbb{Z}^d. \tag{2.6}$$

It is intuitively clear that $\theta(p)$ and $\vec{\theta}(p)$ are monotonically increasing functions in p, but the formal proof takes some steps and needs a technique called coupling.

Proposition 2.2 [18]. *The maps $[0,1] \to [0,1]$, $p \mapsto \theta(p)$ and $[0,1] \to [0,1]$, $p \mapsto \vec{\theta}(p)$ are monotonically increasing.*

Proof. (Only for ordinary bond percolation). Let $(\Omega_Y, \mathcal{F}_Y, \mathbb{P}_Y)$ be a probability space, $p, p' \in [0,1]$ with $p < p'$ and $(Y_e)_{e\in\mathbb{E}^d}$ be a family of independent random variables on $(\Omega_Y, \mathcal{F}_Y, \mathbb{P}_Y)$, which are uniformly distributed on the interval $[0,1]$: $Y_e \sim \mathcal{U}_{[0,1]}$. Now we define for $q \in \{p, p'\}$ a family $(X_e^q)_{e\in\mathbb{E}^d}$ of random variables:

$$X_e^q \coloneqq \mathbb{1}_{\{Y_e\leq q\}} = \begin{cases} 1, & \text{if } Y_e \leq q, \\ 0, & \text{otherwise.} \end{cases}$$

Since the family $(Y_e)_{e\in\mathbb{E}^d}$ is independent, the family $(X_e^q)_{e\in\mathbb{E}^d}$ also is. Furthermore, as it holds $\mathbb{P}(X_e^q = 1) = 1 - \mathbb{P}(X_e^q = 1) = q$, X_e^q is Bernoulli distributed: $X_e^q \sim \mathrm{Ber}_q$. X_e^p and $X_e^{p'}$ both depend on the same Y_e and so they are coupled and for every $e \in \mathbb{E}^d$ the relation $X_e^p \leq X_e^{p'}$ is fulfilled for all $e \in \mathbb{E}^d$, because $\{Y_e \leq p\} \subset \{Y_e \leq p'\}$ $\forall e \in \mathbb{E}^d$. Since we can interpret X_e^q as the state of edges (cf. equation (2.3)), we have constructed two models of ordinary bond percolation for p and p' simultaneously on the same probability space $(\Omega_Y, \mathcal{F}_Y, \mathbb{P}_Y)$. From the relation $X_e^p \leq X_e^{p'}$ for all $e \in \mathbb{E}^d$ it follows for the open clusters: $C_p(x) \subset C_{p'}(x)$ for any $x \in \mathbb{Z}^d$ and hence $\theta(p) \leq \theta(p')$ for $0 \leq p \leq p' \leq 1$. □

The percolation probability defines for a given $x \in \mathbb{Z}^d$ the probability that x belongs to an infinite open cluster, but regarding the whole lattice, we can define $\psi(p)$ or $\vec{\psi}(p)$ as the probability that percolation occurs, which means that at least one infinite open cluster exists:

$$\psi(p) \coloneqq \mathbb{P}_p\left(\bigcup_{x\in\mathbb{Z}^d}\{|C_p(x)| = \infty\}\right), \qquad \vec{\psi}(p) \coloneqq \mathbb{P}_p\left(\bigcup_{x\in\mathbb{Z}^d}\{|\vec{C}_p(x)| = \infty\}\right), \tag{2.7}$$

where $\{|C_x| = \infty\}$ is the empty set if no infinite open cluster for x exists and otherwise it is the event $A_x = \{|C_x| = \infty\}$ that there exists an infinite open cluster at x. Consequently the union over all $x \in \mathbb{Z}^d$ describes the event that there exists at least one infinite open cluster.

Proposition 2.3 [18]. *For any $p \in [0,1]$ it holds*

$$\psi(p) = \begin{cases} 0, & \text{if } \theta(p) = 0, \\ 1, & \text{if } \theta(p) > 0. \end{cases} \qquad \vec{\psi}(p) = \begin{cases} 0, & \text{if } \vec{\theta}(p) = 0, \\ 1, & \text{if } \vec{\theta}(p) > 0. \end{cases}$$

Proof. (Only for ordinary bond percolation). If $\theta(p) = 0$ it follows with equation (2.6):

$$\psi(p) \coloneqq \mathbb{P}_p\left(\bigcup_{x\in\mathbb{Z}^d} \{|C_p(x)| = \infty\}\right) \leq \sum_{y\in\mathbb{Z}^d} \mathbb{P}_p(|C_p(y)| = \infty) = \sum_{y\in\mathbb{Z}^d} \theta(p) = 0.$$

For the case $\theta(p) > 0$ define $A \coloneqq \bigcup_{x\in\mathbb{Z}^d}\{|C_p(x)| = \infty\}$. If we change only the state of finitely many edges $\emptyset \neq \mathbb{F}^d \subset \mathbb{E}^d$, the realisation of percolation $\mathbb{E}_p^d$ differs, but the connected components of infinite cardinality and so also A stay unchanged. Hence for every finite $\emptyset \neq \mathbb{F}^d \subset \mathbb{E}^d$ the event A is an element of the σ-algebra generated by the remaining edges: $A \in \sigma((X_e^p)_{e\in\mathbb{E}^d\setminus\mathbb{F}^d})$. By the definition of the tail σ-algebras (A.15) it follows directly $A \in \mathcal{T}((X_e^p)_{e\in\mathbb{E}^d})$. So Kolmogorov's 0-1 law (A.16) shows $\psi(p) = \mathbb{P}(A) \in \{0,1\}$. The probability that an infinite open cluster exists is larger or equal than the probability that the origin is contained in an infinite open cluster. Therefore it holds $\psi(p) \geq \theta(p)$ and so $\psi(p) \in \{0,1\}$ implies that $\psi(p) = 1$ for $\theta(p) > 0$. □

So for $\theta(p) > 0$, at least one infinite open cluster exists. For ordinary bond percolation, it is almost surely unique, which is proved in [18]:

Theorem 2.4 [18]. *Let N be the number of infinite clusters,*

$$N \coloneqq |\{C_p(x) : |C_p(x)| = \infty \text{ for } x \in \mathbb{Z}^d\}|.$$

Then for any $p \in [0,1]$ it holds $\mathbb{P}_p(N \leq 1) = 1$.

For oriented bond percolation, in [10] a theorem implying the uniqueness of an infinite open cluster is proved. A special case of this theorem is outlined below.

Theorem 2.5 [10]. *Let $d \geq 2$ and $p \in [0,1]$ with $\vec{\psi}(p) = 1$. Then for all $x, y \in \mathbb{Z}^d$:*

$$\mathbb{P}_p\left(\exists z : |\vec{C}_p(z)| = \infty \wedge z \in \vec{C}_p(x) \wedge z \in \vec{C}_p(y) \,\middle|\, |\vec{C}_p(x)| = \infty \wedge |\vec{C}_p(y)| = \infty\right) = 1.$$

This theorem is proved for a sublattice of $\vec{\mathbb{L}}^d = (\mathbb{Z}^d, \vec{\mathbb{E}}^d)$, containing all vertices and edges of $\vec{\mathbb{L}}^d$, whose components are non-negative. For given x and y in $\vec{\mathbb{L}}^d$, the lattice can be translated so that x and y are located in the positive orthant. Every infinite open path starting from a vertex in the positive orthant only contains edges between vertices with non-negative components, because of the directionality of the edges. Consequently, Theorem 2.5 also holds on $\vec{\mathbb{L}}^d = (\mathbb{Z}^d, \vec{\mathbb{E}}^d)$. Hence, even in the case of oriented bond percolation, the infinite cluster is almost surely unique: if there would be at least two different infinite clusters which have no points in common with $x \in \mathbb{Z}^d$ contained in a first and $y \in \mathbb{Z}^d$ contained in a second one, Theorem 2.5 would ensure the existence of a $z \in \mathbb{Z}^d$ contained in both infinite open clusters. This is a contradiction to the assumption of two different infinite open clusters.

2.3. The Critical Phenomenon

As we have shown in Propositions 2.2 and 2.3 that θ, $\vec{\theta}$ and ψ, $\vec{\psi}$ are monotonically increasing functions in p, we can define the critical probability as

$$\begin{aligned} p_c = p_c(\mathbb{L}^d) &\coloneqq \inf\{p \in [0,1] : \theta(p) > 0\} &&= \sup\{p \in [0,1] : \theta(p) = 0\} \\ &= \inf\{p \in [0,1] : \psi(p) = 1\} &&= \sup\{p \in [0,1] : \psi(p) = 0\}, \\ \vec{p}_c = \vec{p}_c(\vec{\mathbb{L}}^d) &\coloneqq \inf\{p \in [0,1] : \vec{\theta}(p) > 0\} &&= \sup\{p \in [0,1] : \vec{\theta}(p) = 0\} \\ &= \inf\{p \in [0,1] : \vec{\psi}(p) = 1\} &&= \sup\{p \in [0,1] : \vec{\psi}(p) = 0\} \end{aligned} \tag{2.8}$$

The percolation probabilities $\theta(p)$ and $\vec{\theta}(p)$ take the following values dependent on p_c and $\vec{p}_c$:

$$\theta(p) \begin{cases} = 0, & \text{if } p < p_c, \\ > 0, & \text{if } p > p_c, \end{cases} \qquad \vec{\theta}(p) \begin{cases} = 0, & \text{if } p < \vec{p}_c, \\ > 0, & \text{if } p > \vec{p}_c. \end{cases} \tag{2.9}$$

There are two phases: the subcritical phase if $p < p_c$ and the supercritical phase if $p > p_c$. In the subcritical phase, all connected components are almost surely finite. In the supercritical phase, the origin and, because of the translation invariance of the lattice, every vertex in $\mathbb{Z}^d$ has a positive probability to be in an infinite open cluster. According to Proposition 2.3 an infinite open cluster almost surely exists and due to Theorems 2.4 and 2.5 it is almost surely unique. From equations (2.8) and (2.9) a couple of questions arise: are there exact values known for p_c and $\vec{p}_c$? What is the probability that an infinite connected component at $p = p_c$ or $p = \vec{p}_c$ exists? How does the percolation system behave for values of p or $\vec{p}$ near the critical probability? In the following, some answers to this critical phenomenon can be given, but there are still many open questions in percolation theory. The theorems outlined below show parallels between ordinary and oriented bond percolation, but the proofs often differ because the directionality of the edges restricts the spatial freedom.

The proof of the following theorem is briefly sketched for ordinary bond percolation in [18] and will be presented here in more detail and also for oriented bond percolation.

Theorem 2.6 [18]. *For $d = 1$ it holds $p_c = \vec{p}_c = 1$ and $\theta(p_c) = \vec{\theta}(\vec{p}_c) = 1$.*

Proof. For $p = 1$ every edge of the lattices $\mathbb{L}^d$ and $\vec{\mathbb{L}}^d$ is open, so an infinite open cluster at the origin exists. Hence $\theta(1) = 1$ and $\vec{\theta}(1) = 1$.

In the case of ordinary bond percolation on the lattice $\mathbb{L}^1 = (\mathbb{Z}^1, \mathbb{E}^1)$ define for $p < 1$ and $n \in \mathbb{Z}$ the events $A_n = \{X^p_{\{n,n+1\}} = 0\}$. Since the family of Bernoulli distributed random variables $(X^p_e)_{e \in \mathbb{E}^1}$ was chosen to be independent, the family of events $(A_n)_{n\in\mathbb{Z}}$, $(B_n)_{n\in\mathbb{N}} := (A_n)_{n\in\mathbb{N}}$ and $(C_n)_{n\in\mathbb{N}} := (A_{1-n})_{n\in\mathbb{N}}$ are each independent. Furthermore $P(A_n) = 1 - p > 0$ and so $\sum_{n=1}^{\infty} B_n = \sum_{n=1}^{\infty} C_n = \sum_{n=1}^{\infty} 1 - p = \infty$. It holds

$$B^* := \limsup_{n\to\infty} B_n := \bigcap_{n=1}^{\infty} \bigcup_{m=n}^{\infty} B_m = \{X^p_{\{n,n+1\}} = 0 \text{ for infinitely many } n \in \mathbb{N}\},$$

$$C^* := \limsup_{n\to\infty} C_n := \bigcap_{n=1}^{\infty} \bigcup_{m=n}^{\infty} C_m = \{X^p_{\{1-n,2-n\}} = 0 \text{ for infinitely many } n \in \mathbb{N}\}.$$

By the Borel-Cantelli Lemma (A.12) it follows $\mathbb{P}(B^*) = \mathbb{P}(C^*) = 1$. Define $A^* = B^* \cap C^*$ to be the event that located to the left and to the right from the origin infinitely many closed edges exist respectively. Because of the independence of the family $(A_n)_{n\in\mathbb{Z}}$, it follows $\mathbb{P}(A^*) = \mathbb{P}(B^*) \cdot \mathbb{P}(C^*) = 1$. As the event that the origin is contained in an infinite open cluster, is a subset of $(A^*)^c$, it holds $\theta(p) \leq \mathbb{P}((A^*)^c) = 0 \Rightarrow p_c = \inf\{p \in [0,1] : \theta(p) > 0\} = 1$.

In the case of oriented bond percolation on the lattice $\vec{\mathbb{L}}^1 = (\mathbb{Z}^1, \vec{\mathbb{E}}^1)$ we define for $p < 1$ and $n \in \mathbb{N}$ the events $A_n = \{X^p_{\langle n,n+1\rangle} = 0\}$. Since the family of Bernoulli distributed random variables $(X^p_e)_{e\in\vec{\mathbb{E}}^1}$ was chosen to be independent, the family of events $(A_n)_{n\in\mathbb{N}}$ is independent. Furthermore, $\mathbb{P}(A_n) = 1 - p > 0$ and so $\sum_{n=1}^{\infty} A_n = \sum_{n=1}^{\infty} 1 - p = \infty$. It holds

$$A^* := \limsup_{n\to\infty} A_n := \bigcap_{n=1}^{\infty} \bigcup_{m=n}^{\infty} B_m = \{X^p_{\langle n,n+1\rangle} = 0 \text{ for infinitely many } n \in \mathbb{N}\}.$$

By the Borel-Cantelli Lemma it follows $\mathbb{P}(A^*) = 1$. Because of the left-right orientation of the edges, only the ones between positive integers play a role for the decision whether the origin is part of an infinite open cluster. So this event is contained in $(A^*)^c$. Hence $\theta(p) \leq \mathbb{P}((A^*)^c) = 0$ $\Rightarrow \vec{p}_c = \inf\{p \in [0,1] : \theta(p) > 1\} = 1$. □

In two dimensions the value for the critical probability of ordinary bond percolation on a square lattice is known, but it takes more steps to prove it than the intuitively clear result looks like, see [8].

Theorem 2.7 [8]. *For $d = 2$ it holds $p_c = \frac{1}{2}$ and $\theta(p_c) = 0$.*

For different lattices like triangular or hexagonial ones, it is also possible to compute exact values of the critical probability in two dimensions [8]. Even there are no exact and not numerically computed values known in higher dimensions, some lower and upper bounds can be found for ordinary and oriented bond percolation.

Theorem 2.8 [9], [18]. *For $d \geq 2$, it holds $0 < \frac{1}{2d-1} \leq p_c(d) \leq \vec{p}_c(d) \leq \frac{2}{3} < 1$.*

Proof. In the undirected case, we consider for the lower bound a self avoiding walk (SAW) on $\mathbb{E}^d$. This is a path that visits each vertex of $\mathbb{Z}^d$ at most once. We denote with σ_n the number of SAWs on $\mathbb{E}^d$, which start at the origin and have length n and with N_n the number of SAWs counted in σ_n, which consist only of open edges. Since the existence of an infinite open cluster is equivalent to the existence of an open self avoiding walk with length infinity, if follows

$$\theta(p) \coloneqq \mathbb{P}_p(|C_p| = \infty) = \mathbb{P}_p(N_n \geq 1 \ \forall n \geq 1) = \lim_{n\to\infty} \mathbb{P}_p(N_n \geq 1).$$

The last equality holds because if an open path of length n exists also an open path of length $n-1$ exists, so $\mathbb{P}_p(N_n \geq 1) \leq \mathbb{P}_p(N_{n-1} \geq 1)$ and consequently $\mathbb{P}_p(N_n \geq 1)$ converges as it is bounded from below through 0. To find an evaluation for the percolation probability $\theta(p)$, we describe the value of $\mathbb{P}_p(N_n \geq 1)$ in terms of the expected value of N_n. This can be expressed as the number of all possible SAWs σ_n times the probability p^n that each of the n vertices is open.

$$\mathbb{P}_p(N_n \geq 1) = \sum_{i=1}^{\infty} \mathbb{P}(N_n = i) \leq \sum_{i=1}^{\infty} i \cdot \mathbb{P}_p(N_n = i) = E_p(N_n) = p^n \cdot \sigma_n.$$

The number of possible SAWs is bounded since for the first step there are $2d$ possible steps away from the origin on $\mathbb{E}^d$ and afterwards there are not more than $2d-1$ possible directions to walk because one edge is already used to reach the regarded vertex. Thus

$$\begin{aligned} & \sigma_n \leq 2d \cdot (2d-1)^{n-1} \\ \Rightarrow \quad & \theta(p) = \lim_{n\to\infty} \mathbb{P}_p(N_n \geq 1) = \lim_{n\to\infty} p^n \cdot \sigma_n \leq \lim_{n\to\infty} p^n \cdot 2d \cdot (2d-1)^{n-1}. \end{aligned}$$

The limit value of the geometric series and so also $\theta(p)$ is zero if $p \cdot (2d-1) < 1$. As $p_c = \inf\{p \in [0,1] : \theta(p) > 0\}$, the critical probability has to fulfil

$$p_c \cdot (2d-1) \geq 1 \quad \Rightarrow \quad p_c \geq \frac{1}{2d-1} > 0 \quad \forall d \geq 2. \tag{2.10}$$

Every oriented path is also a path, so if there exists an infinite open cluster in $\vec{\mathbb{L}}^d$ and we keep the same edges open, there exists also an infinite open cluster in $\mathbb{L}^d$. It follows for the percolation probability $\vec{\theta}(p) \leq \theta(p)$ and because of definition (2.8) for the critical probability $p_c(d) \leq \vec{p}_c(d)$.

For the upper bound, we remark that $\vec{\mathbb{L}}^d$ can be embedded in $\vec{\mathbb{L}}^{d+1}$ as a projection on the subspace generated by the first d coordinates. So if for given $p \in [0,1]$ an infinite open cluster exists in $\vec{\mathbb{L}}^d$, it is also infinite in $\vec{\mathbb{L}}^{d+1}$. Hence $\vec{\theta}_d(p)$ is increasing in d. With the definition of $\vec{p}_c$ it follows

$$\vec{p}_c(d+1) \leq \vec{p}_c(d) \quad \forall\, d \geq 1. \tag{2.11}$$

So to prove $\vec{p}_c(d) \leq \frac{2}{3}$ for all $d \geq 2$ it suffices to show $\vec{p}_c(2) \leq \frac{2}{3}$. Therefore define with the points $(i,0) \in \mathbb{Z}^2$, $i \in \{1,...,N\}$, $N \in \mathbb{N}$ the open cluster of $\{1,...,N\} \times \{0\}$:

$$\vec{C}_N \coloneqq \bigcup_{i=1}^{N} \vec{C}_p((i,0)),$$

where $\vec{C}((x_1, x_2))$ denotes the open cluster of $(x_1, x_2) \in \mathbb{Z}^2$ (cf. equation (2.4)). $\vec{C}_N$ is presented in Figure 2.3. From the σ-subadditivity of probability (A.5) and the translation invariance of the lattice (2.6) it follows for an arbitrary point $y \in \mathbb{Z}^2$ that

$$\begin{aligned}\vec{\theta}(p) = \vec{\mathbb{P}}_p(|\vec{C}_p(y)| = \infty) &= \frac{1}{N}\sum_{i=1}^{N} \mathbb{P}_p(|\vec{C}_p((i,0))| = \infty) \\ &\geq \frac{1}{N}\mathbb{P}_p\left(\bigcup_{i=1}^{N}\{|\vec{C}_p((i,0))| = \infty\}\right) = \frac{1}{N}\mathbb{P}_p(|\vec{C}_N| = \infty). \end{aligned} \tag{2.12}$$

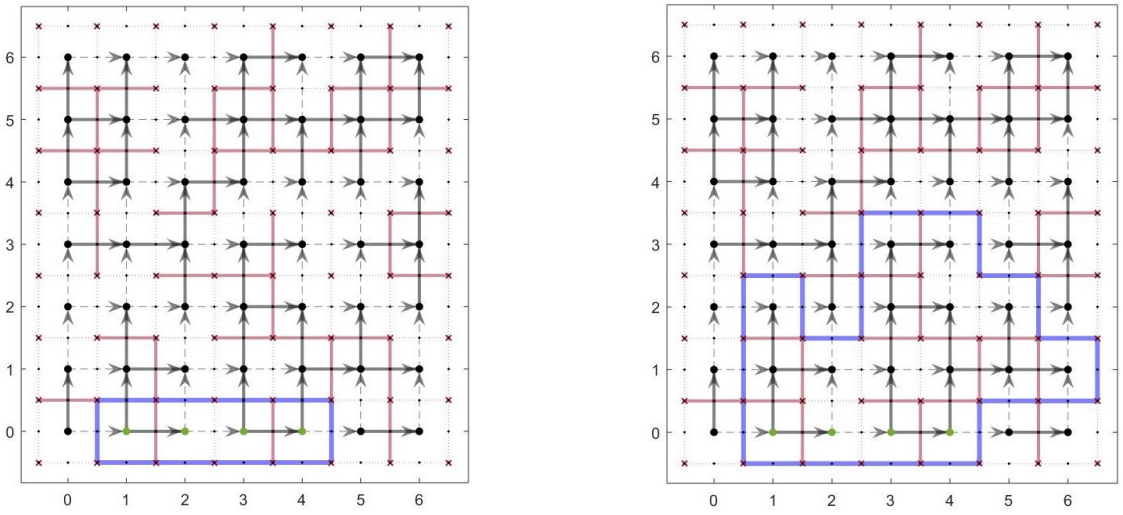
The undirected dual lattice of $(\vec{\mathbb{Z}}^2, \vec{\mathbb{E}}^2)$ is defined by $(\bar{\mathbb{Z}}^2, \bar{\mathbb{E}}^2)$ with

$$\bar{\mathbb{Z}}^2 = \left(\frac{1}{2}, \frac{1}{2}\right) + \mathbb{Z}^2 \qquad \bar{\mathbb{E}}^2 = \{e = \{x, y\} : x, y \in \bar{\mathbb{Z}}^2 \wedge \delta(x, y) = 1\}. \tag{2.13}$$

The realisation of percolation in the dual lattice $(\bar{\mathbb{Z}}^2, \bar{\mathbb{E}}^2_p)$ is obtained in the following way: Each edge of $\bar{\mathbb{E}}^2$ crosses exactly one edge in $\vec{\mathbb{E}}^2$ (cf. equation (2.3)), it is called the corresponding edge. Hence every edge of $\bar{\mathbb{E}}^2$ is defined to be open if and only if the corresponding edge of $\mathbb{E}^2$ is open. A closed cycle of the undirected dual lattice is a sequence $\pi = (x_0, x_1, ..., x_n), n \geq 0$ of points $x_0, x_1, ..., x_n \in \mathbb{Z}^d$ with $x_0 = x_n$, $x_i \neq x_j$ for $i \in \{0, ..., N\}, j \in \{1, ..., N-1\}, i \neq j$, and $\{x_{k-1}, x_k\} \in \bar{\mathbb{E}}^2 \backslash \bar{\mathbb{E}}^2_p$ for $k \in \{1, ..., N\}$. We define the set

$$\begin{aligned} M_n \coloneqq \{\mu : \mu \text{ is a closed cycle of the undirected dual lattice with length } n, \text{ which} \\ \text{surrounds } \{1, ..., N\} \times \{0\}\}. \end{aligned} \tag{2.14}$$

Every closed cycles surrounding $\{1, ..., N\} \times \{0\} \subset \vec{C}_N$ has a length $n \geq 2N + 2 > 2N$, see Figure 2.3(a). We show now that $|M_n|$ is bounded by $n \cdot 3^n$: Every cycle surrounding $\{1, ..., N\} \times \{0\}$ has to cross the axis $\mathbb{Z} \times \{0\}$ at least twice. So there is an integer $r \leq 1$, such that the edge $\{(r - \frac{1}{2}, \frac{1}{2}), (r - \frac{1}{2}, -\frac{1}{2})\}$ crosses $\mathbb{Z} \times \{0\}$ and an integer $m \geq N$, such that the edge $\{(m + \frac{1}{2}, \frac{1}{2}), (m + \frac{1}{2}, -\frac{1}{2})\}$ crosses $\mathbb{Z} \times \{0\}$ as well. Since every closed cycle of M_n has n different vertices and has to contain the points $(r - \frac{1}{2}, -\frac{1}{2})$, $(r - \frac{1}{2}, \frac{1}{2})$, $(m + \frac{1}{2}, -\frac{1}{2})$ and $(m + \frac{1}{2}, \frac{1}{2})$ it holds $n \geq 2(m - r) + 2 > 2m > m$. It follows that there are less than n possibilities to pick the vertex



(a) In blue: minimal circle surrounding $\{1, ..., 4\} \times \{0\}$ with length $2 \cdot N + 2 = 10$.

(b) In blue: closed cycle containing the open cluster $\vec{C}_N$ with length $n = 22 > 10$.

Figure 2.3.: Excerpt of the realisation $(\mathbb{Z}^2, \vec{\mathbb{E}}^2_{0.5})$ of oriented bond percolation, the points $\{1, ..., N\} \times \{0\}$ for $N = 4$ are green, here $m = 4$ and $r = 1$. Solid lines represent open edges and dotted lines closed edges.

$(m+\frac{1}{2},\frac{1}{2}) \in \bar{\mathbb{Z}}^2$ out of the points of the closed cycle containing $\{1,...,N\}\times\{0\}$. Starting from this vertex, there are at most 3 possibilities for the next edge of the closed cycle because the cycle cannot go back to the vertex of the last step. It follows $|M_n| \leq n \cdot 3^n$.

The edges of the dual lattice (2.13) have a one-to-one correspondence to the original lattice, so an edge is also open with probability p and closed with probability $1-p$. Since the open cluster $\vec{C}_N$ is finite if and only if there exists at least one $n > 2N$ with $|M_n| \geq 1$, it follows with the σ-subadditivity of probability (A.5) and the limitation of $|M_n|$:

$$\begin{aligned}\mathbb{P}_p(|\vec{C}_N| < \infty) &\leq \mathbb{P}_p\left(\bigcup_{n=2N}^{\infty}\{|M_n| \geq 1\}\right) \leq \sum_{n=2N}^{\infty}\mathbb{P}_p\left(|M_n| \geq 1\right) \\ &= \sum_{n=2N}^{\infty}|M_n|\cdot(1-p)^n \leq \sum_{n=2N}^{\infty} n\cdot 3^n\cdot(1-p)^n.\end{aligned}$$

In Figure 2.3(b), a closed cycle containing the finite open cluster $\vec{C}_N$ is shown. For $p > \frac{2}{3}$ the last sum converges to zero if N tends to infinity by Lemma B.3, because $3\cdot(1-p) < 1$:

$$\sum_{n=2N}^{\infty} n\cdot 3^n\cdot(1-p)^n = \sum_{n=2N}^{\infty} n\cdot(3\cdot(1-p))^n \xrightarrow{N\to\infty} 0.$$

Hence for $p > \frac{2}{3}$ there exists $N^*(p) \in \mathbb{N}$ large enough such that $\mathbb{P}_p(|\vec{C}_N| < \infty) < 1$ for all $N \geq N^*$. Since $\mathbb{P}_p(|\vec{C}_N| < \infty) < 1 \Leftrightarrow \mathbb{P}_p(|\vec{C}_N| = \infty) > 0$, it follows $\mathbb{P}_p(|\vec{C}_N| = \infty) > 0$ for all $N \geq N^*(p)$. Inserting this inequality in equation (2.12) leads to

$$\vec{\theta}(p) \geq \frac{1}{N}\mathbb{P}_p(|\vec{C}_N| = \infty) > 0 \qquad \forall N \geq N^*(p) \text{ with } p > \frac{2}{3}.$$

So if we consider a sufficiently large number N^* of points on the line $\{1,...,N\}\times\{0\}$, the probability that at least one of these points belongs to an infinite open cluster is positive. It follows for the critical probability:

$$\vec{p}_c = \inf\{p \in [0,1] : \vec{\theta}(p) > 0\} \leq \frac{2}{3} < 1. \tag{2.15}$$

Equations (2.10) and (2.15) provide the result of the theorem. □

At the end of this Chapter, we state a conjecture and a theorem about the continuity of the percolation probability at the critical probability. Even many theorems are easier or only possible to be proved for ordinary bond percolation, the following theorem is so far only provable for oriented bond percolation.

The percolation probability $\theta(p)$ can only be a continuous function if $\theta(p_c) = 0$ since p_c is defined as $p_c = \inf\{p \in [0,1] : \theta(p) > 0\}$. If $\theta(p_c) \neq 0$ a 'jump' would exist in the graph of $\theta(p)$ at p_c. For $\theta(p_c) = 0$, θ is continuous at p_c, as for every series $(p_n)_{n\in\mathbb{N}}$ converging to p_c, $\theta(p_n)$ converges to zero: if there would be a series $(p_n)_{n\in\mathbb{N}}$, where $\theta(p_n)$ converges to $c \in \mathbb{R}_{>0}$, it would hold $\theta(p_c) > 0$, which is a contradiction to $\theta(p_c) = 0$. In the case of ordinary bond percolation, the continuity of θ at p_c is only proved for $d = 2$ and $d \geq 19$ (see [13]), but is believed to hold in all dimensions. For oriented bond percolation, the statement is proved in [10] with block construction arguments.

Conjecture 2.9 [9]. *For $d \geq 2$, we have that $\theta(p_c) = 0$.*

Theorem 2.10 [10]. *For $d \geq 2$, we have that $\vec{\theta}(\vec{p}_c) = 0$.*

3. Dynamic Percolation Processes

Besides bond and site percolation, which were introduced in Chapter 2, a third class of percolation process called dynamic or space-time percolation exists. The name space-time results from time as an additional dimension in the process. In a given discrete space, the sites of the lattice can be active or inactive and their states evolve through time because of interactions of the sites with their neighbours. The updates of the lattice can be modelled synchronously with a discrete time axis or asynchronously with a continuous times axis. There are differing views regarding which model is more realistic. Since in nature there is no artificial cycle or clock, the asynchronous spontaneously occurring updates seem more natural. Nevertheless, in the modelling of traffic flows, synchronous updates lead to better results. Both types have a similar behaviour and their properties can often be proven analogously [15], [23].

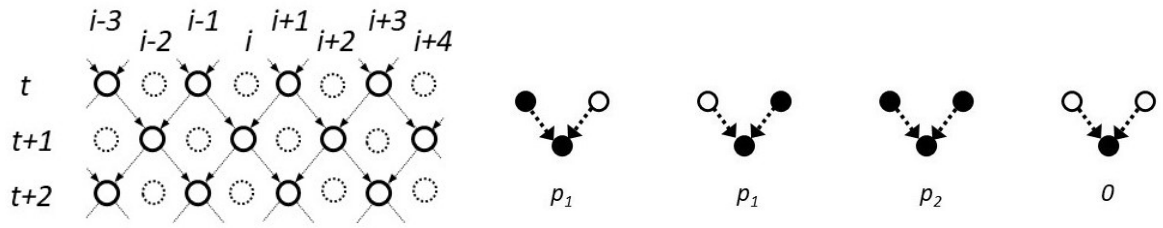
In this Chapter, three of the most popular lattice models for dynamic percolation are presented. First the $1+1$ dimensional cellular automaton defined by Domany and Kinzel is introduced. A special case thereof is directed percolation, whose definition in [15] is generalised in the present work from $1+1$ to $d+1$ dimensions and connected to oriented bond percolation. Afterwards, a continuous time adaption of directed percolation is defined in $d+1$ dimensions, called contact process.

The whole variety of dynamic percolation models works with the same reaction diffusion scheme. Particles on the sites of the lattice can self-destruct (an active particle gets inactive), diffuse (two particles exchange their state), produce offspring (some active particles emerge from one active particle) or coagulate (some active particles merge into one active particle) [15]. Since spontaneous particle creation is forbidden, all lattice models have an absorbing state: if all sites are inactive, it is not possible that any site becomes active again. Above a critical probability, the system does not reach the absorbing state, but self-destruction and offspring production balance each other. This results in a fluctuating steady state, where the average of particles fluctuates around a constant value [15]. For the three models defined here, it is possible to find similar results to the ones given in Chapter 2 regarding the critical probability.

3.1. Domany-Kinzel Cellular Automaton on $\mathbb{Z} \times \mathbb{N}_0$

A cellular automaton is a map from a configuration of a lattice onto another configuration of the same lattice. The map iterates in discrete time steps $t \in \mathbb{N}_0 := \mathbb{N} \cup \{0\}$ and usually the deterministic or stochastic update rules of the sites are locally independent [15].

The $1+1$ dimensional Domany-Kinzel model is a stochastic cellular automaton, which is defined as a homogeneous discrete time Markov chain (A.18), which describes the evolution of the states of sites located on the axis $\mathbb{Z}$. The following definition of the Domany-Kinzel cellular automaton is a more detailed and probabilistic version of the model defined in [15] and [17]. The space axis is $\mathbb{Z}$ or a finite interval of $\mathbb{Z}$, which has without loss of generality the form $[-N, N-1]_{\mathbb{Z}} := \{-N, -N+1, ..., N-2, N-1\}$, $N \in 2\mathbb{N}$. Let $s_i(t) \in \{-1, 0, 1\}$ denote the state of a site i at time t and define the random variables $S^{\infty}(t) := (..., s_{-1}(t), s_0(t), s_1(t), ...)$ and $S^N(t) := (s_{-N}(t), s_{-N+1}(t), ..., s_{N-1}(t))$. Here, 0 means the site is inactive, 1 means the site is active and -1 that it is not existing. This has the following interpretation: the start configuration $S_0^{\infty} := S^{\infty}(0)$ or $S_0^N := S^N(0)$ of the Domany-Kinzel automaton is chosen such that only sites located on even numbers exist and can be active or inactive. In every time iteration, $s_i(t+1)$ depends only on the state of its neighbours $i-1$ and $i+1$ at time t, such that for even time steps only sites with even numbers and for odd time steps only sites with



(a) Extract of the diagonal oriented square lattice, dotted circles represent non-existing sites, solid circles existing sites.

(b) Transition probabilities to become active, active sites are represented by filled circles, inactive sites by hollow circles.

Figure 3.1.: Lattice and transition probabilities of the $1+1$ dimensional Domany-Kinzel model.

odd numbers exist. The obtained lattice of existing sites is a diagonal square lattice with N sites in total in every time step, see Figure 3.1(a) for an example in $1+1$ dimensions. The state space is $\mathcal{E}_\infty := \prod_{i\in\mathbb{Z}}\{-1,0,1\}$ or $\mathcal{E}_N := \prod_{i\in[-N,N-1]_\mathbb{Z}}\{-1,0,1\}$. For a given random variable S_0^∞ or S_0^N and the following simultaneously updated local transition probabilities for the states $i \in \mathbb{Z}$ or $i \in [-N, N-1]_\mathbb{Z}$, a family of random variables $(S_t^\infty)_{t\in\mathbb{N}_0}$ or $(S_t^N)_{t\in\mathbb{N}_0}$ is defined. With $p_1 \in [0,1]$, $p_2 \in [0,1]$ and $i \in [-N, N-1]_\mathbb{Z}$ or $i \in \mathbb{Z}$, the local transition probabilities $\mathbb{P}(s_i(t+1)|s_{i-1}(t), s_{i+1}(t))$ are in both cases given by

$$\mathbb{P}(\,1\ |0,0) = 0, \tag{3.1}$$

$$\mathbb{P}(\,1\ |0,1) = \mathbb{P}(\,1\ |1,0) = p_1, \tag{3.2}$$

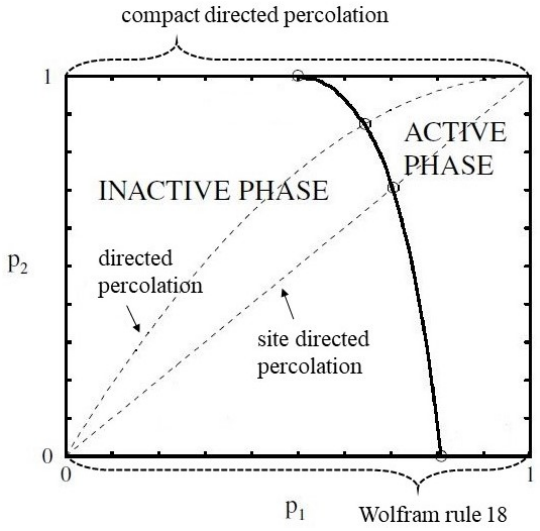
$$\mathbb{P}(\,1\ |1,1) = p_2, \tag{3.3}$$

$$\mathbb{P}(\,0\ |q,r) = 1 - \mathbb{P}(\,1\ |q,r) \qquad \forall (q,r) \in \{0,1\}^2, \tag{3.4}$$

$$\mathbb{P}(-1|q,r) = 1 \qquad \text{if } q = -1 \text{ or } r = -1. \tag{3.5}$$

The transition probabilities (3.1) to (3.3) for sites to become active are illustrated in Figure 3.1(b). If both neighbours exist, a site exists itself in the next time step and can get active or inactive. Equation (3.4) describes the transition probabilities of the counter event of equations (3.1) to (3.3) that a site becomes inactive. The transition probability (3.5) characterises the diagonal square lattice, so that alternating sites with even and odd numbers exist. In the case with the finite space axis $[-N, N-1]_\mathbb{Z}$, the boundary conditions can be chosen free, such that the sites at the boundary have only one neighbour, or periodic. For $i = -N$ the state s_{-N-1} occurs in the local transition probabilities and for $i = N-1$ the state s_N. If we have chosen free boundary conditions, we define $s_{-N-1}(t)$ to be -1 for even t and 0 for odd t and analogously $s_N(t)$ to be 0 for even t and -1 for odd t. So if for a time t the sites $i = -N-1$ or $i = N$ exist, they are inactive and do not influence the system on $[-N, N-1]_\mathbb{Z} \times \mathbb{N}_0$. For periodic boundary conditions, the in the local transition probabilities for $i = -N$ occurring state s_{-N-1} is set to $s_{-N-1}(t) = s_{N-1}(t)$ and the for $i = N-1$ occurring state $s_N(t)$ is set to $s_N(t) = s_{-N}(t)$. It follows that if for a time t the state of the sites $i = -N$ or $i = N-1$ is queried, it is the state of the site which would be located there by arranging the lattice $[-N, N-1]_\mathbb{Z} \times \mathbb{N}_0$ multiple times next to each other.

Depending on the values of $p_1 \in [0,1]$ and $p_2 \in [0,1[$, the Domany-Kinzel cellular automaton is in the inactive phase reaching the empty lattice and therefore an absorbing state, which cannot be left, or in the active phase, where a fluctuating steady state exists. This behaviour is independent of the size of the lattice and the starting configuration S_0^∞ or S_0^N, when starting from at least one active site (explication in Subsection 3.2.3) [15], [26]. The two phases are separated by a phase transition line, see Figure 3.2(a). If $p_2 = 1$ besides the empty lattice also the fully occupied lattice is an absorbing state. The process is then called compact directed percolation, since the clusters of active sites are compact. The behaviour of compact directed percolation is different to the Domany-Kinzel automaton with $p_2 \in [0,1[$, as in the active phase also an absorbing state is reached and no fluctuating steady state exists. Because of the symmetry of compact percolation, its critical probability of the phase transition has to be at $(p_{1,c}, p_{2,c}) = (0.5, 1)$.



(a) The hollow cycles in the phase diagram mark the critical probabilities $(p_{1,c}, p_{2,c})$ of the special cases (edited figure from [15]).

	$p_{1,c}$	$p_{2,c}$	Ref.
compact directed percolation	0.5	1	[17]
directed percolation	0.6447001(1)	0.8737620(2)	[16]
site directed percolation	0.705489(4)	0.705489(4)	[25]
Wolfram rule 18	0.801(2)	0	[26]

(b) Values of the critical probabilities for the special cases.

Figure 3.2.: Phase diagram and critical probabilities of the $1+1$ dimensional Domany-Kinzel model.

There are three other special cases: firstly, directed percolation in $1+1$ dimensions, which is a dynamical adaption from oriented bond percolation on $\mathbb{Z}^2$ with $p \in [0,1[$. It is the main percolation process of this thesis, see also Section 3.2, Chapter 4 and Chapter 5. Analogously to oriented bond percolation in Chapter 2, the transition probabilities are modelled by open or closed edges: if the site i has $k=1$ active neighbours, only one of the two sites $i-1$ and $i+1$ are active at time t and the site i becomes active in the next time step if the incoming edge from the active site is open. The state of the other edge is arbitrary, so $p_1 = p \in [0,1[$. If the number of active neighbours is $k=2$, such that both preprocessors $i-1$ and $i+1$ are active at time t, the site i at time $t+1$ becomes active, if at least one of the two incoming edges is open, so $p_2 = p(1-p)+(1-p)p+p^2 = p(2-p) \in [0,1[$. For an illustration of the transition probabilities of directed percolation in $1+1$ dimensions see Figure 3.3.

The second special case called site directed percolation is obtained by choosing $p_1 = p_2 = p \in [0,1[$. It is connected to ordinary site percolation, which was shortly introduced in Section 2.1: analogously two vertices are connected by an edge if and only if both are active. The site i at time $t+1$ is active, if at least one of its to preprocessors $i-1$ and $i+1$ at time t are active, this is consistent with the choice $p_1 = p_2$. The last special case with $p_2 = 0$ is called Wolfram rule 18. The special cases and their critical probabilities are indicated in the phase diagram of the Domany-Kinzel automaton, which is shown in Figure 3.2.

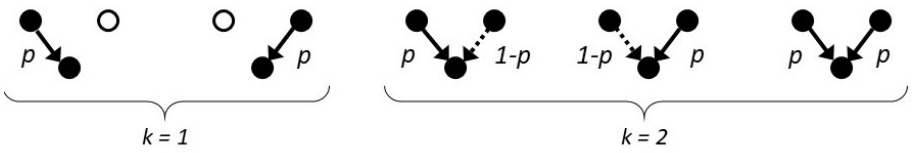


Figure 3.3.: Transition probabilities for directed percolation in $1+1$ dimensions depending on the number k of active neighbours. Edges are open with probability p and represented by solid arrows, closed edges by dotted arrows and edges starting from inactive sites are not presented, because their state does not influence the state of the site where the edge ends.

3.2. Directed Percolation on $\mathbb{Z}^d \times \mathbb{N}_0$

Directed percolation in $1+1$ dimensions was already introduced as a special case of the Domany-Kinzel automaton in Section 3.1. First, we generalize this concept to $d+1$ dimensions, $d \in \mathbb{N}$, then introduce the critical phenomenon and afterwards, we connect directed and oriented bond percolation and show their equivalence in $1+1$ respectively 2 dimensions.

3.2.1. Definition of Directed Percolation in $d+1$ dimensions

Similarly to the Domany-Kinzel automaton, we model the evolution of the states of the vertices of $\mathbb{Z}^d$ or of a d-dimensional hypercube of $\mathbb{Z}^d$, which has with loss of generality the form $[-N, N-1]^d_{\mathbb{Z}}$, $N \in 2\mathbb{N}$, and define the process as a discrete time Markov chain (A.18). The state space is $\mathcal{E}_\infty := \prod_{i\in\mathbb{Z}^d}\{-1,0,1\}$ or $\mathcal{E}_N := \prod_{i\in[-N,N-1]^d_{\mathbb{Z}}}\{-1,0,1\}$ respectively. We denote by $s_i(t) \in \{-1,0,1\}$ the state of a site i at time t and define $S^\infty(t) := (s_i(t) : i \in \mathbb{Z}^d)$ and $S^N(t) := (s_i(t) : i \in [-N, N-1]^d_{\mathbb{Z}})$. Again, 0 means the site is inactive, 1 means the site is active and -1 that it is not existing. Recall from Section 2.1 the graph theoretic distance $\delta(i,j) := \sum_{n=1}^d |i_n - j_n|$. In the start configuration $S_0^\infty := S^\infty(0)$ or $S_0^N := S^N(0)$ as well as in every even time step, only sites $i \in \mathbb{Z}^d$, with an even number $\delta(i,0)$ and for odd time steps, only sites $i \in \mathbb{Z}^d$ with an odd number $\delta(i,0)$ exist.

For the infinite lattice $\mathbb{Z}^d$ we define $k_i^\infty(t) := |\{j \in \mathbb{Z}^d : \delta(i,j) = 1 \wedge s_j(t) = 1\}|$ as the number of active neighbours of i. It is bounded by $2d$, because for every dimension there are two possibilities to change the component i_n, $n \in \{1,...,d\}$ of i, such that the graph theoretic distance δ from i to the new vertex is 1. If the boundary conditions are chosen to be free in the finite dimensional case, such that the boundary points of $[-N, N-1]^d_{\mathbb{Z}}$ have less than $2d$ neighbours, then we define $k_i^{N,free}(t) := |\{j \in [-N, N-1]^d_{\mathbb{Z}} : \delta(i,j) = 1 \wedge s_j(t) = 1\}|$. For periodic boundary conditions, it follows that $k_i^{N,periodic}(t) := |\{j \in \mathbb{Z}^d : \delta(i,j) = 1 \wedge s_{\mathrm{mod}_{[-N,N-1]_{\mathbb{Z}}}(j,2N)}(t) = 1\}|$ describes the number of active neighbours, where modular arithmetic (B.4) was used. For directed percolation in $d+1$ dimensions, the time component can be illustrated by directed edges

$$\bar{\mathbb{E}}^d := \{e = \langle (i,t),(j,t+1)\rangle : i,j \in Z^d, t \in \mathbb{N}_0 \wedge \delta(i,j) = 1 \wedge s_i(t) \in \{0,1\}\}, \tag{3.6}$$

where $Z^d \in \{\mathbb{Z}^d, [-N, N-1]^d_{\mathbb{Z}}\}$. Again, we denote by $\bar{\mathbb{E}}^d_p \subset \bar{\mathbb{E}}^d$ the set of all open edges. Analogously to oriented bond percolation (cf. Chapter 2.1), the transition probabilities of directed percolation are defined in such a way that an edge is open with probability p. For directed percolation, the activity of a site gets transmitted through open bonds to all adjacent sites. From the geometric definition, the following transition probabilities depending on the number of active neighbours result.

Lemma 3.1. *With $p \in [0,1[$ and $k_i(t) \in \{k_i^\infty(t), k_i^{N,free}(t), k_i^{N,periodic}(t)\}$ the local transition probabilities $\mathbb{P}(s_i(t+1)|k_i(t), s_i(t))$ for directed percolation on $\mathbb{Z}^d \times \mathbb{N}_0$ or on $[-N, N-1]^d_{\mathbb{Z}} \times \mathbb{N}_0$ with either free or periodic boundary conditions are in all three cases given by*

$$\mathbb{P}(\ 1\ |0,-1) = 0, \tag{3.7}$$

$$\mathbb{P}(\ 1\ |k,-1) = \sum_{l=1}^{k} \binom{k}{l} p^l (1-p)^{k-l} \qquad \forall k \in \{1,2,...,2d\}, \tag{3.8}$$

$$\mathbb{P}(\ 0\ |k,-1) = 1 - \mathbb{P}(\ 1\ |k,-1) \qquad \forall k \in \{0,1,...,2d\}, \tag{3.9}$$

$$\mathbb{P}(-1|k,\ q\ ) = 1 \qquad \forall k \in \{0,1,...,2d\},\ \forall q \in \{0,1\}. \tag{3.10}$$

Proof. In the hypercube $\mathbb{Z}^d$ for even time steps only sites $i \in \mathbb{Z}^d$ with an even number $\delta(i,0)$ and for odd time steps, only sites $i \in \mathbb{Z}^d$ with an odd number $\delta(i,0)$ exist. Consequently, a site can only become active or inactive, if it was not existing in the time step before. If no neighbour of a site i is active, it is not possible that the site i itself becomes active in the next time step

and equation (3.7) follows. Equation (3.8) adds all probabilities that a site i becomes active, if l of the k active neighbours transmit the activity to the site i. The binomial coefficient counts the number of possibilities to choose l out of k open bonds and then becomes multiplied with the probability p^l that l bond are open and the probability p^{k-l} that the other $k-l$ bond are closed, see also Figure 3.3 for directed percolation on $1+1$ dimensions. Equation (3.9) describes the counter event of equations (3.7) and (3.8) that a non-existing site becomes inactive. Finally, each existing site at time t is inactive at time $t+1$ and so equation (3.10) follows. □

With a given random variable S_0^∞ or S_0^N and the synchronously updated local transition probabilities of Lemma 3.1 for the states $i \in \mathbb{Z}^d$ or $i \in [-N, N-1]_{\mathbb{Z}}^d$, a family of random variables $(S_t^\infty)_{t\in\mathbb{N}_0}$ or $(S_t^N)_{t\in\mathbb{N}_0}$ and so a homogeneous discrete time Markov chain (A.18) is defined.

3.2.2. The Critical Phenomenon

Analogously to Chapter 2, we write $(i,t) \to (j,t+n)$, if there exists a sequence $\pi = (i^0, i^1, ..., i^n)$, $n \geq 0$ of points $i^0, i^1, ..., i^n \in \mathbb{Z}^d$ with $\langle (i^{m-1}, t+m-1), (i^m, t+m) \rangle \in \bar{\mathbb{E}}_p^d$ for all $m \in \{1, ..., n\}$ and $i = i^0$ and $j = i^n$. The open cluster or connected component of a site i at time t is defined as

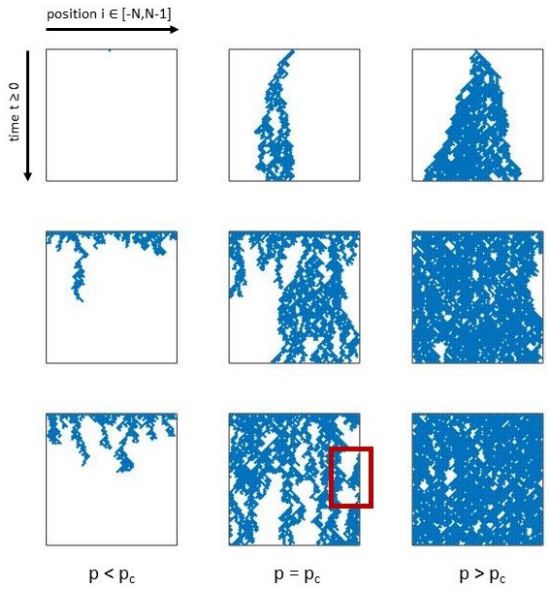
$$\bar{C}_p((i,t)) \coloneqq \{(j, t+n) \in Z^d \times \mathbb{N}_0 : (i,t) \to (j,t+n)\}, \tag{3.11}$$

with $Z^d \in \{\mathbb{Z}^d, [-N, N-1]_{\mathbb{Z}}^d\}$ and we set $\bar{C}_p \coloneqq \bar{C}_p((0,0))$. Similarly to Section 2.1, we can consider a probability space with sample space $\bar{\Omega} \coloneqq \prod_{e\in\bar{\mathbb{E}}^d}\{0,1\}$ and product probability measure $\bar{\mathbb{P}}_p \coloneqq \prod_{e\in\bar{\mathbb{E}}^d} \mathrm{Ber}_p$ and a random variable $X^p : \bar{\Omega} \to \{0,1\}$, whose projection to the e-th component describes the Bernoulli distributed state of an edge $e \in \bar{\mathbb{E}}^d$. The proof of Lemma 2.1 does not depend on the concrete definition of the lattice, so it can also be applied to directed percolation. It follows that $|\bar{C}_p((i,t))|$ is a random variable and we can define the percolation probability $\bar{\theta}(p) \coloneqq \mathbb{P}_p(|\bar{C}_p| = \infty) = \mathbb{P}_p(|\bar{C}_p((i,t))| = \infty)$ for all $i \in \mathbb{Z}^d$ or $i \in [-N, N-1]_{\mathbb{Z}}^d$ and $t \in \mathbb{N}_0$, where the last equality follows from the translation invariance of the lattice. Furthermore, it follows immediately from Proposition 2.2 that $\bar{\theta}(p)$ is a monotonically increasing function in p and we can define the probability that percolation occurs as $\bar{\psi}(p) \coloneqq \mathbb{P}_p\left(\bigcup_{(i,t)\in Z^d\times\mathbb{N}_0}\{|\bar{C}_p((i,t))| = \infty\}\right)$, where $Z^d \in \{\mathbb{Z}^d, [-N, N-1]_{\mathbb{Z}}^d\}$. Since also the proof of Proposition 2.3 is independent of the underlying lattice, it holds that $\bar{\psi}(p)$ is 0, if $\bar{\theta}(p) = 0$ and 1, if $\bar{\theta}(p) > 0$ and so we can define the critical probability $\bar{p}_c = \bar{p}_c(d+1) \coloneqq \inf\{p \in [0,1] : \bar{\theta}(p) > 0\}$. Again, two phases exist: In the subcritical phase $\bar{p} < \bar{p}_c$, all connected components are almost surely finite, and in the supercritical phase $\bar{p} > \bar{p}_c$ every site has a positive probability to be in an infinite open cluster and an infinite open cluster exists almost surely. Directed percolation is one of few processes, where even in the lowest dimension $1+1$, no exact value for the critical probability is known [15]. With the same argument like for equation (2.11) in the proof of Theorem 2.8, it follows $\bar{p}_c((d+1)+1) \leq \bar{p}_c(d+1)$ for all $d \geq 1$.

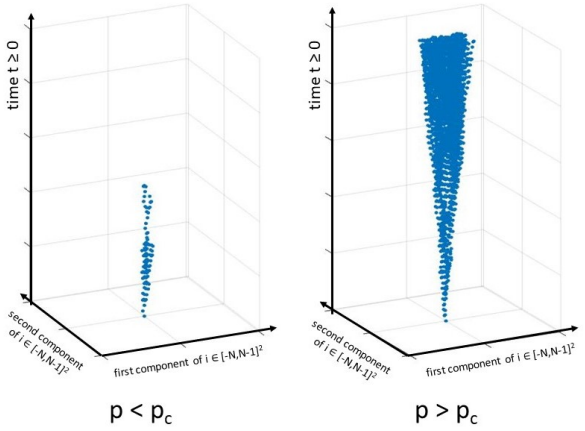
In Figure 3.4 directed percolation is simulated for finitely many sites in $1+1$ and $2+1$ dimensions with free or periodic boundary conditions, starting from a single active site at the origin, which means $S_0^\infty = (0, ..., 0, 1, 0, ..., 0)$, or a lattice, where all existing sites of the start configuration are active, which means $S_0^\infty = (1, 0, 1, ..., 0, 1, 0)$. For further numerical analysis of directed percolation see Section 4.3.

3.2.3. Equivalence of Directed and Oriented Bond Percolation

According to [15], directed percolation in $1+1$ dimensions on the infinite lattice is fully equivalent to oriented bond percolation on $\mathbb{Z}^2$. In the following Proposition 3.2 we prove this claim in the case of finitely many active sites in the start configuration S_0^∞ and argument why the critical probability has to be the same for all start configurations for directed percolation in $1+1$ dimensions.



(a) Directed percolation in $1+1$ dimensions starting from a single active site at 0 (top row) or from a lattice fully occupied with active sites first with free boundary conditions (middle row) and finally with periodic boundary conditions (bottom row). The red box marks active sites on the boundary which can only occur with periodic boundary conditions.



(b) Directed percolation in $2+1$ dimensions starting from a single active site for different values of the critical probability p_c.

Figure 3.4.: Simulations of directed percolation in $1+1$ and $2+1$ dimensions. The numerical code of directed percolation can be found in Appendix C.1.

Proposition 3.2. *Starting from finitely many active sites in S_0^∞, directed percolation in $1+1$ dimensions on the infinite lattice and oriented bond percolation on $\mathbb{Z}^2$ are fully equivalent. Furthermore, the critical probability is the same for all possible start configurations S_0^∞ for directed percolation in $1+1$ dimensions.*

Proof. First, we consider directed percolation starting from a single active site at the origin, which means $S_0^\infty = (0, ..., 0, 1, 0, ..., 0)$. The open cluster $\bar{C}_p$ of the origin is contained in the sublattice $L_1 := \{(i,t) \in \mathbb{Z}^d \times \mathbb{N}_0 : |i| \leq t\}$. For oriented bond percolation, the open cluster $\vec{C}_p$ is contained in the positive quadrant $L_2 := \{(x,y) \in \mathbb{Z}^2 : x, y \geq 0\}$. There is a one to one correspondence between the existing sites of L_1 and the vertices of L_2 via the bijective mapping l, which is illustrated in Figure 3.5:

$$l : L_1 \to L_2,\ (i,t) \mapsto \left(\frac{t-i}{2}, \frac{t+i}{2}\right), \quad l^{-1} : L_2 \to L_1,\ (x,y) \mapsto (y+x, y-x)\,. \tag{3.12}$$

Since the origin gets mapped to itself and in both cases an edge is supposed to be open with probability p, the two processes are equivalent as the open clusters $\bar{C}_p$ and $\vec{C}_p$ are built with the same rules. It follows that the critical probabilities have to be the same: $\bar{p}_c(1+1) = \vec{p}_c(2)$. Due to Theorem 2.8 it holds $\vec{p}_c(2) \leq \frac{2}{3}$ and $\bar{p}_c(1+1) = 0.644700(1) < \frac{2}{3}$ according to [16].

If there are $M < \infty$ active sites in the start configuration S_0^∞ of directed percolation, then a finite interval $[-M^*, M^*] \subset \mathbb{Z}$ exists, where all active sites are contained in, see Figure 3.5. The probability that another directed percolation process starting from a single active site at the origin, has at time M^* the same active sites like S_0^∞, is positive: For every active site i^* we can construct an open path from the origin $(0,0)$ to the vertex (i^*, M^*) without activating any other sites at time M^*, since an open path can only contain one site per time step because of the directionality of the edges. So for every $p \in (0,1)$, the probability is positive that another time-shifted directed percolation process exists, which contains from time M^* on the considered percolation process. As shown before, this time shifted directed percolation process starting from

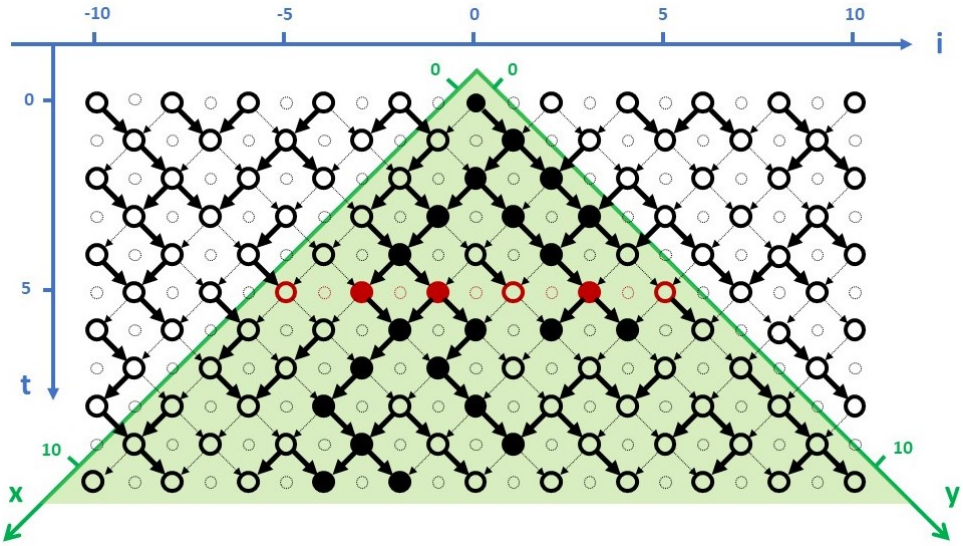


Figure 3.5.: Directed and oriented bond percolation starting from a single active site at the origin: the positive quadrant L_2 of $\mathbb{Z}^2$ is embedded onto the lattice $\mathbb{Z}\times\mathbb{N}_0$. The sublattice L_1 of $\mathbb{Z}\times\mathbb{N}_0$, which corresponds to L_2, is highlighted in green. The open cluster of the origin of directed and oriented bond percolation is given by the active sites, which are represented by filled cycles. Hollow circles denote inactive sites, dotted small circles not existing sites of directed percolation and solid (dotted) arrows open (closed) edges. The red sites represent a possible start configuration S_0^∞ with $M = 3 < \infty$ active sites, contained in the interval $[-M^*, M^*] = [-5, 5]$, embedded in L_1 at time $M^* = 5$.

a single active site at the origin is equivalent to oriented bond percolation. According to theorem 2.5, the infinite open cluster of the origin is unique for oriented bond percolation. It follows that the time-shifted percolation process has to contain all active sites at time $M^* < \infty$ if an infinite open cluster exists. These active sites correspond to the active sites of S_0^∞ and so the sites of S_0^∞ belong to an infinite open cluster if and only if the origin of the time shifted percolation process belongs to an infinite open cluster. It follows from the definition of the critical probability that it has to be the same for directed percolation in $1+1$ dimensions starting from finitely many active sites and oriented bond percolation on $\mathbb{Z}^2$.

Finally, we consider the case with infinitely many active sites in the start configuration S_0^∞. Since the function is constant, which assigns the critical probability to the size $M^* < \infty$ of the interval containing all active sites, the critical probability is also in the limit of the infinite lattice the same as in the two previous cases. Even if the critical probability is the same, we cannot specify concretely a corresponding directed percolation process starting from a single active site at the origin. □

This proof also applies to the $1+1$ dimensional Domany-Kinzel cellular automaton for $p_1, p_2 \in (0, 1)$ as no specific properties of p_1 and p_2 were used. It follows that in this case, the critical probability is also independent of the start configuration.

In higher dimensions, directed and oriented bond percolation cannot be equivalent, since the lattices would need the same dimensions: for directed percolation on $\mathbb{Z}^d \times \mathbb{N}_0 \subset \mathbb{Z}^{d+1}$, every vertex has $2d$ outgoing directed edges, but for oriented bond percolation on $\mathbb{Z}^{d+1}$, every vertex has only $d+1$ outgoing edges. The only solution of $2d = d+1$ is given by $d = 1$, where we already showed equivalence. Nevertheless, according to [10] and [23], the proofs of many (it is believed that all) results of directed percolation can be adapted to oriented bond percolation and vice versa. In particular, the two Theorems 2.5 and 2.10 of [10] hold in both cases. So also for directed percolation the infinite open cluster is unique if it exists and the percolation probability is continuous at $\bar{p}_c$: $\bar{\theta}(\bar{p}_c) = 0$. With the same arguments as in $1+1$ dimensions, it follows for directed percolation in $d+1$ dimensions,that the critical probability $\bar{p}_c$ is independent of the start configuration S_0^∞.

3.3. The Contact Process on $\mathbb{Z}^d \times \mathbb{R}_{\geq 0}$

The contact process in $d+1$ dimensions with $d \in \mathbb{N}$ can be seen as a continuous time adaption of directed percolation in $d+1$ dimensions and is believed to show the same critical behaviour as its discrete time version [23]. Since the contact process includes asynchronous updates, which occur spontaneously and independently in space and time of the other updates, it is modelled as a continuous time Markov chain (A.19). The following definition is a more detailed and probabilistic version of the model defined in [15]. Because of continuity, it is easier to analyse the contact process theoretically than directed percolation, see Section 4.2.

3.3.1. Definition of the Contact Process in $d+1$ dimensions

Analogously to directed percolation, the contact process models the evolution of states of vertices of the d-dimensional square lattice $\mathbb{Z}^d$, $d \in \mathbb{N}$ or of a d-dimensional hypercube of $\mathbb{Z}^d$, which has without loss of generality the form $[1,N]^d_{\mathbb{Z}}$, $N \in \mathbb{N}$. The state space is $\mathcal{E} := \prod_{i \in \mathbb{Z}^d} \{0,1\}$ or $\mathcal{E} := \prod_{i \in [1,N]^d_{\mathbb{Z}}} \{0,1\}$ and we denote again by $s_i(t) \in \{0,1\}$ the state of a site i at time $t \in \mathbb{R}_{\geq 0}$ and by the random variables $S^\infty(t) := (s_i(t) : i \in \mathbb{Z}^d)$ or $S^N(t) := (s_i(t) : i \in [1,N]^d_{\mathbb{Z}})$ the vector of the states of all sites i at time t. $s_i(t) = 1$ means the site i is active and $s_i(t) = 0$ that the site i is inactive at time t. The local transition rates describe the events that one active site gets inactive, or that depending on the number of active neighbours, one inactive site gets active. Therefore we define the number of active neighbours of a site $i \in \mathbb{Z}^d$ on the infinite lattice as $k_i^\infty(t) := |\{j \in \mathbb{Z}^d : \delta(i,j) = 1 \wedge s_j(t) = 1\}|$, where the graph-theoretic distance $\delta(i,j) := \sum_{n=1}^d |i_n - j_n|$ defined in Section 2.1 was used. On the finite lattice the number of active neighbours of a site $i \in [1,N]^d_{\mathbb{Z}}$ is for free boundary conditions given by $k_i^{N,free}(t) := |\{j \in [1,N]^d_{\mathbb{Z}} : \delta(i,j) = 1 \wedge s_j(t) = 1\}|$ and for periodic boundary conditions given by $k_i^{N,periodic}(t) := |\{j \in \mathbb{Z}^d : \delta(i,j) = 1 \wedge s_{\mathrm{mod}_{[1,N]_{\mathbb{Z}}}(j,N)}(t) = 1\}|$, where modular arithmetic (B.4) was used. According to Theorem A.21, a continuous time Markov chain can be defined by a random variable $S_0^\infty := S^\infty(0)$ or $S_0^N := S^N(0)$ describing the start configuration and a generator matrix Q containing the transition rates between different configurations $S^\infty(t)$ or $S^N(t)$, where the state of only one site i differs. As every site has the same transition rates, we can define the Markov Chain by stating the local transition rates without constructing the global transition rate matrix Q. For the standard contact processes the local transition rates $q(s_i(t) \to s_i(t+t'), k_i(t))$ for a site i from time t to time $t+t'$ with $t, t' \in \mathbb{R}_{\geq 0}$ with $k_i(t) \in \{k_i^\infty(t), k_i^{N,free}(t), k_i^{N,periodic}(t)\}$ are given with a parameter $\lambda \in \mathbb{R}_{\geq 0}$ by

$$\begin{aligned} q(0 \to 1, k) &= \frac{\lambda k}{2d} \qquad \forall k \in \{0,1,...,2d\}, \\ q(1 \to 0, k) &= 1 \qquad \forall k \in \{0,1,...,2d\}, \end{aligned} \tag{3.13}$$

where the number of active neighbours is analogously to directed percolation bounded by $2d$. So in the first rate, we divide by $2d$ to norm over the dimensions and obtain comparable rates for all contact processes. The local transition rates q of the $1+1$ dimensional contact process are illustrated in Figure 3.6.

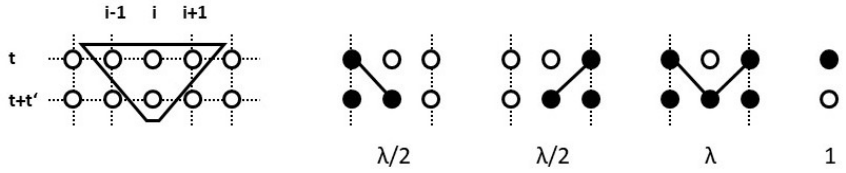


Figure 3.6.: Transition rates of the standard $1+1$ dimensional contact process. Filled (hollow) cycles denote active (inactive) sites. The state of site i changes and depends on the state of its neighbours $i-1$ and $i+1$ if it is inactive. The sites, whose states do not change are joined by dotted vertical lines.

In the graphical representation, we define for a given realisation of the contact process with parameter $\lambda \in \mathbb{R}_{\geq 0}$ the set of directed open time edges as

$$\tilde{\mathbb{T}}^d_\lambda := \Big\{ e = \big\langle (i,t),(i,t+t') \big\rangle : i \in Z^d, t, t' \in \mathbb{R}_{\geq 0} \wedge\ s_i(t) = s_i(t') = 1 \\ \wedge s_i(r) = 1\ \forall\, t < r < t' \Big\}, \tag{3.14}$$

with $Z^d \in \{\mathbb{Z}^d, [1,N]^d_{\mathbb{Z}}\}$. All the edges of $\tilde{\mathbb{T}}^d_\lambda$ are needed, because the transition can appear at every time. The set $\tilde{\mathbb{S}}^d_\lambda$ of directed open space edges, which describe the activation of neighbouring sites, is given for the infinite lattice or the finite lattice with free boundary conditions by

$$\tilde{\mathbb{S}}^d_{\lambda,\text{free}} := \Big\{ e = \big\langle (i,t),(j,t) \big\rangle : i,j \in Z^d, t \in \mathbb{R}_{\geq 0} \wedge \delta(i,j) = 1 \wedge s_i(t) = s_j(t) = 1 \\ \wedge\, \exists \epsilon' > 0 \text{ with } s_j(t-\epsilon) = 0\ \forall\, 0 < \epsilon < \epsilon' \Big\}, \tag{3.15}$$

with $Z^d \in \{\mathbb{Z}^d, [1,N]^d_{\mathbb{Z}}\}$. For the finite lattice with periodic boundary conditions it changes to

$$\tilde{\mathbb{S}}^d_{\lambda,\text{periodic}} := \Big\{ e = \big\langle (i,t),(j,t) \big\rangle : i \in [1,N]^d_{\mathbb{Z}}, j \in \mathbb{Z}^d, t \in \mathbb{R}_{\geq 0} \wedge \delta(i,j) = 1 \wedge s_i(t) = s_{j'}(t) = 1 \\ \wedge\, \exists \epsilon' > 0 \text{ with } s_{j'}(t-\epsilon) = 0\ \forall\, 0 < \epsilon < \epsilon' \Big\}, \tag{3.16}$$

with $j' = \text{mod}_{[1,N]_{\mathbb{Z}}}(j,N)$. The set $\tilde{\mathbb{E}}^d_\lambda$ of all open edges is defined as the union of these two sets:

$$\tilde{\mathbb{E}}^d_\lambda = \tilde{\mathbb{T}}^d_\lambda \cup \tilde{\mathbb{S}}^d_\lambda, \qquad \tilde{\mathbb{S}}^d_\lambda \in \{\tilde{\mathbb{S}}^d_{\lambda,\text{free}}, \tilde{\mathbb{S}}^d_{\lambda,\text{periodic}}\}. \tag{3.17}$$

A realisation of the contact process in 1+1 dimensions on a finite lattice with periodic boundary conditions is given in Figure 3.7.

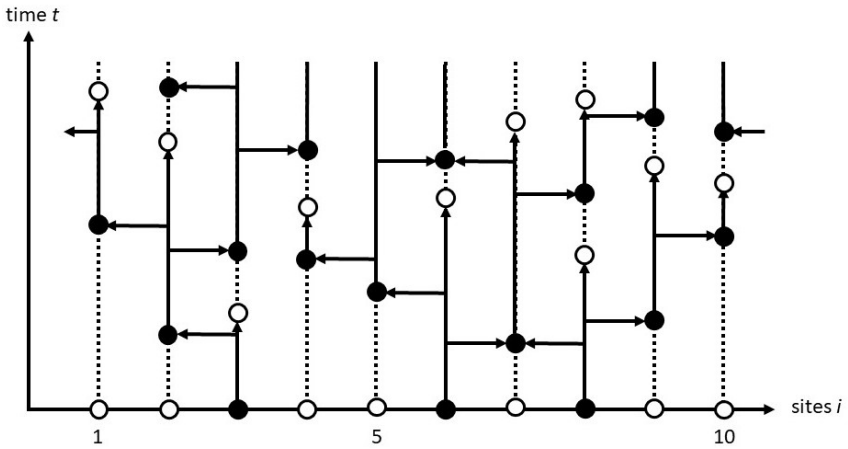


Figure 3.7.: Realisation of the contact process in $1+1$ dimensions with $N = 10$ sites and periodic boundary conditions. Filled (hollow) cycles denote active (inactive) sites and solid (dotted) lines represent open (closed) edges. The start configuration is $S_0 = (0,0,1,0,0,1,0,1,0,0)$, the time edges $\tilde{\mathbb{T}}^d_\lambda$ are vertical lines and the space edges $\tilde{\mathbb{S}}^d_\lambda$ horizontal lines.

3.3.2. Master Equation of the $1+1$ dimensional Contact Process

For the contact process in 1+1 dimensions on a finite lattice, we have the state space $\mathcal{E} = \{0,1\}^N$ with cardinality $|\mathcal{E}| = 2^N$. To order the possible states $S := (s_1, ..., s_N) \in \mathcal{E}$, we use a vector notation, which encodes each configuration S explicitly as a unit vector $u_n = (0, ..., 0, 1, 0..., 0)^T \in \mathbb{R}^{2^N}$. This vector notation is explained in Lemma B.6 in Appendix B. It follows $\mathcal{E} = \{u_n : n \in [2^N]\}$ with $[n] := \{1, 2, ..., n\}$. For every continuous time Markov chain with generator matrix $Q = (q_{mn}) \in \mathbb{R}^{|\mathcal{E}|\times|\mathcal{E}|}$, the transition probability matrix $P(t) = (p_{mn}) \in \mathbb{R}^{|\mathcal{E}|\times|\mathcal{E}|}$ is given as the solution of the forward equation

$$\partial_t P(t) = P(t)Q, \qquad P(0) = I_{|\mathcal{E}|}, \tag{3.18}$$

with identity matrix $I_{|\mathcal{E}|} \in \mathbb{R}^{|\mathcal{E}|\times|\mathcal{E}|}$ (A.21). Its mn-th entry $p_{mn}(t)$ describes the probability to get from the configuration u_m to u_n in time $t \geq 0$ and q_{mn} the rate to get from u_m to u_n for $m \neq n$. We denote by the row vector $\pi(t) \in \mathbb{R}^{1\times 2^N}$ the probability distribution of the contact process at time t. The probability to be at time t in a configuration u_n is

$$\pi_n(t) := \mathbb{P}(S(t) = u_n) = \sum_{m\in[2^N]} \mathbb{P}(S(t) = u_n | S(0) = u_m) \cdot \mathbb{P}(S(0) = u_m) = \sum_{m\in[2^N]} \pi_m(0) \cdot p_{mn}(t).$$

Consequently, the probability distribution vector $\pi(t)$ fulfils

$$\pi(t) = \pi(0)P(t). \tag{3.19}$$

Inserting equation (3.19) in the forward equation (3.18) leads to

$$\partial_t \pi(t) = \pi(0)\partial_t P(t) = \pi(0)P(t)Q = \pi(t)Q. \tag{3.20}$$

This equation describes the conservation of probability: Since $\pi(t)$ is a distribution, the sum of its components has to stay constant 1, which means that its time derivative is zero. Because in a Q-matrix (A.20) the elements of each row have to sum up to zero, it follows

$$\sum_{n\in[2^N]} \partial_t \pi_n(t) = \sum_{n\in[2^N]} \sum_{m\in[2^N]} \pi_m(t) q_{mn} = \sum_{m\in[2^N]} \pi_m(t) \sum_{n\in[2^N]} q_{mn} = 0. \tag{3.21}$$

Regarding the components of the vector equation (3.20) alone, it leads for every configuration u_n to the master equation, which describes the in- and outflow of probability:

$$\begin{aligned} \partial_t \pi_n(t) &= \sum_{m\in[2^N]} \pi_m(t) q_{mn} = \sum_{\substack{m\in[2^N] \\ m\neq n}} \pi_m(t) q_{mn} + \pi_n(t) q_{nn} \\ &= \sum_{\substack{m\in[2^N] \\ m\neq n}} \pi_m(t) q_{mn} - \sum_{\substack{m\in[2^N] \\ m\neq n}} \pi_n(t) q_{nm}, \end{aligned} \tag{3.22}$$

where we have used in the last equation the property of the Q-matrix that the elements in each row have to sum up to zero. The terms of the first sum describe the gain of the state u_n, as q_{mn} is the rate to get from the state u_m, where we are with probability $\pi_m(t)$, to the state u_n. Analogously, the terms of the second sum describe the loss of u_n. The master equation for the contact process with periodic boundary conditions can be expressed with the local transition rates of Figure 3.6, as the state of a site only changes depending on its neighbours. These rates occur for all sites i, so we have to add up over all $i \in [1, N]_{\mathbb{Z}}$ and the master equation for the contact process in $1+1$ dimensions is given by [15]

$$\begin{aligned} \partial_t \pi_{(s_1,..,s_N)}(t) = \sum_{i=1}^{N} (2s_i - 1) \Big\{ &\frac{\lambda}{2} s_{i-1} \pi_{(s_1,..,s_{i-2},1,0,s_{i+1},..,s_N)}(t) \\ &+ \frac{\lambda}{2} s_{i+1} \pi_{(s_1,..,s_{i-1},0,1,s_{i+2},..,s_N)}(t) - \pi_{(s_1,..,s_{i-1},1,s_{i+1},..,s_N)}(t) \Big\}, \end{aligned} \tag{3.23}$$

where we write $\pi_{(s_1,...,s_N)}(t)$ for the component of $\pi(t)$, which corresponds to the configuration $(s_1, ..., s_N)$. If the site i is active, $(2s_i - 1) = 1$ and the 'gain'-terms correspond to the first three illustrations of Figure 3.6 and the 'loss' term corresponds to the last illustration of Figure 3.6. If both neighbours $i-1$ and $i+1$ are active, the first and second term sum up to the term, which would represent the rate of the third illustration, so for the 'gain'-terms only two summands are needed. Due to the factors s_{i-1} and s_{i+1}, the summands only exist if the corresponding site is active and so the transition can be possible. If the site i is inactive, the roles of gain and loss replace each other. In equation (3.23) this is expressed by the term $(2s_i - 1)$, which is 1 for $s_i = 1$ and -1 for $s_i = 0$.

3.3.3. Generator Matrix Q of the $1+1$ dimensional Contact Process

In order to determine the matrix Q from the local transition probabilities q we construct, with help of the master equation, a two-site process being equivalent to the contact process in $1+1$ dimensions with periodic boundary conditions, for which an easier representation of Q exists. Since we consider periodic boundary conditions, we can carry out index transformations and still sum up the same terms. The aim is to transform the indices in such a way that only the state of the sites i and $i+1$ appear in the master equation. Additionally, the concrete state of the sites i and $i+1$ should occur in every component $\pi_{(s_1,\dots,s_N)}(t)$ of $\pi(t)$, which is part of the master equation. Therefore we transform the index of the first summand from i to $i+1$ and let the index of the second summand persist. Then, we first split the last summand in two equal parts by multiplication with $\frac{1}{2}$, make an index transformation from i to $i+1$ in the second part and then split both parts up again depending on the state of site $i+1$ in the third and fourth summand or on the the state of site i in the fifth and sixth summand of equation (3.24). We obtain:

$$\partial_t \pi_{(s_1,..,s_N)}(t) = \sum_{i=1}^{N} (2s_{i+1}-1)\frac{\lambda}{2} s_i \pi_{(s_1,..,s_{i-1},1,0,s_{i+2},..,s_N)}(t) + (2s_i-1)\frac{\lambda}{2} s_{i+1}\pi_{(s_1,..,s_{i-1},0,1,s_{i+2},..,s_N)}$$
$$(t) - (2s_i-1)\frac{1}{2}(s_{i+1}-1)\pi_{(s_1,..,s_{i-1},1,0,s_{i+2},..,s_N)}(t) - (2s_i-1)\frac{1}{2} s_{i+1}\pi_{(s_1,..,s_{i-1},1,1,s_{i+2},..,s_N)}(t) -$$
$$(2s_{i+1}-1)\frac{1}{2}(s_i-1)\pi_{(s_1,..,s_{i-1},0,1,s_{i+2},..,s_N)}(t) - (2s_{i+1}-1)\frac{1}{2} s_i \pi_{(s_1,..,s_{i-1},1,1,s_{i+2},..,s_N)}(t). \qquad (3.24)$$

From the representation of the master equation (3.24), we can read out the transition rates of the equivalent two-site process with periodic boundary conditions: the first summand is only non-zero if $s_i = 1$ and the state of site i is also 1 in the subsequent factor $\pi_{(s_1,..,s_{i-1},1,0,s_{i+2},..,s_N)}(t)$, so it has to be site $i+1$, whose state changes and the transition rate from $s_{i+1} = 1$ to $s_{i+1} = 0$ is $\frac{\lambda}{2}$. With the same procedure the other local transition rates can be obtained and they are illustrated in Figure 3.8 and correspond from left to the right to the summands of equation (3.24). Since the transitions rates including the sites N and $N+1$ only correspond to periodic boundary conditions of the two-site process, the master equation of the two site process with free boundary conditions is given by equation (3.24) when summing up from $i = 1$ to $i = N-1$.

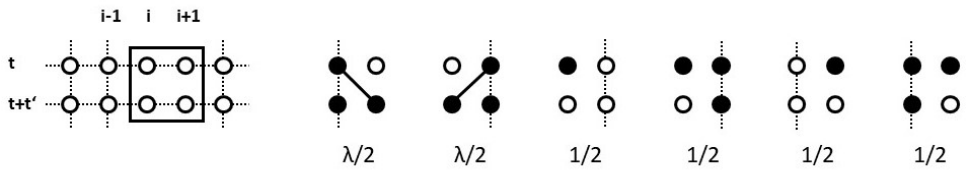


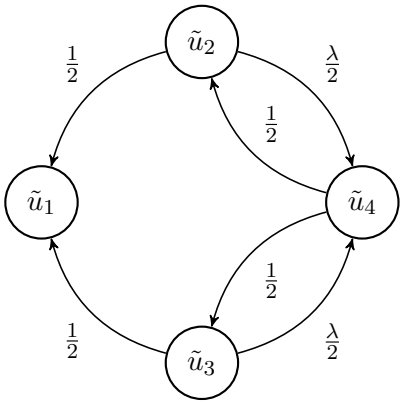
Figure 3.8.: Transition rates of the two-site process, which is equivalent to the contact process in $1+1$ dimensions (definition see text). Filled (hollow) cycles denote active (inactive) sites. The state of the site i or $i+1$ changes and depends on the state of its neighbour $i+1$ or i if it is inactive. The sites, whose states do not change from time t at time $t+t'$ are joined by dotted vertical lines.

Consider now the sublattice, which consists only of the two sites i and $i+1$. According to Corollary B.7, for given $i \in [1,N]_{\mathbb{Z}}$ we can also encode each configuration (s_i, s_{i+1}) as a unit vector in $\mathbb{R}^4$ and have the following correspondences:

$$(0,0) \leftrightarrow \tilde{u}_1 = \begin{pmatrix}1\\0\\0\\0\end{pmatrix}, \quad (0,1) \leftrightarrow \tilde{u}_2 = \begin{pmatrix}0\\1\\0\\0\end{pmatrix}, \quad (1,0) \leftrightarrow \tilde{u}_3 = \begin{pmatrix}0\\0\\1\\0\end{pmatrix}, \quad (1,1) \leftrightarrow \tilde{u}_4 = \begin{pmatrix}0\\0\\0\\1\end{pmatrix}.$$

The local transition rate diagram and the corresponding local transition rate matrix $Q_{[i,i+1]} = (\tilde{q}_{mn}) \in \mathbb{R}^{4\times 4}$ of the two site process, which are obtained from the local transition rates of Figure

3.8, are given in Figure 3.9. Its mn-th entry corresponds to the rate to get from state $\tilde{u}_m$ to the state $\tilde{u}_n$. Between different states without a given rate, we insert a 0 into the matrix. As we want that also the matrix $Q_{[i,i+1]}$ is a Q-matrix (A.20), the entries of every row have to sum up to 0, and we set the entries on the diagonal to $\tilde{q}_{mm} = -\sum_{n\in[4]\setminus\{m\}} \tilde{q}_{mn}$.



$$Q_{[i,i+1]} = \begin{pmatrix} 0 & 0 & 0 & 0 \\ \frac{1}{2} & -\frac{1+\lambda}{2} & 0 & \frac{\lambda}{2} \\ \frac{1}{2} & 0 & -\frac{1+\lambda}{2} & \frac{\lambda}{2} \\ 0 & \frac{1}{2} & \frac{1}{2} & -1 \end{pmatrix}$$

Figure 3.9.: Local transition rate diagram and corresponding local transition matrix of the to the contact process equivalent two-site process

Out of the local transition rate matrices, we can construct Q-matrices $Q_i \in \mathbb{R}^{2^N\times 2^N}$ for $i \in [1, N-1]_{\mathbb{Z}}$ and in the case of periodic boundary conditions a Q-matrix $Q^* \in \mathbb{R}^{2^N\times 2^N}$ for $i = N$, see Lemma B.8 and Proposition B.9 in Appendix B. The global Q-matrices Q_i, $i \in [1, N-1]_{\mathbb{Z}}$ and Q^* contain the same information as local transition matrices $Q_{[i,i+1]}$, $i \in [1, N]_{\mathbb{Z}}$ and describe the transitions between the different global configurations u_m, $m \in [2^N]$. The matrix Q of the whole contact process has to describe the transition rates between all possible configurations of the two-site system at once, so we have to add all the matrices Q_i, $i \in [1, N]_{\mathbb{Z}}$ to obtain the matrix Q^{free} in the case of free boundary conditions:

$$Q^{\text{free}} = \left(\sum_{i=1}^{N-1} Q_i\right) = \left(\sum_{i=1}^{N-1} I_{2^{i-1}} \otimes Q_{[i,i+1]} \otimes I_{2^{N-1-i}}\right). \tag{3.25}$$

In the case of periodic boundary conditions, we have to add additionally the matrix Q^* to obtain the matrix Q^{periodic}:

$$Q^{\text{periodic}} = \left(\sum_{i=1}^{N-1} Q_i\right) + Q^* = \left(\sum_{i=1}^{N-1} I_{2^{i-1}} \otimes Q_{[i,i+1]} \otimes I_{2^{N-1-i}}\right) + Q^*. \tag{3.26}$$

3.3.4. The Critical Phenomenon

To define an open cluster of the contact process analogously to bond percolation (cf. equation (2.4)) or directed percolation (cf. equation (3.11)), we write $(i,t) \to (j,t+t')$, if there exists a sequence $\pi = \big((i^0,t^0),(i^0,t^1),(i^1,t^1),(i^1,t^2),...,(i^n,t^{n+1})\big)$, $n \geq 0$ of points $(i^l,t^m) \in Z^d \times \mathbb{R}$ with $Z^d \in \{\mathbb{Z}^d, [1,N]^d_{\mathbb{Z}}\}$ and $l,m \in \mathbb{N}_0$ with $\langle(i^{k-1},t^{k-1}),(i^{k-1},t^k)\rangle \in \tilde{\mathbb{T}}^d_\lambda$ for all $k \in [n+1]$ and $\langle(i^{k-1},t^k),(i^k,t^k)\rangle \in \tilde{\mathbb{S}}^d_\lambda \in \{\tilde{\mathbb{S}}^d_{\lambda,\text{free}}, \tilde{\mathbb{S}}^d_{\lambda,\text{periodic}}\}$ for all $k \in [n]$ and $(i,t) = (i^0,t^0)$ and $(j,t+t') = (i^n,t^{n+1})$ [9]. Here the open directed time and space edges introduced in equations (3.14) to (3.16) are used. The open cluster or connected component of a site i at time t is defined as

$$\tilde{C}_\lambda((i,t)) \coloneqq \{(j,t+t') \in Z^d \times \mathbb{R}_{\geq 0} : (i,t) \to (j,t+t') \wedge t' \in \mathbb{R}_{\geq 0}\}, \tag{3.27}$$

with $Z^d \in \{\mathbb{Z}^d, [1,N]^d_{\mathbb{Z}}\}$ and we set $\tilde{C}_\lambda \coloneqq \tilde{C}_\lambda((0,0))$. Even though it is possible to define the open cluster analogously to bond percolation and directed percolation, we cannot define the percolation probability as the probability that the cardinality of the open cluster is infinity. This

is the case, because the time axis is now continuous and so $|\tilde{C}_\lambda| = \infty$ always except the case, where all active sites of the start configuration get inactive at time 0.

An equivalent expression to the infinite open cluster is obtained as follows: if we start at a single active site (whose exact position does not matter because of the translation invariance of the lattice as we have periodic boundary conditions) and look at the probability that this site is contained in an open infinite cluster, we can also look at the probability that the number of active sites does not become zero for all $t \in \mathbb{R}_{\geq 0}$. These two approaches are equivalent, because otherwise the contact process would reach the absorbing state: if all sites are inactive, it is impossible to leave this state [9], [21].

We denote by $\mathbb{P}_\lambda$ the appropriate probability measure for the contact process. According to [9], the following duality relation for the contact process holds:

Theorem 3.3 [9]. *For $A, B \subset [1,N]^d_{\mathbb{Z}}$, $d \geq 1$ with periodic boundary conditions or $A, B \in \mathbb{Z}^d$, $d \geq 1$, we have*

$$\begin{aligned}&\mathbb{P}_\lambda(\{i : s_i(t) = 1 \wedge s_j(0) = 1 \; \forall j \in A\} \cap \{j : j \in B\} \neq \emptyset)\\ &= \mathbb{P}_\lambda(\{i : s_i(t) = 1 \wedge s_j(0) = 1 \; \forall j \in B\} \cap \{j : j \in A\} \neq \emptyset).\end{aligned}$$

Proof. The event on the left hand side of the equality is the union over all events that $(a,0) \to (b,t)$ for $a \in A$ and $b \in B$. By reversing the direction of the time axis and the direction of all open edges contained in $\tilde{\mathbb{E}}^d_\lambda$, we obtain the event on the right hand side of the equality. As we have not changed the open edges, the probability stays the same. □

Because of the translation invariance of the infinite and the finite lattice with periodic boundary conditions for arbitrary $x \in Z^d \in \{\mathbb{Z}^d, [1,N]^d_{\mathbb{Z}}\}$, the percolation probability is given by

$$\begin{aligned}\tilde{\theta}(\lambda) &\coloneqq \lim_{t\to\infty} \mathbb{P}_\lambda(\{i : s_i(t) = 1 \wedge s_x(0) = 1\} \neq \emptyset)\\ &= \lim_{t\to\infty} \mathbb{P}_\lambda(\{i : s_i(t) = 1 \wedge s_x(0) = 1\} \cap Z^d \neq \emptyset)\\ &= \lim_{t\to\infty} \mathbb{P}_\lambda(\{i : s_i(t) = 1 \wedge s_j(0) = 1 \; \forall j \in Z^d\} \cap \{x\} \neq \emptyset)\\ &= \lim_{t\to\infty} \mathbb{P}_\lambda(s_x(t) = 1 \wedge s_j(0) = 1 \; \forall j \in Z^d),\end{aligned} \tag{3.28}$$

where Theorem 3.3 was applied in the third line. To simplify the expression in equation (3.28), we introduce the upper invariant measure as the limit of the probability distribution $\pi^*(t)$, when starting from all sites active, such that $\pi^*(0)$ is one at the component belonging to $S_0^N = (1,1,...,1)$ or $S_0^\infty = (...,1,1,...)$ and zero at all other components. It is given by [9], [21]

$$\mu_\lambda \coloneqq \lim_{t\to\infty} \pi^*(t) = \lim_{t\to\infty} \pi^*(0)P(t), \tag{3.29}$$

where $P(t)$ is the transition probability matrix of the Markov chain, defined in (A.21). With Measure Theory arguments it can be shown that the limit exists and so μ_λ is well defined [9], [21]. μ_λ is called upper invariant measure, as the configuration $S_0^N = (1,1,...,1)$ or $S_0^\infty = (...,1,1,...)$ and so also the invariant measure dominates the distributions of processes starting with at least one active site and it is an invariant measure (A.22), because

$$\mu_\lambda P(s) = \lim_{t\to\infty} \pi^*(0)P(t)P(s) = \lim_{t\to\infty} \pi^*(0)P(t+s) = \lim_{(t+s)\to\infty} \pi^*(0)P(t+s) = \mu_\lambda \quad \forall s \in \mathbb{R}_{\geq 0},$$

which follows from equation (3.29) and the semigroup property of the Markov chain (A.21). As $\mathbb{P}_\lambda(s_x(t) = 1 \wedge s_j(0) = 1 \; \forall j \in Z^d)$ converges for $t \to \infty$ for every $x \in Z^d \in \{\mathbb{Z}^d, [1,N]^d_{\mathbb{Z}}\}$ to $\mu_\lambda\{S : s_x = 1\}$ [9], we can also define the percolation probability as

$$\tilde{\theta}(\lambda) = \mu_\lambda\{S : s_x = 1\}, \tag{3.30}$$

with arbitrary $x \in Z^d \in \{\mathbb{Z}^d, [1,N]_{\mathbb{Z}}^d\}$. Analogously to Proposition 2.2 it follows with probabilistic coupling that also $\tilde{\theta}(\lambda)$ is a monotonically increasing function in λ [21]. So we can define the critical probability

$$\lambda_c = \lambda_c(d+1) \coloneqq \inf\{\lambda \in \mathbb{R}_{\geq 0} : \tilde{\theta}(\lambda) > 0\}.$$

Again, there exist two phases: In the subcritical phase $\lambda < \lambda_c$, the number of active sites per time step is almost surely zero for $t \geq T$, $T \in \mathbb{R}_{\geq}0$ and in the supercritical phase $\lambda > \lambda_c$ the probability is positive that the number of active sites per time step is greater than zero for all $t \in \mathbb{R}_{\geq 0}$. For the critical probability of the contact process on the infinite lattice, which is defined with the transition rates of equation (3.13) on the lattice $\mathbb{Z}^d \times \mathbb{R}$, the following estimate is valid:

Theorem 3.4 [21]. *For $d \geq 1$, we have $0 < \frac{2}{2d-1} \leq \lambda_c(d+1) \leq \frac{4}{d} < \infty$.*

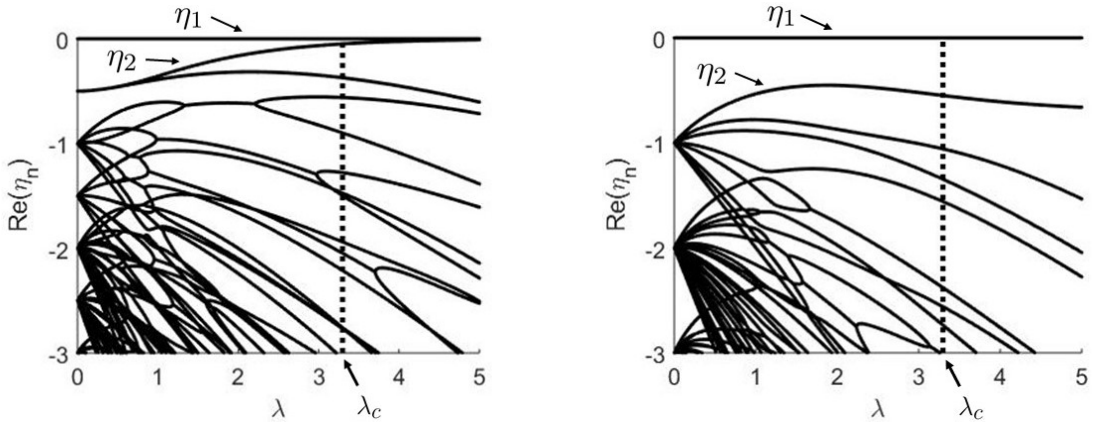
In $1+1$ dimensions, the critical value of the contact process can be approximated by $\lambda_c \simeq 3.29785(8)$ [15]. Analogously to oriented and directed percolation, also the contact process on the infinite lattice has a continuous percolation probability at the critical rate λ_c:

Theorem 3.5 [2]. *For $d \geq 1$ it holds $\tilde{\theta}(\lambda_c) = 0$.*

In the case of a finite lattice, there is always a positive probability to die out, so the percolation probability $\tilde{\theta}$ is zero for all values of λ [15]. In $1+1$ dimension this can also be seen via the eigenvalues η_n, $n \in [2^N]$ of the Q-matrices Q^{free} and Q^{periodic} (cf. equations (3.25) and (3.26)). They are shown in Figure 3.10 and defined as the solutions of the equation

$$\pi Q = \eta \pi, \tag{3.31}$$

with $\pi \in \mathbb{R}^{1\times 2^N}$. According to equation (3.20) it holds $\partial_t \pi(t) = \pi(t)Q$, so for all stationary distributions with $\partial_t \pi(t) = 0$, zero has to be an eigenvalue. In both Figures 3.10(a) and 3.10(b), 0 is an eigenvalue and corresponds to the eigenvector $u_1 = (1, 0, ..., 0) \in \mathbb{R}^{1\times 2^N}$, which represents the absorbing state of the empty lattice. The second eigenvalue corresponds to the active state of the contact process [15]. For the infinite lattice, the second eigenvalue η_2 vanishes at $\lambda = \lambda_c$, for the finite lattice we have $\eta_2 < 0$ for all values of λ, which corresponds to the fact that for finite lattices, there is always a positive probability to die out. All other eigenvalues converge to $-\infty$ as λ converges to ∞, which corresponds to the fact that in higher dimensions, the stationary solutions are reached faster. The differences of the behaviour of the eigenvalues in Figures 3.10(a) and 3.10(b) originate from the matrix Q^*, which has a different structure than the matrices Q_i, $i \in [1,N]_{\mathbb{Z}}$.



(a) Eigenvalues of Q^{free} for $N = 8$.

(b) Eigenvalues of Q^{periodic} for $N = 8$.

Figure 3.10.: Numerical diagonalization of the Q-matrices of the $1+1$ dimensional contact process with $N = 8$ sites for free and periodic boundary conditions.

4. Critical Exponents of Dynamic Percolation

In Chapters 2 and 3 percolation models and the critical phenomenon were analysed. For dynamic percolation processes it was shown that depending on the probability parameter, the process is either in the subcritical phase, where the absorbing state is reached, or in the supercritical phase, where an infinite open cluster almost surely exists. Furthermore, it was stated for directed percolation and the contact process that the percolation probability vanishes at the critical probability. However, we want to know how the system behaves near the critical probability.

Phase transitions also appear in equilibrium statistical physics, where universal scaling laws are used to describe the critical behaviour. Percolation processes are non-equilibrium processes, as they describe the time evolution of a system. They have a more complex dynamical behaviour than the equilibrium systems and the understanding is still at its beginning. To classify the phase transitions of percolation systems, we introduce in Section 4.1 a phenomenological scaling theory similar to the one of statistical physics. The occurring critical exponents describe the behaviour of the systems near the critical probability [15].

Depending on the critical behaviour, models can be divided in universality classes, the one including directed percolation is called directed percolation (DP) universality class. It is believed that different systems belonging to the same universality class are scaling invariant: this means the critical exponents and scaling functions, which describe probabilistic properties of the system, are the same for all models in the same universality class. The critical exponents only depend on the dimension, but not on the specific lattice and the microscopic interaction rules of the model. It is suspected that a model is part of the DP universality class, if the phase transition from the unique absorbing state to the fluctuating steady state is continuous, the update rules include only short-range processes such as nearest-neighbours reaction-diffusion schemes, there are no additional symmetries, the transition is characterized by finitely many positive probability transition parameters and no further random components are used. This classification is not proven rigorously, but numerical experiments support the conjecture. There is strong numerical evidence that the contact process in $d+1$ dimensions (cf. Section 3.3) and the Domany-Kinzel automaton for $p_2 \neq 1$ (cf. Section 3.1) belong to the DP universality class [15], [17].

Discrete systems like directed percolation can be implemented efficiently on parallel computers. They are analysed numerically by a Monte Carlo method in Section 4.3. Because of continuity, the contact process is easier to analyse theoretically. This will be done in Section 4.2 with a mean-field approximation [15].

4.1. Phenomenological Scaling Theory

The scaling theory introduced in this chapter follows [15]. The phenomena are shown in the case of directed percolation (cf. Section 3.2), but can be applied analogously to all percolation processes. The critical probability is in the following for all spreading processes denoted by p_c and the percolation probability by $\theta(p)$.

4.1.1. The Critical Exponents β, β', $\nu_\perp$, $\nu_\parallel$ and the Dynamic Exponent z

An order parameter, which characterises the behaviour of a spreading process, is given by the ensemble average $\rho(t)$ of the density of active sites at time t. It averages the particle density over all possible configurations S the process can be in at time t, when it started from a fixed state, weighted with their probability respectively. We denote it for a spreading process starting

from a finite number of active sites on a finite lattice by

$$\rho(t) = \sum_{S \in \mathcal{E}} \mathbb{P}(S(t) = S) \cdot \frac{1}{n} \sum_j s_j(t)_{[S(t)=S]}, \tag{4.1}$$

where n is the number of sites on the spatial lattice and $\mathcal{E}$ the underlying state space. For spreading processes starting from an infinite number of active sites on an infinite lattice, the particle density is defined as the limit $n \to \infty$ of a series of finite sublattices with n particles. For a spreading process starting from finitely many active sites on an infinite lattice, we set the number n of sites in each time step to be the maximal distance between the most left and the most right possible active site. If directed percolation in $1+1$ dimensions starts with a single active site at the origin, the open cluster at time t can reach all sites i with $-t \leq i \leq t$ and we obtain a maximal distance cone, see Figure 4.1(b) in orange.

Starting from a fully occupied lattice in the active phase, $\rho(t)$ decays and evens out at a stationary density ρ^{stat}. In the inactive phase ($p < p_c$), no infinite open cluster exists and $\rho(t) = 0$ for $t > T$ with an appropriate $T \in \mathbb{N}$. Since oriented and directed percolation are equivalent (cf. Subsection 3.2.3), the percolation probability $\theta(p_c)$ at the critical probability p_c is zero for an infinite lattice according to Theorem 2.10. Consequently, the density of active sites vanishes for $p = p_c$. For $p > p_c$, numerical experiments show that ρ^{stat} varies continuously with the difference $\Delta \coloneqq p - p_c$ and behaves near the phase transition as

$$\rho^{\text{stat}} \sim \Delta^{\beta}, \qquad p > p_c, \tag{4.2}$$

with the critical exponent $\beta > 0$.

The survival probability $P(t)$ is a similar order parameter like the density of active sites $\rho(t)$. It is defined as the probability that the cluster generated by a single active site still exists after t time steps. The limit value $P_\infty \coloneqq \lim_{t\to\infty} P(t)$ is the percolation probability $\theta(p)$ that the open cluster grown from a single active site is infinitely large. The critical exponent $\beta' > 0$ describes the behaviour of the percolation probability near the phase transition and is given by

$$P_\infty = \theta(p) \sim \Delta^{\beta'}, \qquad p > p_c. \tag{4.3}$$

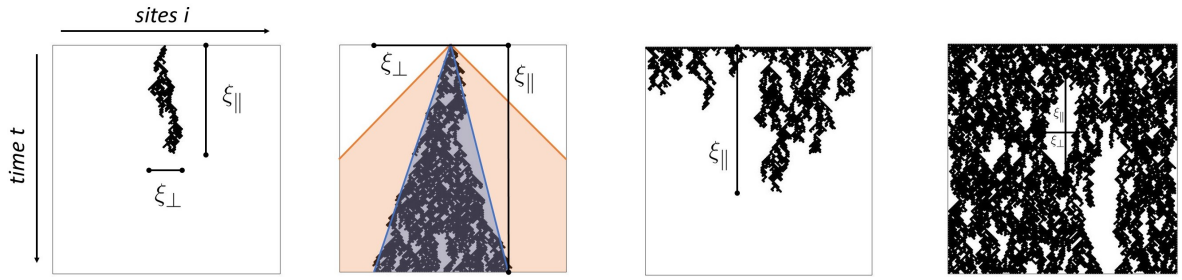
The proof of the duality relation in Theorem 3.3, can analogously be applied to the graphical representation of directed percolation and is proven rigorously in [7]. It follows for the percolation probability $\theta(p)$ that $\theta(p) = \rho^{\text{stat}}$. Consequently $\beta = \beta'$, which has to be valid for all models belonging to the DP universality class. There are many other non-equilibrium processes with multiple absorbing states or fluctuations, which do not belong to the DP universality class, for which $\beta \neq \beta'$.

Spreading processes evolve in time, so in contrast to models of equilibrium statistical physics, they can additionally be characterized by two independent correlation lengths corresponding to space and time. The spatial length scale $\xi_\perp$ is defined for $p < p_c$ as the maximal width of active sites averaged over all spatial dimensions and all possible realisations of the process when starting from a single active site. The temporal length scale $\xi_\parallel$ is analogously defined for $p < p_c$ as the mean time of survival, when starting from a single active site. In Figure 4.1(a), both correlation lengths are shown for directed percolation in $1+1$ dimensions. Near the critical probability, these length scales are supposed to diverge as

$$\xi_\perp \sim |\Delta|^{-\nu_\perp}, \qquad \xi_\parallel \sim |\Delta|^{-\nu_\parallel}, \tag{4.4}$$

with the two critical exponents $\nu_\perp, \nu_\parallel > 0$. Out of these two critical exponents, the dynamic exponent z is defined as $z = \nu_\parallel / \nu_\perp$, such that the two correlation lengths are linked by $\xi_\parallel \sim \xi_\perp^z$. It describes the relation of the spatial and the temporal scale depending on the probability and is in that way connected to the shape of the droplet in Figure 4.1(a).

Above the critical probability p_c, the active sites of directed percolation starting from a single active site form approximately a cone. For directed percolation in $1+1$ dimensions, the approximation cone is shown in Figure 4.1(b) in blue. Analogously to the subcritical phase, the term



(a) Extenison of the droplet, when starting from a single active site with $p < p_c$.

(b) Approximation cone in blue and maximal width cone in orange, when starting from a single active site with $p > p_c$.

(c) Mean survival time, when starting from a fully occupied lattice with $p < p_c$

(d) Mean extension of inactive islands, when starting from a fully occupied lattice with $p > p_c$

Figure 4.1.: Interpretation of the correlation lengths $\xi_\perp$ and $\xi_\parallel$ of directed percolation in $1+1$ dimensions. The numerical code of directed percolation can be found in Appendix C.1.

$\xi_\perp/\xi_\parallel$ describes the ratio of spatial and temporal expansion, which is connected to the opening angle of the approximation cone via trigonometric relations. Starting from a fully occupied lattice, the temporal length scale $\xi_\parallel$ describes in the subcritical phase again the mean survival time (Figure 4.1(c)). In the supercritical phase, the two correlation lengths represent the average extensions of inactive islands (Figure 4.1(d)).

For general spreading processes, the four defined exponents β, β', $\nu_\perp$ and $\nu_\parallel$ describe the phase transition into absorbing states. As $\beta = \beta'$ for processes belonging to the DP universality class, the triplet $(\beta, \nu_\perp, \nu_\parallel)$ is the fundamental set of critical exponents, all other exponents like the dynamic exponent z are related to these three.

4.1.2. Universal Scaling Functions and the Hyperscaling Relation

In Subsection 4.1.1 the critical exponent β was introduced depending on the stationary density of active sites. To describe the time evolution of quantities like the particle density $\rho(t)$, universal scaling functions are used. They are called universal, as they have the same form for all models in the same universality class. Furthermore, scaling functions only depend on scale-invariant combinations, which are obtained as outlined below.

We consider a spreading process in the supercritical phase $p > p_c$ and denote by $i \in \mathbb{Z}^d$ the position of a site. The spreading process should be invariant under the dilatation $i \to \Lambda i$, $\Lambda \in \mathbb{N}$, if the time t and the deviation from criticality $|\Delta| = \Delta = p - p_c$ become also rescaled. The spatial correlation length is proportional to the position i of a site and the temporal correlation length is proportional to the time t, hence $t \sim \xi_\parallel \sim \xi_\perp^z \sim i^z$. With the proportionality of equation (4.4) we obtain

$$i \;\to\; \Lambda i, \tag{4.5}$$

$$t \sim i^z \;\to\; \Lambda^z i^z \sim \Lambda^z t, \tag{4.6}$$

$$\Delta \sim \xi_\perp^{-1/\nu_\perp} \sim i^{-1/\nu_\perp} \;\to\; \Lambda^{-1/\nu_\perp} i^{-1/\nu_\perp} \sim \Lambda^{-1/\nu_\perp} \xi_\perp^{-1/\nu_\perp} \sim \Lambda^{-1/\nu_\perp} \Delta. \tag{4.7}$$

Out of these relations we can construct scale-invariant combinations, which do not change under the dilatation $i \to \Lambda i$. The general product $i^a \cdot t^b \cdot \Delta^c$ with $a, b, c \in \mathbb{R}$ transforms as

$$i^a \cdot t^b \cdot \Delta^c \;\to\; \Lambda^a i^a \cdot (\Lambda^z)^b t^b \cdot (\Lambda^{-1/\nu_\perp})^c \Delta^c = \Lambda^{a+zb-c/\nu_\perp} \cdot i^a \cdot t^b \cdot \Delta^c.$$

If and only if $a + zb - c/\nu_\perp = 0$, the general product $i^a \cdot t^b \cdot \Delta^c$ does not change under the dilatation $i \to \Lambda i$. It follows that for example the combinations $\Delta t^{1/\nu_\parallel}$ with $a = 0$, $b = 1/\nu_\parallel = 1/(z\nu_\perp)$, $c = 1$ and $i/t^{1/z}$ with $a = 1$, $b = -1/z$, $c = 0$ are scale-invariant. For spreading processes on a finite lattice, denote by M the number of existing particles in each time step. A further scale-invariant composition is given by $\xi_\perp^d/M \sim \xi_\parallel^{d/z}/M \sim t^{d/z}/M$, as the spatial correlation

length is proportional to the position of a site i and the number of sites grows exponentially with the dimension.

Starting from a fully occupied (fo) lattice in the active phase, numerical simulations show that the particle density $\rho_{\mathrm{fo}}(t)$ first decays exponentially and then saturates at the stationary density. The survival probability $P(t)$ also first decays exponentially and then evens out at a constant value. The scaling forms for a finite lattice are given by

$$\rho_{\mathrm{fo}}(t) \sim t^{-\alpha} f(\Delta t^{1/\nu_\parallel}, t^{d/z}/M), \qquad P(t) \sim t^{-\delta} g(\Delta t^{1/\nu_\parallel}, t^{d/z}/M), \tag{4.8}$$

where f and g are universal scaling functions and $\alpha, \delta > 0$ critical exponents. On an infinite lattice, f and g each not depend on their second argument in equation (4.8) respectively. The functions f and g have the property that they are constant for small arguments and scale for large arguments so that, regarding each argument alone, the time dependency is omitted. This is shown afterwards in equations (4.13) and (4.14).

$$f(x,y) \sim 1, \qquad g(x,y) \sim 1 \qquad ((x,y) \to (0,0)), \tag{4.9}$$
$$f(x,y) \sim x^{\alpha\nu_\parallel}, \qquad g(x,y) \sim x^{\delta\nu_\parallel} \qquad (x \to \infty), \tag{4.10}$$
$$f(x,y) \sim y^{\alpha z/d}, \qquad g(x,y) \sim y^{\delta z/d} \qquad (y \to \infty). \tag{4.11}$$

With these properties, for small arguments the exponential decay is represented and for large arguments the steady state of the particle density and the survival property are modelled. Inserting equations (4.9) to (4.11) into equation (4.8) leads in each case to

$$\rho_{\mathrm{fo}}(t) \sim t^{-\alpha}, \qquad P(t) \sim t^{-\delta} \qquad (t \to 0), \tag{4.12}$$
$$\rho_{\mathrm{fo}}(t) \sim t^{-\alpha}(\Delta t^{1/\nu_\parallel})^{\alpha\nu_\parallel} \sim \Delta^{\alpha\nu_\parallel}, \qquad P(t) \sim t^{-\delta}(\Delta t^{1/\nu_\parallel})^{\delta\nu_\parallel} \sim \Delta^{\delta\nu_\parallel} \qquad (t \to \infty), \tag{4.13}$$
$$\rho_{\mathrm{fo}}(t) \sim t^{-\alpha}(t^{d/z}/M)^{\alpha z/d} \sim M^{-\alpha z/d}, \qquad P(t) \sim t^{-\delta}(t^{d/z}/M)^{\delta z/d} \sim M^{-\delta z/d} \qquad (t \to \infty). \tag{4.14}$$

Comparison of equations (4.2) and (4.3) with equation (4.13) leads to $\beta = \alpha\nu_\parallel$ and $\beta' = \delta\nu_\parallel$. For models belonging to the DP universality class we conclude $\alpha = \delta$ from $\beta = \beta'$.

Starting from a single active site (sa), the particle density first grows exponentially as

$$\rho_{\mathrm{sa}}(t) = t^{\mu} \quad (t \to 0), \tag{4.15}$$

where μ is the critical initial slip exponent. After this critical initial slip of the spreading process, the density of active sites decays exponentially and in the case of an active phase, it saturates at the stationary density.

A further possibility to characterize spreading processes is the pair connectedness function $c(i', t', i, t)$. It is the probability that an open path from the site i' at time t' to the site i at time $t > t'$ exists. For translation invariant models like directed percolation, we can define $c(i - i', t - t') \coloneqq c(i', t', i, t)$. Starting from a single active site at the origin, the pair connectedness function $c(i, t)$ is supposed to scale as

$$c(i,t) \sim t^{\mu - d/z} F(i/t^{1/z}, \Delta t^{1/\nu_\parallel}), \tag{4.16}$$

where d is the spatial dimension, z the dynamic exponent and μ the initial slip exponent of the spreading process. F is a universal scaling function with the additional property that

$$F(0,x) \sim x^{(d/z-\mu)\nu_\parallel} \quad (x \to \infty), \tag{4.17}$$

so that the pair connectedness function of the origin $c(0, t)$ saturates in the active phase for $t \to \infty$ at a constant value with the scaling behaviour

$$c(0,\infty) \sim \lim_{t\to\infty} t^{\mu-d/z} F(0, \Delta t^{1/\nu_\parallel}) \sim t^{\mu-d/z} (\Delta t^{1/\nu_\parallel})^{(d/z-\mu)\nu_\parallel} \sim \Delta^{(d/z-\theta)\nu_\parallel}. \tag{4.18}$$

On the other hand, the probability $c(0,\infty)$ that an open path between the site 0 at time 0 to itself at an infinite large time exists, can be expressed by other probabilities: $c(0,\infty)$ has to be proportional to the percolation probability $\theta(p)$ that an infinite open cluster containing the site 0 exists. Furthermore, the probability that the site 0 is active, can be approximated by the stationary density of active sites ρ^{stat} if we assume that the active sites are distributed uniformly in the maximal distance cone. If follows that $c(0,\infty)$ scales as

$$c(0,\infty) \sim \theta(p) \cdot \rho^{\text{stat}} \sim \Delta^{\beta}\Delta^{\beta'} = \Delta^{\beta+\beta'}. \tag{4.19}$$

Comparing equations (4.18) and (4.19), the generalized hyperscaling relation for processes with phase transitions into absorbing states is obtained:

$$\left(\frac{d}{z} - \mu\right)\nu_{\parallel} = \beta + \beta' \quad \Rightarrow \quad \mu = \frac{d}{z} - \frac{\beta+\beta'}{\nu_{\parallel}} = \frac{d\nu_{\perp} - (\beta+\beta')}{\nu_{\parallel}}, \tag{4.20}$$

where the last equation follows from $z = \nu_{\parallel}/\nu_{\perp}$. For the DP universality class, equation (4.20) can be simplified with $\beta = \beta'$ and is then called hyperscaling relation. Numerical experiments show that the generalized hyperscaling relation is only valid below a upper critical dimension d_c. For $d < d_c$, the cluster of active sites surrounds the site 0, and the assumption of uniformly distributed active sites over the maximal distance cone is reasonable. Above the upper critical dimension, the approximation cone (cf. Figure 4.6(b)) can diffuse to one side, such that the site 0 is not contained inside the approximation cone for all $t > T$ with an appropriate $T \in \mathbb{N}$, hence $c(0,\infty) = 0$. For the DP universality class the upper critical dimension is $d_c = 4$ [15].

4.2. Mean-Field Approximation of the Contact Process

There are several possibilities to approximate the critical exponents of the contact process, like series expansions, field theoretic approximations and the analysis of the scaling behaviour of the eigenvalues of the contact process, which were shown in Subsection 3.3.3. [15]. Here we will approximate the critical exponents of the contact process by the analysis of the mean-field rate equation, as these estimates are accurate in comparison with other methods and become exact above the upper critical dimension $d_c = 4$ [15]. Therefore we consider again the ensemble average of the density of active sites at time t (cf. equation (4.1)). In the special case of the $1+1$ dimensional contact process on the finite lattice $[1,N]_{\mathbb{Z}} \times \mathbb{R}$ with start configuration S_0, we can explicitly specify the particle density. It is given by

$$\rho(t) = \sum_{n=1}^{2^N} \mathbb{P}(S(t) = u_n) \cdot \frac{1}{N}\sum_{n=1}^{N} s_i(t)_{[S(t)=u_n]} = \sum_{n=1}^{2^N} (\pi(0)P(t))_n \cdot \frac{1}{N}\sum_{n=1}^{N} s_i(t)_{[S(t)=u_n]}, \tag{4.21}$$

where $S(t) = (s_1(t), ..., s_N(t))$ is the random variable describing the configuration at time t (cf. Subsection 3.1.1), which can be encoded as a unit vector in $\mathbb{R}^{2^N}$ (cf. Lemma (B.6)). We sum up over all possible configurations u_n, $n \in [2^N]$ and multiply the probability that the contact process is in the configuration u_n at time t, with the fraction of active sites of the configuration u_n. The probability $\mathbb{P}(S(t) = u_n)$ can be calculated by the probability distribution $\pi(0)$ of the start configuration and the probability matrix $P(t)$ of the Markov chain (cf. equation (3.19)).

The mean-field rate equation approximates the derivation of the density of active sites under the assumption that each site is active at time t with probability $\rho(t)$. It follows that the mean-field approximation becomes exact in infinitely many dimensions, when all sites are neighboured [15]. In higher dimensions, the mean-field approximation is more accurate, as the behaviour is less dependent on the concrete configuration. For the $1+1$ dimensional contact process the mean-field rate equation is given by [15]

$$\begin{aligned}\partial_t\rho(t) &= \frac{\lambda}{2}\rho(t)(1-\rho(t))^2 + \frac{\lambda}{2}\rho(t)(1-\rho(t))^2 + \lambda\rho^2(t)(1-\rho(t)) - \rho(t) \\ &= \lambda\rho(t)(1-\rho(t))\left(1-\rho(t)+\rho(t)\right) - \rho(t) = (\lambda-1)\rho(t) - \lambda\rho^2(t).\end{aligned} \tag{4.22}$$

It is obtained from the rates of Figure 3.6 as follows: regarding an arbitrary site $i \in [1, N]_{\mathbb{Z}}$, the particle density $\rho(t)$ increases with rate $\frac{\lambda}{2}$ if the left neighbour is active, the site i is inactive and the right neighbour is also inactive. As we approximate the mean-field behaviour, this happens with probability $\rho(t)(1-\rho(t))^2$. The same probability and rate arises from an inactive left neighbour, an inactive site i and an active right neighbour. In the mean-field, both neighbours are active and the site i is inactive with probability $\rho^2(t)(1-\rho(t))$. In this case, the particle density $\rho(t)$ increases with rate λ. Finally, a site is active with probability $\rho(t)$ and becomes inactive with rate 1. Adding up the first three terms, where the particle density increases and subtracting the last term, where the particle density decays, leads to equation (4.22).

The mean-field rate differential equation (4.22) has a quadratic right hand site and hence two stationary solutions, which are given by

$$\partial_t \rho(t) = 0 \quad \Leftrightarrow \quad \rho_1^{\text{stat}} = 0 \ \vee \ \rho_2^{\text{stat}} = \frac{\lambda - 1}{\lambda}, \tag{4.23}$$

where ρ_1^{stat} corresponds the absorbing state of the empty lattice and ρ_2^{stat} represents the average particle density of the fluctuating steady state. The bifurcation diagram of the mean-field rate equation can be seen in Figure 4.2. It shows the stationary solutions of the differential equation depending on the parameter λ. At $\lambda_c = 1$ the two stationary solutions coincide and a fundamental change in the phase portrait of $\rho(t)$ occurs, see Figure 4.3. The indicated flow in the phase portrait of $\rho(t)$ is obtained from the sign of the derivative $\partial_t \rho(t)$: $\rho(t)$ grows if $\partial_t \rho(t) > 0$ and $\rho(t)$ decays if $\partial_t \rho(t) < 0$. A stationary solution is called stable, if all trajectories in a neighbourhood of the stationary solution converge to the stationary solution as $t \to \infty$, otherwise the stationary solution is called unstable [11]. It follows that ρ_1^{stat} is stable for $\lambda < \lambda_c$ and unstable for $\lambda \geq \lambda_c$ and ρ_2^{stat} is unstable for $\lambda \leq \lambda_c$ and stable for $\lambda > \lambda_c$. For $\lambda < \lambda_c$, the stationary solution ρ_2^{stat} is negative and therefore not relevant, since a particle density has only values in $[0, 1]$. $\lambda_c = 1$ is the mean-field value for the critical rate of the $1+1$ dimensional contact process, since in the subcritical phase $\lambda < \lambda_c$, the stable stationary solution of the absorbing state is reached and in the supercritical phase $\lambda > \lambda_c$, the trajectories converge to the stable fluctuating steady state, when starting from a configuration different to the absorbing state. As the two stationary solutions exchange their stability at $\lambda_c = 1$, the mean-field rate equation undergoes a transcritical bifurcation at $\lambda_c = 1$ [11].

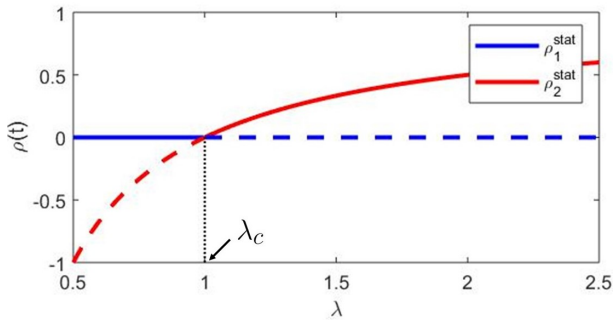
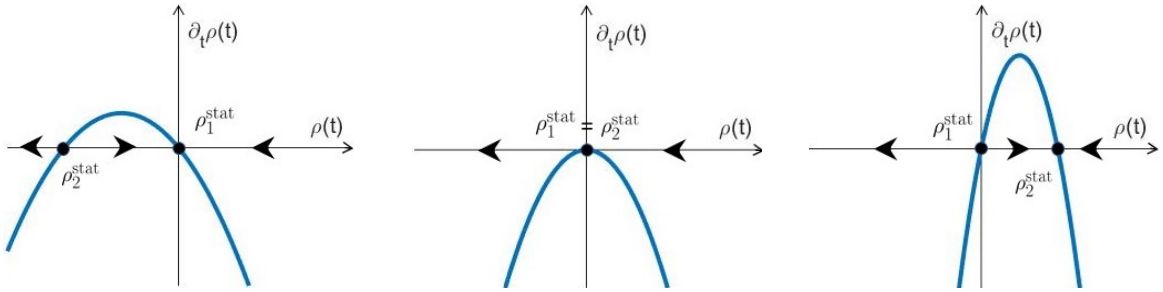


Figure 4.2.: Bifurcation diagram of the mean-field rate equation of the $1+1$ dimensional contact process. Solid lines represent stable stationary solutions, dotted lines represent unstable stationary solutions. At the critical rate $\lambda_c = 1$ a transcritical bifurcation occurs.

With a rescaling argument of the mean-field rate equation (4.22), when starting from a fully occupied infinite lattice, the critical exponents β and $\nu_{\parallel}$ can be obtained [19]. To determine also the spatial critical exponent $\nu_{\perp}$, the spatial argument i and a particle diffusion term depending on i has to be added. This diffusion term does not change the mean-field rate equation (4.22) without the spatial argument i, as it describes the time-behaviour of the particle density, which stays constant if particles diffuse [15]. According to [15], the extended mean-field rate equation is given by

$$\partial_t \rho_{\text{fo}}(i,t) = \Delta \rho_{\text{fo}}(i,t) - \lambda \rho_{\text{fo}}^2(i,t) + D\nabla^2 \rho_{\text{fo}}(i,t), \tag{4.24}$$



(a) Phase portrait of $\rho(t)$ for $0 \leq \lambda < \lambda_c$ (b) Phase portrait of $\rho(t)$ for $\lambda = \lambda_c$ (c) Phase portrait of $\rho(t)$ for $\lambda > \lambda_c$

Figure 4.3.: Phase portrait of the one dimensional phase spaces of $\rho(t)$ depending on the value of λ. The flow of $\rho(t)$ is indicated by arrows: $\rho(t)$ grows if $\partial_t\rho(t) > 0$ and $\rho(t)$ decays if $\partial_t\rho(t) < 0$.

where $\Delta := \lambda - \lambda_c$, D is a diffusion constant and ∇^2 is the Laplace Operator, which sums up the second spatial derivatives of all spatial dimensions. The extended mean-field rate equation (4.24) should be invariant under the dilatation $i \to \Lambda i$. According to equations (4.6) and (4.7), t and Δ rescale as $t \to \Lambda^z t$ and $\Delta \to \Lambda^{-1/\nu_\perp}\Delta$. It follows for the scaling law (4.8) of $\rho_{\text{fo}}(t)$ on an infinite lattice:

$$\rho_{\text{fo}}(t) \sim t^{-\alpha} f(\Delta t^{1/\nu_\parallel}) \to \Lambda^{-\alpha z} t^{-\alpha} f(\Lambda^{-1/\nu_\perp}\Delta \cdot \Lambda^{z/\nu_\parallel} t^{1/\nu_\parallel}) \sim \Lambda^{-\beta/\nu_\perp}\rho_{\text{fo}}(\Lambda^z t), \tag{4.25}$$

because $\alpha = \beta/\nu_\parallel$ and $z = \nu_\parallel/\nu_\perp$ (cf. Subsection 4.1.2) and so $-\alpha z = -(\beta/\nu_\parallel)\cdot(\nu_\parallel/\nu_\perp) = -\beta/\nu_\perp$. Including the additional spatial component i of the particle density, the following scaling form is obtained:

$$\rho_{\text{fo}}(i,t) \to \Lambda^{-\beta/\nu_\perp}\rho_{\text{fo}}(\Lambda i, \Lambda^z t). \tag{4.26}$$

With the rescaling relations $i \to \Lambda i$, $t \to \Lambda^z t$ and $\Delta \to \Lambda^{-1/\nu_\perp}\Delta$ (cf. equations (4.5) to (4.7)) and equation (4.26), the extended mean-field equation (4.24) rescales as

$$\begin{aligned}&\Lambda^{-\beta/\nu_\perp}\Lambda^{-z}\partial_t\rho_{\text{fo}}(\tilde{i},\tilde{t})\\ &= \Lambda^{-\beta/\nu_\perp}\Lambda^{-1/\nu_\perp}\Delta\rho_{\text{fo}}(\tilde{i},\tilde{t}) - \Lambda^{-2\beta/\nu_\perp}\lambda\rho_{\text{fo}}^2(\tilde{i},\tilde{t}) + \Lambda^{-\beta/\nu_\perp}\Lambda^{-2}D\nabla^2\rho_{\text{fo}}(\tilde{i},\tilde{t}),\end{aligned} \tag{4.27}$$

where $\tilde{i}$ and $\tilde{t}$ are the rescaled variables $\tilde{i} = \Lambda i$ and $\tilde{t} = \Lambda^z t$ [19]. The factors Λ^{-z} and Λ^{-2} compensate the factors, which arise by the chain rule when differentiating $\rho_{\text{fo}}(\tilde{i},\tilde{t})$. Equation (4.27) is invariant under rescaling if each summand is multiplied by the same power of Λ. Consequently, the factors have to fulfil

$$\Lambda^{-(\beta+\nu_\parallel)/\nu_\perp} = \Lambda^{-(\beta+1)/\nu_\perp} = \Lambda^{-2\beta/\nu_\perp} = \Lambda^{-(\beta+2\nu_\perp)/\nu_\perp}, \tag{4.28}$$

where $z = \nu_\parallel/\nu_\perp$ was used. Comparing the equalities leads to the mean-field critical exponents

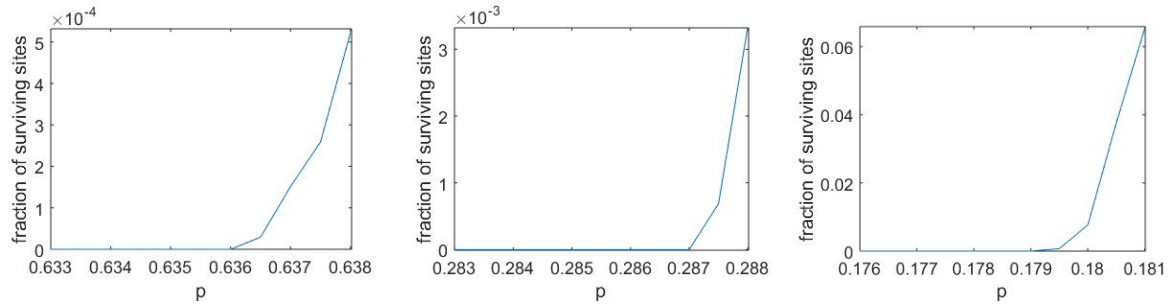
$$\beta^{\text{MF}} = 1, \qquad \nu_\parallel^{\text{MF}} = 1, \qquad \nu_\perp^{\text{MF}} = 0.5. \tag{4.29}$$

Above the upper critical dimensions $d_c = 4$. the mean filed critical exponents of equation (4.29) become exact for the DP universality class [15]. In $1+1$, $2+1$ and $3+1$ dimensions the critical exponents take non-trivial values, which are probably irrational [20]. In the following Section 4.3, the critical exponents for $d = 1, 2, 3$ are approximated numerically.

4.3. Numerical Analysis of Directed Percolation

To analyse directed percolation numerically, we use Monte Carlo simulations. Therefore we average over many realisations of the probabilistic process. The numerical code applied is listed in Appendix C.1. In order to approximate the triplet $(\beta, \nu_\parallel, \nu_\perp)$ of critical exponents of directed percolation, the critical probability p_c is needed.

A first way to obtain the critical probability is to simulate directed percolation in $d+1$ dimensions, $d = 1, 2, 3$ each K times starting from a fully occupied lattice with periodic boundary conditions until a finite, but high time T. We choose $K = 100$ and $T = 10000$ and simulate in each of the dimensions $d = 1, 2, 3$ a total number of 2048 particles. As in the definition of directed percolation (cf. Section 3.2) only every second site of the lattice $[-N, N-1]^d$ is existing, we choose in $1+1$ dimensions $N = 2048$, in $2+1$ dimensions $N = 32$, such that the total number of particles is $0.5 \cdot (2 \cdot 32)^2 = 2048$ and in $3+1$ dimensions $N = 8$, such that the total number of particles is also $0.5 \cdot (2 \cdot 8)^3 = 2048$.



(a) $d = 1$, $N = 2048$, $K = 100$ (b) $d = 2$, $N = 32$, $K = 100$ (c) $d = 3$, $N = 8$, $K = 100$

Figure 4.4.: Fraction of surviving sites over $K = 100$ simulations of directed percolation in d dimensions with N sites until time $T = 10000$ depending on the probability parameter p. The numerical code can be found in Appendix C.2.

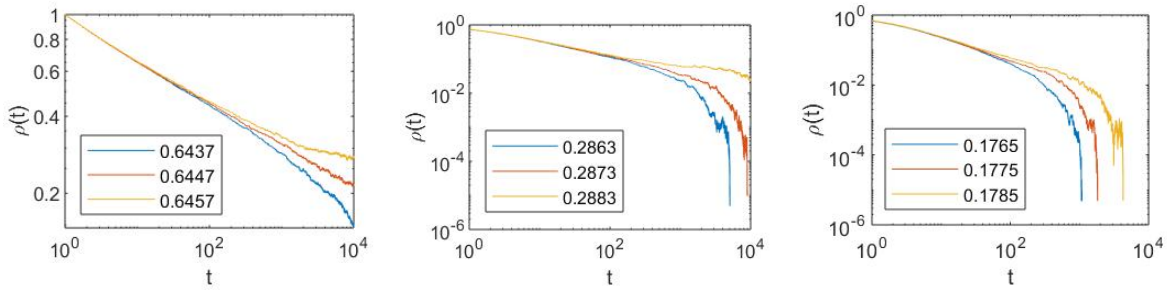
In the subcritical phase $p < p_c$, the probability is zero that a site is contained in an infinite cluster. Consequently, according to Figure 4.4 we obtain $p_c(1) \approx 0.636$, $p_c(2) \approx 0.287$ and $p_c(3) \approx 0.179$. These values are very inaccurate, as we only simulated 100 times, the absorbing state could be reached after more than $T = 10000$ time steps and in finite size simulations, there is always a positive probability to reach the absorbing state [15].

A more precise way is to measure deviations from the power law decay of the particle density $\rho_{\text{fo}}(t) \sim t^{-\alpha}$ (cf. equation (4.12)). In a double-logarithmic graph, the exponential decay is represented as a line with slope $-\alpha$, as $\log(\rho_{\text{fo}}(t)) = -\alpha \log(t) + c$, $c \in \mathbb{R}$. Figures 4.5(a) to 4.5(c) show the average over $K = 100$ simulations of directed percolation with 2048 particles for $d = 1, 2, 3$ respectively for three values of p: The blue line represents a probability smaller than p_c, the red line represents p_c and the yellow line a probability greater than p_c. For clarity, further lines were omitted. In Figure 4.5(a) for directed percolation in $1+1$ dimensions we observe the following: in the active phase $p > p_c$ the stationary density is reached and the slope of the curve grows until it is constant. In the inactive phase, the particle density decays faster than exponentially and the slope of the curve decreases. The slope of the red curve stays constant, so we obtain the critical probability $p_c(1) = 0.6447$, which is a good approximation of the value $p_c^*(1) = 0.644700185(5)$ of [4]. In $2+1$ and $3+1$ dimensions (Figures 4.5(b) and 4.5(c)), the size of the lattice is too small, such that finite size effects occur and the process also dies out in the active phase $p > p_c$ [15]. For the simulations the critical probabilities

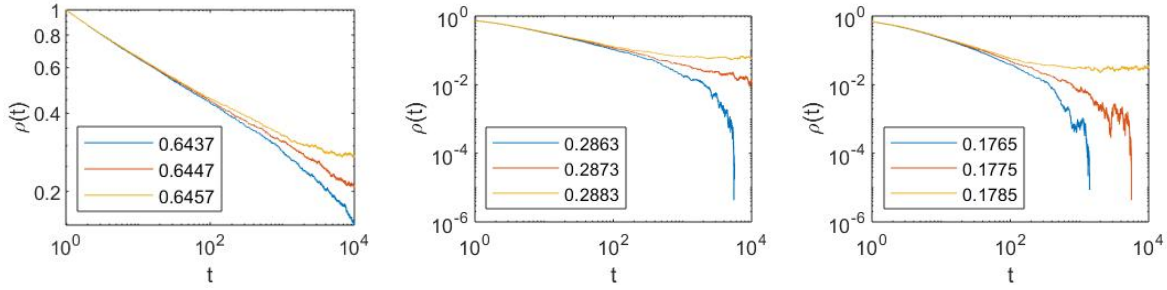
$$p_c^*(1) = 0.644700185(5), \qquad p_c^*(2) = 0.287338(3), \qquad p_c^*(3) = 0.1774970(5),$$

of [4] rounded to four decimals were used. To obtain better results, we average additionally directed percolation over $K = 10$ simulations with 32328 particles for $d = 1, 2, 3$, see Figures 4.5(d) to 4.5(f). These plots confirm the correctness of the values $p_c^*(2)$ and $p_c^*(3)$. Therefore we choose $N = 108$ in $2+1$ dimensions, as $0.5 \cdot (2 \cdot 108)^2 = 32328$ and $N = 18$ in $3+1$ dimensions, as $0.5 \cdot (2 \cdot 18)^3 = 32328$.

From Figures 4.5(d) to 4.5(f) the critical exponent $\alpha(d) = \delta(d)$ can be obtained, which is the negative of the slope of the red lines in the double-logarithmic plot. We have $\alpha(1) \approx 0.162$, $\alpha(2) \approx 0.481$ and $\alpha(3) \approx 0.761$, see Appendix C.3. These are slightly higher, but good approximations to the values $\alpha^*(1) = 0.159464(6)$, $\alpha^*(2) = 0.4505(10)$ and $\alpha^*(3) = 0.737(5)$ given in [4].



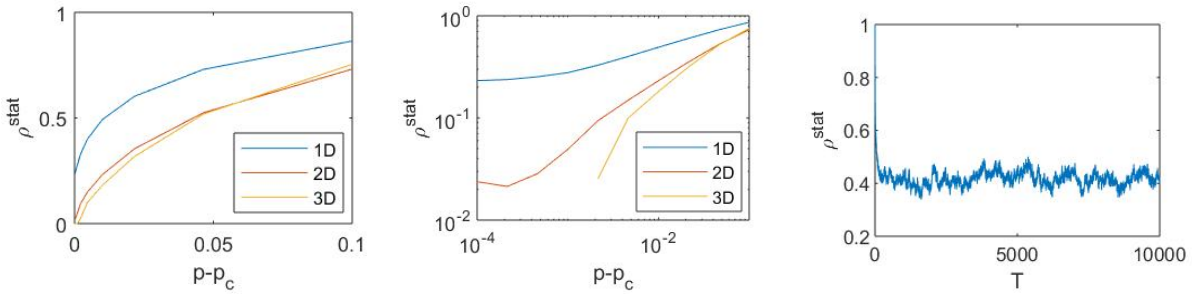
(a) $d = 1$, $N = 2048$, $K = 100$ (b) $d = 2$, $N = 32$, $K = 100$ (c) $d = 3$, $N = 8$, $K = 100$



(d) $d = 1$, $N = 32328$, $K = 10$ (e) $d = 2$, $N = 108$, $K = 10$ (f) $d = 2$, $N = 18$, $K = 10$

Figure 4.5.: Fraction of surviving sites over K simulations of directed percolation in d dimensions with N sites until time $T = 10000$ depending on the probability parameter p represented in a double-logarithmic plot. The numerical code can be found in Appendix C.2.

A first way to determine β is to use the scaling relation $\rho^{\text{stat}} \sim \Delta^{\beta}$ for $\Delta = p - p_c > 0$. In Figures 4.6(a) and 4.6(b) the stationary density depending on $p - p_c$ for directed percolation in $1+1$, $2+1$ and $3+1$ dimensions is shown. β is represented as the slope in the double-logarithmic graph 4.6(b), as $\log(\rho^{\text{stat}}) = \beta \log(\Delta) + c$, $c \in \mathbb{R}$. As there are still many fluctuations especially in $1+1$ dimensions (see Figure 4.6(c)), we averaged the particle density from time $T_0 = 5000$ to time $T = 10000$ over $K = 100$ simulations and obtain $\beta(1) \approx 0.247$, $\beta(2) \approx 0.534$ and $\beta(3) \approx 0.658$, see Appendix C.3. These values are especially in $2+1$ and $3+1$ dimensions inaccurate, as the closer p is p_c, the longer is the time to reach the stationary density [15]. Furthermore, in $3+1$ dimensions it happens that even in the active phase, the process dies out and the absorbing state is reached, such that the logarithm of the particle density is $-\infty$ and not represented in the double-logarithmic plot. According to [15], the values for the critical exponent β are given by $\beta^*(1) = 0.276486(8)$, $\beta^*(2) = 0.584(4)$ and $\beta^*(3) = 0.81(1)$.



(a) Linear plot of ρ_p^{stat} depending on $p - p_c$ (b) Double-logarithmic plot of ρ_p^{stat} depending on $p - p_c$ (c) Fluctuations of directed percolation on $1+1$ dimensions, $p = 0.65 > p_c$.

Figure 4.6.: Stationary density ρ_p^{stat} depending on the difference $p - p_c$ for directed pond percolation in $1+1$, $2+1$ and $3+1$ dimensions with 2048 particles and $K = 100$ simulations each. Because of fluctuations, the stationary density was averaged from $T_0 = 5000$ to $T = 10000$. The numerical code can be found in Appendix C.3.

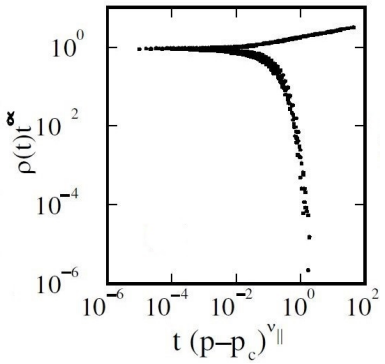
The finite size and near criticality problems can be avoided by using the scaling law $\rho_{\text{fo}}(t) \sim t^{-\alpha} f(\Delta t^{1/\nu_\parallel})$ (cf. equation (4.8)) and determining $\nu_\parallel$ [15]. β is then obtained with the relation $\beta = \alpha\nu_\parallel$. Because of insufficient computing power, we explain the approach and refer in $1+1$ dimensions to the plots of [15].

By plotting $\rho_{\text{fo}}(t) \cdot t^\alpha$ against $\Delta t^{1/\nu_\parallel}$ for constant Δ, the function $f(\Delta t^{1/\nu_\parallel})$ is shown. According to equation (4.10) it holds $f(\Delta t^{1/\nu_\parallel}) \sim (\Delta t^{1/\nu_\parallel})^{\alpha\nu_\parallel} = (t\Delta^{\nu_\parallel})^\alpha$ for $t \to \infty$, such that f is linear with slope α for $t \to \infty$ when plotting it against $t\Delta^{\nu_\parallel}$ in a double-logarithmic graph, see Figure 4.7(a). The critical exponent $\nu_\parallel$ can be obtained by tuning $\nu_\parallel$ in such a way that all curves collapse in the double-logarithmic graph [15]. This is the case, because already small perturbations $\epsilon \in \mathbb{R}$ of the appreciated value $\nu'_\parallel = \nu_\parallel + \epsilon$ lead to high deviations of $f(\Delta t^{1/\nu'_\parallel})$ for $t \to \infty$:

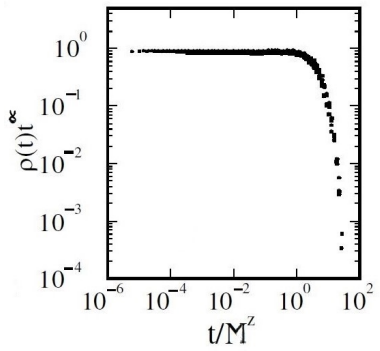
$$\begin{aligned} f(\Delta t^{1/\nu'_\parallel}) &\sim (\Delta t^{1/\nu'_\parallel})^{\alpha\nu_\parallel} = (\Delta t^{1/(\nu_\parallel+\epsilon)})^{\alpha\nu_\parallel} = (\Delta t^{1/\nu_\parallel})^{\alpha\nu_\parallel} \cdot t^{(1/(\nu_\parallel+\epsilon)-1/\nu_\parallel)\alpha\nu_\parallel} \\ &\sim f(\Delta t^{1/\nu_\parallel}) \cdot t^{(\nu_\parallel/(\nu_\parallel+\epsilon)-1)\alpha} = f(\Delta t^{1/\nu_\parallel}) \cdot t^{-\epsilon\alpha/(\nu_\parallel+\epsilon)}. \end{aligned} \tag{4.30}$$

Since $\alpha \neq 0$, the factor $t^{-\epsilon\alpha/(\nu_\parallel+\epsilon)}$ is one if and only if $\epsilon \neq 0$ and converges to 0 or ∞ depending on the sign of ϵ. It can be seen in Figure 4.7(a) that the curves collapse to 0 or ∞.

Analogously, the critical exponent z can be determined by only considering the second argument in the scaling law of equation (4.8), such that $\rho_{\text{fo}}(t) \sim t^{-\alpha} f(t^{d/z}/M)$ is obtained. The critical exponent $\nu_\perp$ is then given by $z = \nu_\parallel/\nu_\perp$. Therefore $\rho_{\text{fo}}(t) \cdot t^\alpha$ is plotted against t/M^z for constant Δ and $\nu_\parallel$ is tuned in such a way that all curves collapse, see Figure 4.7(b) [15].



(a) Data collapse of off-critical simulations



(b) Data collapse of finite-size simulations

Figure 4.7.: Double-logarithmic plots of [15] of the scaling law $\rho_{\text{fo}}(t) \sim t^{-\alpha} f(\Delta t^{1/\nu_\parallel}, t^{d/z}/M)$ (cf. equation (4.8)) considering only the first or only the second argument for directed percolation in $1+1$ dimensions.

In the following tabular, the values for the critical exponents $\alpha = \delta$, β, $\nu_\perp$, $\nu_\parallel$, z and μ stated in [15] are shown. They are obtained by numerical and field theoretic methods. Above the upper critical dimension $d_c = 4$, the mean-field critical exponents of Section 4.2. become exact [15].

critical exponent	d = 1	d = 2	d=3	mean-field
$\alpha = \delta$	0.159 464 (6)	0.451	0.73	1
β	0.276 486 (8)	0.584(4)	0.81(1)	1
$\nu_\perp$	1.096 854 (4)	0.734(4)	0.581(5)	0.5
$\nu_\parallel$	1.733 847 (6)	1.295(6)	1.105(5)	1
z	1.580 745 (10)	1.76(3)	1.90(1)	2
μ	0.313 686 (8)	0.230	0.12	0

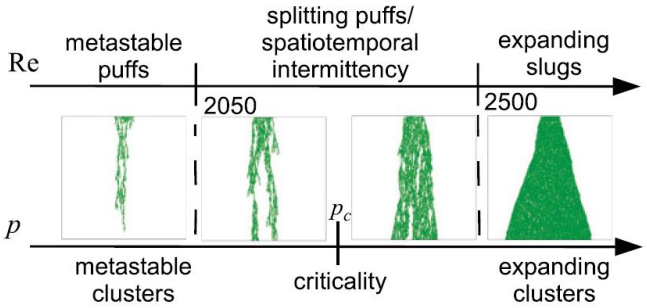
Table 4.1.: Critical Exponents of the DP universality class, stated in [15].

5. Directed Percolation in Fluid Dynamics

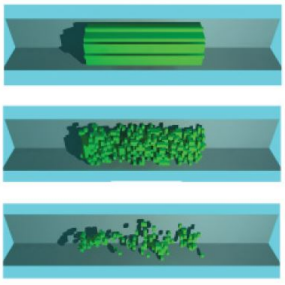
Besides examples discussed in the introduction chapter, percolation processes can also be used to describe transitions from a laminar to a turbulent flow, since this transition shows many similarities to the non-equilibrium phase transition of the DP universality class. After the theory, simulation and analysis of models related to directed percolation, this chapter is a small outlook on the connections of percolation theory and fluid dynamics.

The dimensionless Reynolds number Re is a parameter in fluid dynamics describing the turbulence in flows. It is defined as $Re = \frac{UL}{\nu}$, where U is the mean flow velocity, L the characteristic length scale and ν the kinematic viscosity [24]. If the Reynolds number is sufficiently small, every turbulent disturbance decays immediately, resulting in a laminar flow. For higher Reynolds numbers, the turbulence of the flow in a pipe behaves differently: For $1650 < Re < 2050$, local clusters of turbulence, also called puffs, are metastable. With growing Reynolds number the characteristic life-time τ grows and the clusters of turbulence can split and show a more complex spatio-temporal behaviour. Above the critical value $R_c \sim 2500$, turbulence expands uniformly and a slug of turbulence arises [24]. This transition to turbulence is shown in Figure 5.1(a) and compared with the similar phenomena of directed percolation in $1+1$ dimensions (cf. Section 3.2) starting from a number of neighboured sites depending on the probability parameter p. In the subcritical phase $p < p_c$, the open cluster is almost surely finite and in the supercritical phase $p > p_c$, an infinite open cluster exists almost surely, which expands like a slug. The closer p is the critical probability p_c, the higher is the complexity of the geometry of the open cluster.

To model turbulence of a flow in a three dimensional pipe with length D and radius R, the following 3+1 dimensional model is proposed by [24]. The flow is discretized as a regular lattice of cubes. All cubes, where the turbulence intensity is higher than a given threshold, are represented as active sites; all laminar regions as inactive sites [1], [24]. The obtained lattice is a sublattice of $\mathbb{Z}^3$. Sites of the lattice are called neighboured or adjacent in the case they are joined by an edge as in the definition of directed percolation (cf. equation (3.6) in Subsection 3.2.1). The start configuration models the inlet disturbance of the flow. The configurations are updated in discrete time steps: every turbulent site stays turbulent with probability p and becomes laminar with probability $1-p$. Furthermore the fluid dynamical behaviour of the flow is simplified as follows: each active site with coordinates (x, y, z) activates simultaneously with probability p its neighbours $(x+1, y, z)$, $(x, y+1, z)$ and $(x, y, z+1)$ at even time steps and its neighbours



(a) Comparison of the phenomena of turbulence in a pipe as a function of the Reynolds number Re with the phenomena of directed percolation in $1+1$ dimensions starting from a number of neighboured sites depending on the probability parameter p.



(b) Decay of the model of [24] with $p < p_c$. Active sites are represented as green cubes.

Figure 5.1.: Phenomena and properties of the directed percolation model proposed by [24]. The Figures are taken from [24].

$(x-1,y,z)$, $(x,y-1,z)$ and $(x,y,z-1)$ at odd time steps if they are laminar respectively. The boundary conditions are not prescribed, but have to stay fixed. In Figure 5.1(b) the decay of an active cluster of the model of [24] is shown for $p < p_c$.

When p is near the critical probability p_c, the spatial correlation length $\xi_\perp \sim |p - p_c|^{-\nu_\parallel}$ becomes larger than the radius R of the pipe, as $\nu_\parallel$ is a positive critical exponent. Consequently, the $3+1$ dimensional model is effectively $1+1$ dimensional and can be approximated by a corresponding $1+1$ dimensional percolation process on a lattice, which has the length D of the pipe. Each turbulent site x of the one dimensional lattice stays turbulent with probability p and becomes laminar with probability $1-p$. Furthermore, each turbulent site x activates at even time steps with probability p its neighbour $x+1$ and at odd time steps with probability p its neighbour $x-1$ [24].

Analogously to directed percolation, the survival probability $P(p,t)$ is defined as the probability that there are still active sites after t time steps. Figure 5.2 shows the survival probability of the $1+1$ dimensional model of [24] depending on the parameter p for four different values of t. The numerical data is shown for $t = 300$ as red crosses, for $t = 1000$ as green dots, for $t = 6000$ as blue pluses and for $t = 80000$ as cyan triangles [24]. The critical probability p_c is defined analogously to Chapter 3 as

$$p_c \coloneqq \inf\{p \in [0,1] : P(p,\infty) > 0\}. \tag{5.1}$$

The numerical data of Figure 5.2 indicates that the critical value p_c of the $1+1$ dimensional model is slightly higher than 0.653, as at this value the first cyan triangle of $t = 80000$ is bigger than zero. This approximation is close to the critical value of directed percolation in $1+1$ dimensions, which is given by $p_c^*(1) = 0.644700185(5)$ [4]. The numerical data of the $1+1$ dimensional percolation process of [24] fits very well with the predicted survival probability of turbulent puffs of fluid dynamics theory. It is given by

$$P(Re,t) = \exp\left(-\frac{t-t_0}{\tau(Re)}\right), \tag{5.2}$$

with $t > t_0$, where t_0 is the formation time of the puff [24]. The exponential distribution is normed by the average life-time $\tau(Re)$ of a puff. The average life-time τ scales super-exponentially as

$$\tau(Re) = \tau_0 \exp[\exp(c_1 Re + c_2)], \tag{5.3}$$

with two constants c_1 and c_2 and a parameter $\tau_0 \sim \frac{R}{U}$, where R is the radius of the pipe and U the mean flow velocity [24]. For the concrete choices of the formation time t_0, the parameter τ_0 and the constants c_1 and c_2 in Figure 5.2, see [24]. In that paper, also further similarities of fluid dynamics and the DP universality class are shown.

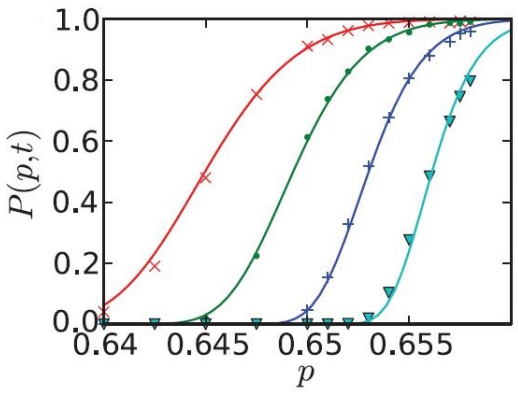


Figure 5.2.: Survival probablity $P(p,t)$ depending on the probability paramter p for different values of t. For an explication of the lines, points and colours, see text. The Figure is taken from [24].

Another $1+1$ dimensional percolation model for a flow in a (very long) pipe is proposed by [1]. The flow in the pipe is simplified as an infinite one dimensional lattice with turbulent and laminar regions, represented as active or inactive sites. Each active site stays turbulent with probability p and becomes inactive with probability $1-p$. Additionally, each turbulent site activates simultaneously its left or right inactive neighbour with probability r respectively, see Figure 5.3.

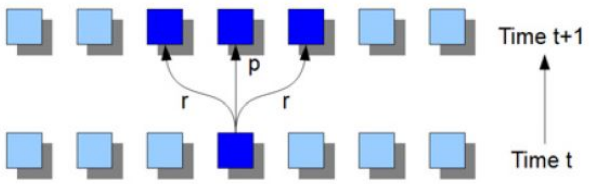
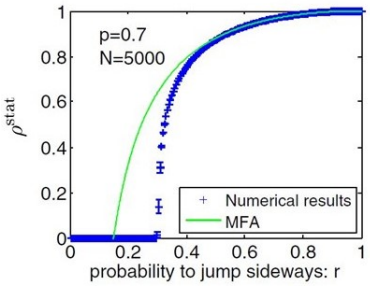
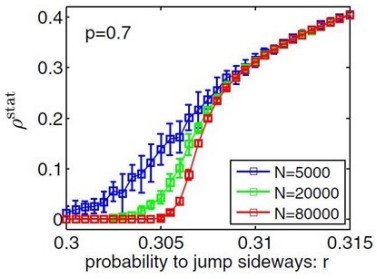


Figure 5.3.: Transition probabilities of the model proposed by [1]. The Figure is taken from [1].

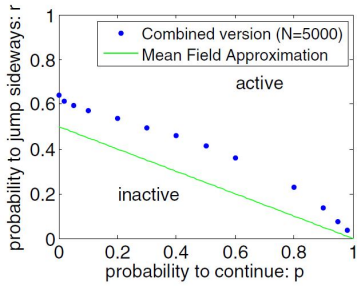
For a fixed probability p to stay active, the critical value r_c of the probability to jump sideways is determined numerically as well as with a mean-field approximation in [1], see Figures 5.4(a) and 5.4(b) for $p = 0.7$. In Figure 5.4(c) the numerically and mean-field approximated critical probability pairs (p_c, r_c) are shown in a $p-r$ parameter plane.



(a) Numerical and mean-field approximation to determine r_c



(b) Numerial approximation of r_c for different system sizes



(c) Numerical and mean-field approximated pairs (p_c, r_c).

Figure 5.4.: Numerical experiments of the model proposed in [1]. The Figures are taken from [1].

Given the pairs (p_c, r_c) of critical probabilities, the critical exponents β, $\nu_\parallel$ and $\nu_\perp$ can be approximated numerically as in Section 4.3, see Figure 5.5. In the fluid dynamical context, $L_\perp$ is defined as the mean length of laminar regions and $L_\parallel$ as the mean time interval to stay laminar [1]. With the definitions of $\xi_\perp$ and $\xi_\perp$ of directed percolation starting from a fully occupied lattice in the active phase $p > p_c$ (cf. Figure 4.1(d) of Section 4.1), it follows $L_\perp = \xi_\perp$ and $L_\parallel = \xi_\parallel$. Comparing the critical exponents $\beta^* = 0.276486(8)$, $\nu_\perp^* = 1.096854(4)$ and $\nu_\parallel^* = 1.733847(6)$ of Table 4.1 of Section 4.3. with the numerically obtained values of Figure 5.5 leads to the conclusion that the model of [1] belongs quite certainly to the DP universality class.

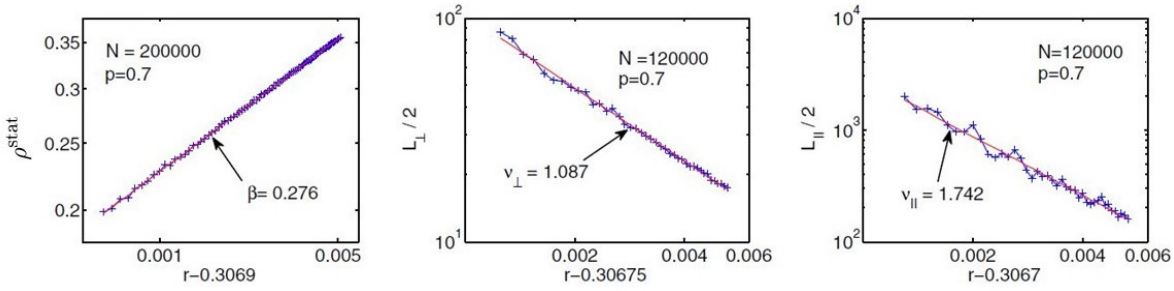


Figure 5.5.: Numerical approximation of the critical exponents β, $\nu_\perp$ and $\nu_\parallel$. The Figure is taken from [1].

A. Basics Probability Theory

Appendix A contains definitions, lemmas and theorems of the topics probability theory and Markov chains which can be found in [3] and [18]. The notations used and the formulation of the definitions, lemmas and theorems are sometimes adapted to the present thesis.

Definition A.1 (Power Set) [18]. *For a set Ω the Power Set $\mathcal{P}(\Omega)$ is defined as the set of all subsets of Ω:*

$$\mathcal{P}(\Omega) := \{A : A \subset \Omega\}.$$

Definition A.2 (σ-algebra) [18]. *A class of sets $\mathcal{A} \subset \mathcal{P}(\Omega)$ is called a a σ-algebra if it fulfils the following three conditions:*

(*i*) $\Omega \in \mathcal{A}$

(*ii*) *$\mathcal{A}$ is closed under complements: For $A \in \mathcal{A}$ it holds $A^c := \Omega \backslash A \in \mathcal{A}$*

(*iii*) *$\mathcal{A}$ is closed under countable unions: For $A_1, A_2, ... \in \mathcal{A}$ it holds $\bigcup_{n=1}^{\infty} A_n \in \mathcal{A}$.*

Definition A.3 (Generated σ-algebra) [18]. *Let $\mathcal{E} \subset \mathcal{P}(\Omega)$. Then there exists a smallest σ-algebra $\sigma(\mathcal{E})$ with $\mathcal{E} \subset \sigma(\mathcal{E})$:*

$$\sigma(\mathcal{E}) := \bigcap_{\substack{\mathcal{A} \subset \mathcal{P}(\Omega) \text{ is a } \sigma\text{-algebra} \\ A \supset \mathcal{E}}} .$$

$\sigma(\mathcal{E})$ is called the generated σ-algebra by the generator $\mathcal{E}$.

Definition A.4 (Measure) [18]. *Let Ω be a nonempty set and $\mathcal{A} \subset \mathcal{P}(\Omega)$ a σ-algebra. A set function $\mu : \mathcal{A} \to [0, \infty]$ is called a measure on $\mathcal{A}$ if the following conditions hold:*

(*i*) $\mu(\emptyset) = 0$

(*ii*) *μ is σ-additive: For countable many mutually disjoint sets $A_1, A_2, ... \in \mathcal{A}$ it holds*

$$\mu\left(\bigcup_{n=1}^{\infty} A_n\right) = \sum_{i=1}^{\infty} \mu\left(A_i\right)$$

If additionally $\mu(\Omega) = 1$, μ is called a probability measure.

Lemma A.5 (σ-Subadditivity) [18]. *Let Ω be a nonempty set, $\mathcal{A} \subset \mathcal{P}(\Omega)$ a σ-algebra and $\mu : \mathcal{A} \to [0, \infty]$ a measure on $\mathcal{A}$. Then it holds for countably many sets $A_1, A_2, ... \in \mathcal{A}$ and $A \subset \bigcup_{n=1}^{\infty} A_n$ with $A \in \mathcal{A}$:*

$$\mu(A) \leq \sum_{i=1}^{\infty} \mu\left(A_i\right).$$

Definition A.6 (Measure and Probability Space) [18]. *A pair $(\Omega, \mathcal{A})$ of a nonempty set Ω and a σ-algebra $\mathcal{A} \subset \mathcal{P}(\Omega)$ is called a measurable space. The sets $A \in \mathcal{A}$ are called measurable sets.*
A triple $(\Omega, \mathcal{A}, \mu)$ is called a measure space if $(\Omega, \mathcal{A}, \mu)$ is a measurable space and μ is a measure on $\mathcal{A}$. If in addition μ is a probability measure, then $(\Omega, \mathcal{A}, \mu)$ is called a probability space and the sets $A \in \mathcal{A}$ are called events.

Definition A.7 (Almost surely) [18]. *Let $(\Omega, \mathcal{A}, \mathbb{P})$ be a probability space and $E(\omega)$ be a property that a point $\omega \in \Omega$ can have or not have. We say E holds $(\mathbb{P}-)$ almost surely if $E(\omega)1$ holds for all $\omega \in \Omega \backslash N$, where N denotes a null set to $\mathbb{P}$: $\mathbb{P}(N) = 0$.*

Definition A.8 (Measurable map) [18]. *A map $X : \Omega \to \Omega'$ is called $\mathcal{A} - \mathcal{A}'$-measurable (or briefly, measurable) if $X^{-1}(A') \coloneqq \{X^{-1}(A') : A' \in \mathcal{A}'\} \subset \mathcal{A}$; that is, if*

$$X^{-1}(A') \in \mathcal{A} \text{ for any } A' \in \mathcal{A}'.$$

Definition A.9 (Random Variable) [18]. *Let $(\Omega, \mathcal{A}, \mathbb{P})$ be a probability space, $(\Omega', \mathcal{A}')$ a measurable space and $X : \Omega \to \Omega'$ measurable. Then X is called a random variable (with values in $(\Omega', \mathcal{A}')$).*

Definition A.10 (Distribution, Distribution Function) [18]. *Let $(\Omega, \mathcal{A}, \mathbb{P})$ be a probability space and $X : \Omega \to \mathbb{R}$ be a real random variable. The probability measure $\mathbb{P}_X \coloneqq \mathbb{P} \circ X^{-1}$ is called the distribution of X or rather $\mathbb{P}_x$.*
The map $F_X : x \mapsto \mathbb{P}(X \leq x)$ is called the distribution function of X. If $\mu = \mathbb{P}(X)$, X has the distribution μ. Notation: $X \sim \mu$.
Let I be an index set. A family $(X_i)_{i \in I}$ of random variables is called identically distributed if $\mathbb{P}_{X_i} = \mathbb{P}_{X_j}$ for all $i, j \in I$. Notation: $X \overset{\mathcal{D}}{=} Y$ if $\mathbb{P}_X = \mathbb{P}_X$ ($\mathcal{D}$ for distribution).

Definition A.11 (Independence) [18]. *Let I be an arbitrary index set and $(A_i)_{i \in I}$ be an arbitrary family of events on a probability space $(\Omega, \mathcal{A}, \mathbb{P})$. The family $(A_i)_{i \in I}$ is called independent if for any finite subset $\emptyset \neq J \subset I$ the following product formula holds:*

$$\mathbb{P}\left(\bigcap_{j \in J} A_j\right) = \prod_{j \in J} \mathbb{P}(A_j).$$

An arbitrary family of σ-algebras $(\mathcal{A}_i)_{i \in I}$ is called independent if the events $(A_i)_{i \in I}$ are independent for $A_i \in \mathcal{A}_i \ \forall i \in I$.
The family $(X_i)_{i \in I}$ of random variables is called independent if the family $(\sigma(X_i)_{i \in I})$ of σ-algebras is independent.

Theorem A.12 (Borel-Cantelli Lemma) [18]. *Let $(A_n)_{n \in \mathbb{N}}$ be a family of events in the probability space $(\Omega, \mathcal{A}, \mathbb{P})$. With $A^* \coloneqq \limsup_{n \to \infty} A_n$ the two following two statements hold:*

(i) *If $\sum_{n=1}^{\infty} \mathbb{P}(A_n) < \infty$, then $\mathbb{P}(A^*) = 0$.*

(ii) *If $(A_n)_{n \in \mathbb{N}}$ is independent and $\sum_{n=1}^{\infty} P(A_n) = \infty$, then $P(A^*) = 1$.*

Theorem A.13 (Product measure) [18]. *For every $n \in \mathbb{N}_0$, let $\mathbb{P}_n$ be a probability measure on the measurable space $(\Omega_n, \mathcal{A}_n)$. Denote by $\Omega \coloneqq \prod_{i=0}^{\infty} \Omega_i$ the Cartesian product space of the Ω_i and by $\mathcal{A} \coloneqq \prod_{i=0}^{\infty} \mathcal{A}_i$ the product σ-algebra of the $\mathcal{A}_i$. This is the smallest σ-algebra on Ω such that for all $i \in \mathbb{N}$ the coordinate map $X_i : \Omega \to \Omega_i$ is measurable with respect to $\mathcal{A} - \mathcal{A}_i$. Then there exists a uniquely determined probability measurable $\mathbb{P}$ on the product measure space $(\Omega, \mathcal{A})$ with*

$$\mathbb{P}\left(A_0 \times ... \times A_n \times \bigtimes_{i=n+1}^{\infty} \Omega_i\right) = \prod_{k=0}^{n} \mathbb{P}_k(A_k),$$

for $A_i \in \mathcal{A}_i$, $i = 0, .., n$ and $n \in \mathbb{N}_0$.
$\prod_{i=0}^{\infty} \mathbb{P}_i \coloneqq \mathbb{P}$ is called the product probability measure of the probability measures $\mathbb{P}_0, \mathbb{P}_1, ...$ Under $\mathbb{P}$, the coordinate maps $(X_i)_{i \in \mathbb{N}_0}$ are independent.

Definition A.14 (Cylinder Set, special case) (similar to [18], adapted)**.** *For an countably infinitely often repeated random experiment with finitely many possible outcomes $c_1, c_2, ..., c_n$ with $n \in \mathbb{N}$ let $C \coloneqq \{c_1, c_2, ..., c_n\}$ and $\Omega \coloneqq \prod_{n\in\mathbb{N}} C$ the sample space of all possible outcomes. Let for given $m \in \mathbb{N}$:*

$$I_m \coloneqq \{(i_1, ..., i_m) : i_k \in \mathbb{N}\ \forall\ k \in \{1, .., m\} \wedge i_k < i_l \text{ for } k, l \in \{1, .., m\} \text{ with } k < l\},$$
$$J_m \coloneqq \{(j_1, ..., j_m) : j_k \in \{1, ..., n\}\ \forall\ k \in \{1, .., m\}.$$

For given $m \in \mathbb{N}$ let $i \in I_m$ and $j \in J_m$. The cylinder set $\Omega_{i,j}$ is defined as

$$\Omega_{i,j} \coloneqq \{\omega \in \Omega : \omega_{i_k} = c_{j_k}\ \forall\ k \in \{1, .., m\}\}.$$

Now, with $\mathcal{E} \coloneqq \bigcup_{m=1}^{\infty} \bigcup_{i\in I_m} \bigcup_{j\in J_m} \Omega_{i,j} \subset \mathcal{P}(\Omega)$ the generated σ-algebra of the finite dimensional cylinder sets is given by $\sigma(\mathcal{E})$.

Definition A.15 (Tail σ-algebra) [18]**.** *Let I be a countably infinite index set and let $(A_i)_{i\in I}$ be a family of σ-algebras. Then*

$$\mathcal{T}\left((\mathcal{A}_i)_{i\in I}\right) \coloneqq \bigcap_{\substack{J\subset I \\ |J|<\infty}} \sigma\left(\bigcup_{j\in I\setminus J} \mathcal{A}_j\right),$$

is called the tail σ-algebra of $(\mathcal{A}_i)_{i\in I}$. If $(A_i)_{i\in I}$ is a family of events, then the tail σ-algebra is defined as

$$\mathcal{T}\left((A_i)_{i\in I}\right) \coloneqq \mathcal{T}\left((\{\emptyset, A_i, A_i^c, \Omega\})_{i\in I}\right).$$

If $(X_i)_{i\in I}$ is a family of random variables, then the tail σ-algebra is defined as

$$\mathcal{T}\left((X_i)_{i\in I}\right) \coloneqq \mathcal{T}\left((\sigma(X_i))_{i\in I}\right).$$

Theorem A.16 (Kolmogorov's 0-1 Law) [18]**.** *Let $(\Omega, \mathcal{A}, \mathbb{P})$ be a probability space, I a countably infinite index set and $(\mathcal{A}_i)_{i\in I}$ an independent family of σ-algebras contained in $\mathcal{A}$. Then the tail σ-algebra is $\mathbb{P}$-trivial, that is*

$$\mathbb{P}(A) \in \{0, 1\} \quad \text{for any } A \in \mathcal{T}((\mathcal{A}_i)_{i\in I}).$$

Since for mutually independent random variables $(X_i)_{i\in I}$ the generated σ-algebras $(\sigma(X_i))_{i\in I}$ are also independent, Kolmogorov's 0-1 law also holds for this case.

Definition A.17 (Conditional Probability) [3]**.** *The conditional probability of the event A given the event B is defined when $\mathbb{P}(B) > 0$ as*

$$\mathbb{P}(A|B) \coloneqq \frac{\mathbb{P}(A \cap B)}{\mathbb{P}(B)}.$$

Definition A.18 ((Homogeneous) discrete time Markov chain) [3]**.** *Let $(X_t)_{t\in\mathbb{N}_0}$ be a sequence of random variables on a probability space $(\Omega, \mathcal{A}, \mathbb{P})$ with values in $(\mathcal{E}, \mathcal{P}(\mathcal{E}))$, where $\mathcal{E}$ is a countable state space. If for all $t \in \mathbb{N}_0$ and for all $i_0, i_1, ..., i_{n-1}, i, j \in \mathcal{E}$*

$$\mathbb{P}(X_{t+1} = j | X_t = i, X_{t-1} = i_{n-1}, ..., X_0 = i_0) = \mathbb{P}(X_{t+1} = j | X_t = i),$$

whenever both sides are well-defined, this stochastic process is called a discrete time Markov chain. It is called a homogeneous discrete time Markov chain if additionally the right hand side of the formula above is independent of t.

Definition A.19 (Continuous time Markov chain) [5]. *Let $(X_t)_{t\geq 0} = (X_t : 0 \leq t < \infty)$ be a sequence of random variables on a probability space $(\Omega, \mathcal{A}, \mathbb{P})$ with values in $(\mathcal{E}, \mathcal{P}(\mathcal{E}))$, where $\mathcal{E}$ is a countable state space. If for all $0 \leq t_0 \leq t_1 \leq ... \leq t_n \leq t_{n+1}$ with $n \in \mathbb{N}_0$ and for all $i_0, i_1, ..., i_{n-1}, i, j \in \mathcal{E}$*

$$\mathbb{P}(X_{t_{n+1}} = j | X_{t_n} = i, X_{t_{n-1}} = i_{n-1}, ..., X_{t_0} = i_0) = \mathbb{P}(X_{t_{n+1}} = j | X_{t_n} = i),$$

whenever both sides are well-defined and the right hand side of the formula above is independent of the difference $t_{n+1} - t_n$, this stochastic process is called a continuous time Markov chain.

Definition A.20 (Q-matrix) [22]. *Let $\mathcal{E}$ be a countable set. A Q-matrix on $\mathcal{E}$ is a matrix $Q = (q_{ij}) \in \mathbb{R}^{|\mathcal{E}|\times|\mathcal{E}|}$ with the following properties:*

$$\begin{aligned} &(i) && 0 \leq -q_{ii} < \infty && \forall i \in [|\mathcal{E}|], \\ &(ii) && q_{ij} \geq 0 && \forall i \neq j \wedge i, j \in [|\mathcal{E}|], \\ &(iii) && \sum_{j\in\mathcal{E}} q_{ij} = 0 && \forall i \in [|\mathcal{E}|], \end{aligned}$$

where $[n] \coloneqq \{1, 2, ..., n\}$. From this conditions, it follows $q_{ii} = -\sum_{j\in\mathcal{E}, j\neq i} q_{ij} < \infty$.

Theorem A.21 (Continuous time Markov chain with generator matrix Q) [22]. *Let $(X_t)_{t\geq 0} = (X_t : 0 \leq t < \infty)$ be a sequence of random variables on a probability space $(\Omega, \mathcal{A}, \mathbb{P})$ with values in $(\mathcal{E}, \mathcal{P}(\mathcal{E}))$, where $\mathcal{E}$ is a countable state space, and let Q be a Q-matrix on $\mathcal{E}$. Denote by $\hat{i} \in \mathbb{N}$ the position of the state i in $\mathcal{E}$. If for all $0 \leq t_0 \leq t_1 \leq ... \leq t_n \leq t_{n+1}$ with $n \in \mathbb{N}_0$ and for all $i_0, i_1, ..., i_{n-1}, i, j \in \mathcal{E}$*

$$\mathbb{P}(X_{t_{n+1}} = j | X_{t_n} = i, X_{t_{n-1}} = i_{n-1}, ..., X_{t_0} = i_0) = p_{\hat{i}\hat{j}}(t_{n+1} - t_n),$$

whenever both sides are well-defined and $P(t) = (p_{\hat{i}\hat{j}}(t) : i, j \in \mathcal{E}) \in [0, 1]^{|\mathcal{E}|\times|\mathcal{E}|}$ is the solution of the forward equation

$$\partial_t P(t) = P(t)Q, \quad P(0) = I_{|\mathcal{E}|},$$

with identity matrix $I_{|\mathcal{E}|} \in \mathbb{R}^{|\mathcal{E}|\times|\mathcal{E}|}$, then $(X_t)_{t\geq 0} = (X_t : 0 \leq t < \infty)$ is a continuous time Markov chain (A.19)*. It is explicitly determined, if besides the matrix Q, a start configuration is given. The solution $P(t)$ of the forward equation is a stochastic matrix, that means that*

$$0 \leq p_{\hat{i}\hat{j}}(t) < \infty \quad \forall i, j \in \mathcal{E}, t \in \mathbb{R}_{\geq 0} \quad \wedge \quad \sum_{j\in\mathcal{E}} p_{\hat{i}\hat{j}}(t) = 1 \quad \forall i \in \mathcal{E}, t \in \mathbb{R}_{\geq 0}.$$

Furthermore, it follows from ODE theory that $P(t) = e^{tQ}$ is the unique solution of the ordinary differential equation given above. Additionally, it holds

$$P(s + t) = P(s)P(t) \text{ for all } s, t \in \mathbb{R}_{\geq 0},$$

which is called the semigroup property. The entries $q_{\hat{i}\hat{j}} \geq 0, i \neq j$ of the matrix Q describe the rates of the Markov Chain to get from state i to state j.

Definition A.22 (Invariant probability measure of a Markov Chain) [9]. *Given a continuous time Markov Chain with probability matrix $P(t)$, a probability measure μ is called invariant for the Markov chain, if*

$$\mu P(t) = \mu \qquad \forall t \in \mathbb{R}_{\geq 0}.$$

B. Basics Analysis and Algebra

Lemma B.1 (Geometric Series) [6]. *For the partial sums and the limiting value of the geometric series we have*

$$\sum_{i=0}^{n} x^i = \frac{1-x^{n+1}}{1-x} \quad \forall x \in \mathbb{R}, \qquad \sum_{i=0}^{\infty} x^i = \frac{1}{1-x} \quad \forall x \in \mathbb{R} : \ |x| < 1.$$

Proof. Multiplying the formula for the partial sums by $1-x$ leads to

$$\left(\sum_{i=0}^{n} x^i\right) \cdot (1-x) = \left(\sum_{i=0}^{n} x^i\right) - \left(\sum_{i=0}^{n} x^{i+1}\right) = \left(\sum_{i=0}^{n} x^i\right) - \left(\sum_{i=1}^{n+1} x^i\right) = 1 - x^{n+1}$$

and the results follows. Furthermore

$$\sum_{i=0}^{\infty} x^i = \lim_{n\to\infty} \sum_{i=0}^{n} x^i = \lim_{n\to\infty} \frac{1-x^{n+1}}{1-x} = \frac{1}{1-x} \quad \text{for } |x| < 1,$$

since $\lim_{n\to\infty} x^n = 0$ for $|x| < 1$. □

Corollary B.2 (Derivative of the Geometric Series). *It holds*

$$\sum_{i=1}^{n} i x^{i-1} = \frac{nx^{n+1} - (n+1)x^n + 1}{(1-x)^2} \quad \forall x \in \mathbb{R}, \qquad \sum_{i=1}^{\infty} i x^{i-1} = \frac{1}{(1-x)^2} \quad \forall x \in \mathbb{R} : \ |x| < 1.$$

Additionally, for the sequence $(ix^i)_{i\in\mathbb{N}}$ we have $\lim_{i\to\infty} ix^i = 0$ $\forall x \in \mathbb{R} : \ |x| < 1$.

Proof. Derivation of the formulas in lemma (B.1) leads to

$$\begin{aligned}
\sum_{i=1}^{n} i x^{i-1} &= \frac{\partial}{\partial x}\left(\sum_{i=0}^{n} x^i\right) = \frac{\partial}{\partial x}\left(\frac{1-x^{n+1}}{1-x}\right) \\
&= \frac{-(n+1)x^n(1-x) - (1-x^{n+1})(-1)}{(1-x)^2} = \frac{nx^{n+1} - (n+1)x^n + 1}{(1-x)^2}, \\
\sum_{i=1}^{\infty} i x^{i-1} &= \frac{\partial}{\partial x}\left(\sum_{i=0}^{\infty} x^i\right) = \frac{\partial}{\partial x}\left(\frac{1}{1-x}\right) = \frac{1}{(1-x)^2} \quad \text{for } |x| < 1.
\end{aligned}$$

The second statement follows since the sum $\sum_{i=1}^{\infty} ix^{i-1}$ converges for $|x| < 1$, the sequence $(ix^{i-1})_{i\in\mathbb{N}}$ has to tend to zero for $i \to \infty$. So also $\lim_{i\to\infty} ix^i = x \cdot \lim_{i\to\infty} ix^{i-1} = 0$ for $|x| < 1$. □

Lemma B.3 (Further converging series). *It holds*

$$\lim_{m\to\infty} \sum_{i=m}^{\infty} i x^i = 0 \quad \forall x \in \mathbb{R} : \ |x| < 1.$$

Proof. With corollary (B.2) it follows

$$\begin{aligned}
\sum_{i=m}^{\infty} i x^i &= x \sum_{i=m}^{\infty} i x^{i-1} = x\left(\sum_{i=1}^{\infty} i x^{i-1} - \sum_{i=1}^{m-1} i x^{i-1}\right) \\
&= x\left(\frac{1}{(1-x)^2} - \frac{(m-1)x^m - mx^{m-1} + 1}{(1-x)^2}\right) = \frac{(1-m)x^{m+1} + mx^m}{(1-x)^2}.
\end{aligned}$$

The limit value of the term above follows with the second statement of corollary (B.2):

$$\lim_{m\to\infty}\sum_{i=m}^{\infty} ix^i = \lim_{m\to\infty}\frac{(1-m)x^{m+1}+mx^m}{(1-x)^2}$$
$$= \frac{x^2\cdot\lim_{m\to\infty}(m-1)x^{m-1}+\lim_{m\to\infty}mx^m}{(1-x)^2} = 0 \quad \text{for } |x|<1. \qquad \square$$

Definition B.4 (Modular arithmetic). *Let $n\in\mathbb{N}$ be a positive integer and $a,b\in\mathbb{Z}$. We say a is congruent b modulo n and write*

$$a \equiv b \mod n,$$

if there exists an integer $k\in\mathbb{Z}$, such that $a-b=k\cdot n$. Furthermore, with $m\in\mathbb{Z}$, we denote by

$$c = \mathrm{mod}_{[m,m+n-1]_\mathbb{Z}}(a,n),$$

the unique integer $c\in\{m,m+1,...,m+n-1\}$ with $c\equiv a \mod n$. For $m=0$ we define

$$\mathrm{mod}\ (a,n) \coloneqq \mathrm{mod}_{[0,n-1]_\mathbb{Z}}(a,n).$$

For a vector $x\in\mathbb{Z}^d$ with $d\in\mathbb{N}$ and $m\in\mathbb{Z}$ we write abbreviating

$$\mathrm{mod}_{[m,m+n-1]_\mathbb{Z}}(x,n) = (\mathrm{mod}_{[m,m+n-1]_\mathbb{Z}}(x_1,n),...,\mathrm{mod}_{[m,m+n-1]_\mathbb{Z}}(x_d,n))\in\mathbb{Z}^d.$$

Definition B.5 (Kronecker Product) [14]. *The Kronecker product is the tensor product of two matrices $A=(a_{ij})\in\mathbb{R}^{k\times l}$ and $B=(b_{ij})\in\mathbb{R}^{m\times n}$ with $k,l,m,n\in\mathbb{N}$ and defined as*

$$A\otimes B \coloneqq \begin{pmatrix} a_{11}B & a_{12}B & \cdots & a_{1l}B \\ a_{21}B & a_{22}B & \cdots & a_{2l}B \\ \vdots & \vdots & \ddots & \vdots \\ a_{k1}B & a_{k2}B & \cdots & a_{kl}B \end{pmatrix} = \begin{pmatrix} a_{11}b_{11} & \cdots & a_{11}b_{1n} & a_{12}b_{11} & \cdots & a_{1l}b_{1n} \\ \vdots & \ddots & \vdots & \vdots & \ddots & \vdots \\ a_{11}b_{m1} & \cdots & a_{11}b_{mn} & a_{12}b_{m1} & \cdots & a_{1l}b_{mn} \\ a_{21}b_{11} & \cdots & a_{21}b_{1n} & a_{22}b_{11} & \cdots & a_{2l}b_{1n} \\ \vdots & \ddots & \vdots & \vdots & \ddots & \vdots \\ a_{k1}b_{m1} & \cdots & a_{k1}b_{mn} & a_{k2}b_{m1} & \cdots & a_{kl}b_{mn} \end{pmatrix},$$

which is a matrix in $\mathbb{R}^{km\times ln}$. Especially, the Kronecker product of two vectors $a\in\mathbb{R}^{m\times 1}$, $b\in\mathbb{R}^{n\times 1}$ with $m,n\in\mathbb{N}$ is given by

$$\begin{pmatrix} a_1 \\ a_2 \\ ... \\ a_m \end{pmatrix} \otimes \begin{pmatrix} b_1 \\ b_2 \\ ... \\ b_n \end{pmatrix} \coloneqq \begin{pmatrix} a_1b_1 \\ a_1b_2 \\ ... \\ a_1b_n \\ a_2b_1 \\ ... \\ a_mb_n \end{pmatrix} \in \mathbb{R}^{mn\times 1}.$$

Since the matrix multiplication is associative, also the Kronecker product is.

Lemma B.6 (Vector notation for one-dimensional lattice models). *Each configuration of a one-dimensional lattice model with sites $i\in[1,N]_\mathbb{Z}\subset\mathbb{Z}$, $N\in\mathbb{N}$, which can be active (then we write $s_i=1$) or inactive ($s_i=0$), is given by a vector $S\coloneqq(s_1,...,s_N)$. Since for every site i, there is the possibility to be active or not, there exist 2^N possible different configurations S. To encode each S as a unit vector $u_n=(0,...,0,1,0...,0)^T\in\mathbb{R}^{2^N}$, $n\in[2^N]\coloneqq\{1,2,...,2^N\}$, we introduce the following notation, which can also be found in [15]: Let*

$$\langle 0\rangle = \begin{pmatrix} 1 \\ 0 \end{pmatrix}, \qquad \langle 1\rangle = \begin{pmatrix} 0 \\ 1 \end{pmatrix},$$

be the encoded states $\langle s_i \rangle \in \{\langle 0 \rangle, \langle 1 \rangle\}$. *Define for a given configuration* $S = (s_1, ..., s_N)$ *the corresponding vector* $r_S \in \mathbb{R}^{2^N}$ *as the* $(N-1)$*-fold Kronecker product* (B.5) *of the encoded states* $\langle s_i \rangle$ *of each site* i*:*

$$r_S = \langle s_1 \rangle \otimes \langle s_2 \rangle \otimes ... \otimes \langle s_N \rangle.$$

These vectors r_s *are the unit vectors of* $\mathbb{R}^{2^N}$*, since the* $(N-1)$*-fold Kronecker product* c *of the vectors* $\begin{pmatrix} a_i \\ b_i \end{pmatrix} \in \left\{ \begin{pmatrix} 1 \\ 0 \end{pmatrix}, \begin{pmatrix} 0 \\ 1 \end{pmatrix} \right\}$, $i \in [N]$ *is*

$$\begin{pmatrix} a_1 \\ b_1 \end{pmatrix} \otimes \begin{pmatrix} a_2 \\ b_2 \end{pmatrix} \otimes \cdots \otimes \begin{pmatrix} a_N \\ b_N \end{pmatrix} = \begin{pmatrix} a_1 a_2 \\ a_1 b_2 \\ b_1 a_2 \\ b_1 b_2 \end{pmatrix} \otimes \cdots \otimes \begin{pmatrix} a_N \\ b_N \end{pmatrix} = \cdots = \begin{pmatrix} a_1 a_2 \cdots a_{N-1} a_N \\ a_1 a_2 \cdots a_{N-1} b_N \\ a_1 a_2 \cdots b_{N-1} a_N \\ a_1 a_2 \cdots b_{N-1} b_N \\ \vdots \\ b_1 b_2 \cdots b_{N-1} a_N \\ b_1 b_2 \cdots b_{N-1} b_N \end{pmatrix} =: c-$$

For every $i \in [N]$ *either* a_i *or* b_i *is* 1*, so there is exactly one row of* c*, in which only the digit one becomes multiplied, all other rows have at least one zero in it, such that the product is also zero, hence a unit vector of* $\mathbb{R}^{2^N}$ *is obtained. The other way round, if we have given a unit vector of* $\mathbb{R}^{2^N}$*, we take the line of the Kronecker product that corresponds to the one, and encode with the given* a_i *or* b_i *the unique configuration* $(s_1, ..., s_N)$ *of the lattice model. So there is a one-to-one correspondence between the states* $S = (s_1, ..., s_N)$ *of the lattice model and the unit vectors* $u_n = (0, ..., 0, 1, 0..., 0)^T \in \mathbb{R}^{2^N}$, $n \in [2^N]$*.*

Corollary B.7 (Vector notation for a two-site model). *From Lemma B.6 follows that for a two site process, which is an one dimensional lattice with two sites* $i \in [1, 2] \subset \mathbb{Z}$*, every configuration* (s_1, s_2) *with* $s_i = 1$ *if the site* i *is active and* $s_1 = 0$ *if the site* i *is inactive for* $i \in \{1, 2\}$*, can be encoded as a unit vector in* $\mathbb{R}^4$*:*

$$(s_1, s_2) = (0, 0) \quad \Rightarrow \quad r_{(0,0)} = \langle 0 \rangle \otimes \langle 0 \rangle = \begin{pmatrix} 1 \\ 0 \end{pmatrix} \otimes \begin{pmatrix} 1 \\ 0 \end{pmatrix} = \begin{pmatrix} 1 \\ 0 \\ 0 \\ 0 \end{pmatrix},$$

$$(s_1, s_2) = (0, 1) \quad \Rightarrow \quad r_{(0,1)} = \langle 0 \rangle \otimes \langle 1 \rangle = \begin{pmatrix} 1 \\ 0 \end{pmatrix} \otimes \begin{pmatrix} 0 \\ 1 \end{pmatrix} = \begin{pmatrix} 0 \\ 1 \\ 0 \\ 0 \end{pmatrix},$$

$$(s_1, s_2) = (1, 0) \quad \Rightarrow \quad r_{(1,0)} = \langle 1 \rangle \otimes \langle 0 \rangle = \begin{pmatrix} 0 \\ 1 \end{pmatrix} \otimes \begin{pmatrix} 1 \\ 0 \end{pmatrix} = \begin{pmatrix} 0 \\ 0 \\ 1 \\ 0 \end{pmatrix},$$

$$(s_1, s_2) = (1, 1) \quad \Rightarrow \quad r_{(1,1)} = \langle 1 \rangle \otimes \langle 1 \rangle = \begin{pmatrix} 0 \\ 1 \end{pmatrix} \otimes \begin{pmatrix} 0 \\ 1 \end{pmatrix} = \begin{pmatrix} 0 \\ 0 \\ 0 \\ 1 \end{pmatrix}.$$

Lemma B.8 (Kronecker product of Q- and identity matrices). *Let $Q = (q_{mn}) \in \mathbb{R}^{k\times k}, k \in \mathbb{N}$, $Q' = (q'_{mn}) \in \mathbb{R}^{k\times k}, k \in \mathbb{N}$ be a Q-matrix* (A.20) *and denote by $I_l, l \in \mathbb{N}$ the identity matrix in $\mathbb{R}^{l\times l}$. Then it holds*

$$\hat{Q} \coloneqq \left(\bigotimes_{i=1}^{j} I_2\right) \otimes Q \otimes \left(\bigotimes_{i=1}^{l} I_2\right) = I_{2^j} \otimes Q \otimes I_{2^l} \qquad \forall j, l \in \mathbb{N}, \tag{B.1}$$

where $\otimes$ denotes the Kronecker product (B.5)*. Furthermore, $\hat{Q} \in \mathbb{R}^{k\cdot 2^{j+l}\times k\cdot 2^{j+l}}$ and $Q + Q'$ are also Q-matrices.*

Proof. First, we notice

$$I_a \cdot I_b = \begin{pmatrix} I_b & 0 & \cdots & 0 \\ 0 & I_b & \cdots & 0 \\ \vdots & \vdots & \ddots & \vdots \\ 0 & 0 & \cdots & I_b \end{pmatrix} = I_{ab}.$$

Repeated use of this formula leads to equation (B.1). We show now that $\hat{Q} = (\hat{q}_{mn})$ is also a Q-matrix. Since

$$\hat{Q} = I_{2^j} \otimes Q \otimes I_{2^l} = \begin{pmatrix} Q & 0 & \cdots & 0 \\ 0 & Q & \cdots & 0 \\ \vdots & \vdots & \ddots & \vdots \\ 0 & 0 & \cdots & Q \end{pmatrix} \otimes I_{2^l}$$

$$= \begin{pmatrix} q_{11}I_{2^l} & \cdots & q_{1k}I_{2^l} & & & & & \\ \vdots & \ddots & \vdots & & & 0 & & \\ q_{k1}I_{2^l} & \cdots & q_{kk}I_{2^l} & & & & & \\ & & & \ddots & & & & \\ & & & & q_{11}I_{2^l} & \cdots & q_{1k}I_{2^l} \\ & 0 & & & \vdots & \ddots & \vdots \\ & & & & q_{k1}I_{2^l} & \cdots & q_{kk}I_{2^l} \end{pmatrix}, \tag{B.2}$$

it holds for each diagonal element $\hat{q}_{mm}$ of $\hat{Q}$: $\hat{q}_{mm} \in \{q_{nn} : n \in [k]\}$ and as Q is a Q-matrix, it follows also for the matrix $\hat{Q}$ that $0 \leq -\hat{q}_{mm} < \infty$ for all $m \in [k \cdot 2^{j+l}]$.

Analogously, all elements which are not located on the diagonal of $\hat{Q}$ are 0 or non-diagonal elements of Q, so they are also non-negative: $\hat{q}_{mn} \geq 0$ for all $m \neq n$ and $m, n \in [k \cdot 2^{j+l}]$.

All elements $q_{mn}, n \in [k]$ of the m-th row of Q appear exactly once in each of the rows of $\hat{Q}$ with index i, which fulfil $\mathrm{mod}_{[1,k\cdot 2^l]}(i, k \cdot 2^l) \in \{(m-1)\cdot 2^l + 1, (m-1)\cdot 2^l + 2, ..., m \cdot 2l\}$, where modular arithmetic was used (B.4). We take modulo $k \cdot 2^l$, because this is the size of every block in the matrix of equation (B.2) and select then the lines, where the elements $q_{mn}, n \in [k]$ become multiplied with I_{2^l}. It follows that the sum of elements in a row of $\hat{Q}$ is the same like in a row of Q, so it is both times zero, as Q is a Q-matrix.

In total, all three properties of a Q-matrix are fulfilled and so $\hat{Q}$ is also a Q-matrix.

The sum of two Q-matrices Q and Q' is also a Q matrix: The first two properties are obvious as sums of positive numbers, the last property follows also immediately from

$$\sum_{j\in[k]} (q_{ij} + q'_{ij}) = \sum_{j\in[k]} q_{ij} + \sum_{j\in[k]} q'_{ij} = 0. \qquad \square$$

Proposition B.9 (Q-matrix for a two-site process). *Given the local transition rate matrix $Q_{[i,i+1]} = (\tilde{q}_{mn}) \in \mathbb{R}^{4\times 4}$ for every site $i \in [1,N]_{\mathbb{Z}} \subset \mathbb{Z}$ of a two site process on a one dimensional lattice with periodic boundary conditions, the Q-matrix of this process is given by*

$$Q = \left(\sum_{i=1}^{N-1} I_{2^{i-1}} \otimes Q_{[i,i+1]} \otimes I_{2^{N-1-i}} \right) + Q^* \quad \in \mathbb{R}^{2^N \times 2^N},$$

with a matrix $Q^* \in \mathbb{R}^{2^N \times 2^N}$ defined in the proof. This formula is an adaption for the two-site process with periodic boundary conditions from the formula stated in [15].

Proof. Let $i \in [1, N-1]$. According to Lemma B.6 we can encode each configuration of the two-site process as a unit vector $u_l \in \mathbb{R}^{2^N}$, the local configurations of the sites i and $i+1$ are given by unit vectors $\tilde{u}_k \in \mathbb{R}^4$. For a given $\tilde{u}_k$ we find now the set U_k of unit vectors u_l, which are configurations with the same states of the sites i and $i+1$ like $\tilde{u}_k$. From Lemma B.6 also follows that these vectors can be calculated as

$$\begin{aligned} U_k = \big\{ &\big\langle s_1 \big\rangle \otimes ... \otimes \big\langle s_{i-1} \big\rangle \otimes \tilde{u}_k \otimes \big\langle s_{i+2} \big\rangle \otimes ... \otimes \big\langle s_N \big\rangle : \\ &\big\langle s_j \big\rangle \in \big\{ \big\langle 0 \big\rangle, \big\langle 1 \big\rangle \big\} \, \forall j \in [N] \backslash \{i, i+1\} \big\}, \end{aligned}$$

with $[N] \coloneqq \{1, ..., N\}$ because the Kronecker product is associative (B.5) and so we can multiply the states $\big\langle s_i \big\rangle$ and $\big\langle s_{i+1} \big\rangle$ first. In this Lemma we have also seen that the $(n-1)$-fold Kronecker product of n vectors of the form $\begin{pmatrix} 1 \\ 0 \end{pmatrix}$ or $\begin{pmatrix} 0 \\ 1 \end{pmatrix}$ gives a unit vector in $\mathbb{R}^{2^n}$ and all unit vectors in $\mathbb{R}^{2^n}$ can be constructed like this. Hence

$$U_k = \left\{ u_j^{(2^{i-1})} \otimes \tilde{u}_k \otimes u_m^{(2^{N-i-1})} : \forall j \in [2^{i-1}], m \in [2^{N-i-1}] \right\}.$$

Executing the second tensor product first, we see that $\tilde{u}_k \otimes u_m^{(2^{N-i-1})}$ is for arbitrary m a unit vector $u_{m'}^{(2^{N-i+1})} \in \mathbb{R}^{2^{N-i+1}}$, where the unit vectors $u^{(2^{N-i+1})}_{(k-1)\cdot 2^{N-i-1}+c}, c \in [2^{N-i-1}]$ correspond to $\tilde{u}_k$. Building now with an arbitrary unit vector $u_j^{(2^{i-1})}$ from left the Kronecker product with $u_{m'}^{(2^{N-i+1})}$ yields to a unit vector $u_l \in \mathbb{R}^{2^N}$, where the unit vectors

$$u_{(k-1)\cdot 2^{N-i-1}+c+\rho\cdot 2^{N-i+1}}, c \in [2^{N-i-1}], \rho \in [2^{i-1}-1], \tag{B.3}$$

correspond to $\tilde{u}_k$. From Lemma B.8 we know that

$$Q_i \coloneqq I_{2^{i-1}} \otimes Q_{[i,i+1]} \otimes I_{2^{N-1-i}}, \tag{B.4}$$

is for all $i \in [N-1]$ a Q-matrix. We show now that Q_i contains all transition rates between states of the sites i and $i+1$. Analogously to equation (B.2), it follows that

$$Q_i = \begin{pmatrix} \tilde{q}_{11} I_{2^{N-1-i}} & \cdots & \tilde{q}_{14} I_{2^{N-1-i}} & & & & \\ \vdots & \ddots & \vdots & & & 0 & \\ \tilde{q}_{41} I_{2^{N-1-i}} & \cdots & \tilde{q}_{44} I_{2^{N-1-i}} & & & & \\ & & & \ddots & & & \\ & & & & \tilde{q}_{11} I_{2^{N-1-i}} & \cdots & \tilde{q}_{14} I_{2^{N-1-i}} \\ & 0 & & & \vdots & \ddots & \vdots \\ & & & & \tilde{q}_{41} I_{2^{N-1-i}} & \cdots & \tilde{q}_{44} I_{2^{N-1-i}} \end{pmatrix}.$$

So the entry $\tilde{q}_{mn}$ of $Q_{[i,i+1]}$ occurs as a entry in $Q_i = (q^{(i)}_{m'n'})$ if the indices (m', n') fulfil

$$\begin{aligned} (m', n') = &((m-1)\cdot 2^{N-i-1} + \lambda + \mu \cdot 2^{N-i+1}, (n-1)\cdot 2^{N-i-1} + \lambda + \mu \cdot 2^{N-i+1}), \\ &\lambda \in [2^{N-i-1}], \mu \in [2^{i-1}-1]). \end{aligned} \tag{B.5}$$

All other entries of Q_i are zero. Comparing equations (B.3) and (B.5) leads to the result that $q^{(i)}_{m'n'}$ is the transition rate between the configurations $u_{m'}$ and $u_{n'}$ and if it holds $q^{(i)}_{m'n'} = \tilde{q}_{mn}$, the configurations $u_{m'}$ and $u_{n'}$ correspond to the local configurations $\tilde{u}_m$ and $\tilde{u}_n$. So we have constructed a matrix Q_i, which has transferred the local information of $Q_{[i,i+1]}$ to the whole system for $i \in [1, N-1]$.

For $i = N$, the site $i+1 = N+1$ is not contained in the lattice, but it has the same state like site 1 because of the periodic boundary conditions. To construct a matrix $Q^* \in \mathbb{R}^{2^N} \times \mathbb{R}^{2^N}$, which transfers the local information of $Q_{[N,N+1]}$ to the whole system, we expand our lattice and consider first a two site system with sites $i \in [1, N+1]$. Similarly to the construction of Q_i, $i \in [1, N-1]$ (see equation (B.4)), we construct

$$Q_N = I_{2^{N-1}} \otimes Q_{[N,N+1]} \in \mathbb{R}^{2^{N+1} \times 2^{N+1}}.$$

With the same argumentation like above, the entries of Q_N with value $\tilde{q}_{mn}$ are the transition rates between the configurations, which correspond to the local configuration $\tilde{u}_m$ and $\tilde{u}_n$. As we have twice as much configurations for Q_N than for the matrices Q_i, $i \in [1, N-1]$, we have to delete half of them: we only want to remain these configurations $u_l^{(2^{N+1})} \in \mathbb{R}^{2^{N+1}}$ and those entries of Q_N, which correspond to configurations, where the state of site i is the same like the state of site $i+1$. Since the unit vectors of $\mathbb{R}^{2^{N+1}}$ are calculated as

$$\langle s_1 \rangle \otimes \langle s_2 \rangle \otimes ... \otimes \langle s_N \rangle \otimes \langle s_{N+1} \rangle, \qquad \langle s_j \rangle \in \{\langle 0 \rangle, \langle 1 \rangle\} \, \forall j \in [N+1],$$

we observe the following: For $s_1 = 0$ the vectors $u_l^{(2^{N+1})}$, $l \in \{1, 2, ..., 2^N\}$ and for $s_1 = 1$ the vectors $u_l^{(2^{N+1})}$, $l \in \{2^N + 1, 2^N + 2, ..., 2^{N+1}\}$ result, because the state s_1 is the left component of the Kronecker product and it is associative, so we can multiply the most left component at last. Analogously it follows for the state s_{N+1}, which becomes multiplied from the right that for $s_{N+1} = 0$ the vectors $u_l^{(2^{N+1})}$, $l \in \{1, 3, 5, ..., 2^{N+1} - 1\}$ and for $s_{N+1} = 1$ the vectors $u_l^{(2^{N+1})}$, $l \in \{2, 4, 6..., 2^{N+1}\}$ result. It follows that the sites 1 and $N+1$ have the same state in the configurations with index

$$l^* \in \{1, 3, 5, ..., 2^N - 3, 2^N - 1, 2^N + 2, 2^N + 4, ..., 2^{N+1} - 2, 2^{N+1}\}, \qquad |l^*| = 2^N.$$

Since the $\langle s_{N+1} \rangle$ becomes multiplied to the unit vectors $u_l \in \mathbb{R}^{2^N}$ from the right, each configuration $u_m \in \mathbb{R}^{2^N}$ corresponds to the two configurations $u^{(2^{N+1})}_{2m-1}$ and $u^{(2^{N+1})}_{2m}$, where the first N elements have the same state like in u_m. When we consider only the configurations $u_l^{(2^{N+1})} \in \mathbb{R}^{2^N}$ with $l \in l^*$, we have for every $m \in [2^N]$ chosen exactly one of the two possibilities $u^{(2^{N+1})}_{2m-1}$ and $u^{(2^{N+1})}_{2m}$ and so the configurations $u_l^{(2^{N+1})}$, $l \in l^*$ and the corresponding configuration u_m, $m \in [2^N]$ appear in the same order. It follows that the matrix $Q^* \in \mathbb{R}^{2^N \times 2^N}$, which arises by deleting all rows and columns with indices, which are not contained in l^*, contains all the transition rates on the right positions for the configurations u_m, $m \in [2^N]$. We denote it by

$$Q^* = (Q_N)_{l^* l^*}.$$

Altogether, as the sum of Q-matrices is again a Q-matrix (B.8) and the matrix Q has to describe all transition rates between all possible configurations of the two-site system at once, we have to add all the matrices Q_i, $i \in [1, N]_{\mathbb{Z}}$ and the matrix Q^* to obtain the matrix Q:

$$Q = \left(\sum_{i=1}^{N-1} Q_i \right) + Q^* = \left(\sum_{i=1}^{N-1} I_{2^{i-1}} \otimes Q_{[i,i+1]} \otimes I_{2^{N-1-i}} \right) + Q^*. \qquad \square$$

C. Numerical Code and Computations

C.1. Directed Percolation in $d+1$ dimensions, $d \in \{1,2,3\}$

For the simulation of directed percolation in $1+1$ dimensions, the finite lattice $[-N, N-1]_{\mathbb{Z}}$ is represented as a vector of length $m := 2N$, whose entries become updated according to the rules of subsection 3.2.1. For the $2+1$ dimensional directed percolation process, the finite lattice $[-N, N-1]^2_{\mathbb{Z}}$ is represented as a matrix with m rows and m columns. In $3+1$ dimensions, the finite lattice $[-N, N-1]^3_{\mathbb{Z}}$ is represented as a three dimensional array. In the following, only the function DP3 used for directed percolation $3+1$ dimensions will be explained, because it includes all properties of the code of both lower dimensions. The functions DP1 and DP2 can easily obtained from this DP3 by omitting the unnecessary dimensions.

The three dimensional array has length m in each direction and is numbered as shown in Figure C.1. Additionally, each entry of the array is characterised by a triplet $(i,j,l) \in [m]^3$. From the definition in Subsection 3.2.1. it follows that at time t even, only sites with $i+j+l$ odd and at time t odd, only sites with $i+j+l$ even exist. In x-direction we talk about the left and right neighbour, in y-direction about the front and back neighbour and in z-direction about the bottom and top neighbour.

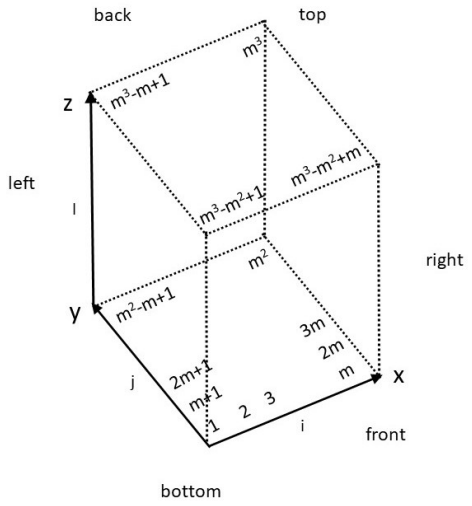


Figure C.1.: Numbering of the three dimensional array representing the finite lattice $[-N, N-1]^3_{\mathbb{Z}}$

The following function programmed in Matlab has the input parameters N for the grid size, p the probability parameter of the percolation process, T for the time until which is simulated, e for the start configuration and b for the boundary conditions. The output is the vector rho, describing the particle density from time 0 to T. The update process starts in line 65. From line 325 to line 349 the points in the interior of cube are considered, the other cases from line 73 to line 323 check the boundary points, which have dependent on the boundary condition different update rules. In lines 61 to 63 the start configuration is plotted and in lines 382 to 384 it is updated in every time step. Additionally, it is possible to visualize in $1+1$ and $2+1$ dimensions the process with a time component, see Figure 3.4 in Section 3.2. Therefore, in each time step the configuration vector of the $1+1$ dimensional process at time t is stored as the $t+1$-th row of a matrix in $\{0,1\}^{m\times(T+1)}$ or the configuration matrix of the $2+1$ dimensional process at time t is stored as the $t+1$-th level of a three dimensional array in $\{0,1\}^{m\times m\times(T+1)}$.

```
function rho = DP3(N,p,T,e,b)

%N: parameter of the finite grid [-N,N-1]^3, has to be even
%p: probability parameter of directed percolation
%T: time until we simulate
%e: start configuration, 1=fully occupied lattice, else: single active site in the middle
%b; boundary conditions, 1=periodic, otherwise free

m = 2*N; %length of the cube, only every second site can be occupied
M = 0.5*(m^3); %number of existing sites in each time step
A = zeros(m,m,m); %3D diagonal array
x = []; %storage vector for x coordinates of active sites at time t=0
y = []; %storage vector for y coordinates of active sites at time t=0
z = []; %storage vector for z coordinates of active sites at time t=0
a1 = zeros(1,M); %matrix indices with i+j+l odd for sites which can exist at time t even
a2 = zeros(1,M); %matrix indices with i+j+l even for sites which can be occupied at t odd
rho = zeros(1,T+1); %storage vector for the particle density

k1 = 1; %counter of sites existing at time t odd
k2 = 1; %counter of sites existing at time t even
k = 1; %counter of all sites

for j = 1:m
    for i = 1:m
        for l = 1:m
            if mod(i+j+l,2) == 1 %i+j+l odd
                a1(1,k1) = k;
                k = k+1;
                k1 = k1+1;
            else %i+j+l even
                a2(1,k2) = k;
                k = k+1;
                k2 = k2+1;
            end
        end
    end
end

if e == 1
    A(a1) = 1; %all sites existing at time t=0 are active
    rho(1,1) = 1; %particle density at time t=0
else
    A(N+1,N+1,N+1) = 1; %single active seed in the 'middle' of the cube at time t=0
    rho(1,1) = 1/M; %particle density at time t=0
end

k = 1;
for i = 1:m
    for j = 1:m
        for l = 1:m
            if A(i,j,l) == 1
                x(k) = i; %x coordinates of active sites to time t=0
                y(k) = j; %y coordinates of active sites to time t=0
                z(k) = l; %z coordinates of active sites to time t=0
                k = k+1;
            end
        end
    end
end

scatter3(x,y,z,'filled') %plot all active sites in a 3D coordinate system
```

```
62  axis([0 m+1 0 m+1 0 m+1])
63  pause(1) %show start configuration for one second
64
65  for t = 1:T %update the three dimensional array for every time step
66      for i = 1:M %loop over every of the M existing sites
67          if mod(t,2) == 1
68              j = a2(i); %sites existing at time t-1 odd
69          else
70              j = a1(i); %sites existing at time t-1 even
71          end
72
73          if j <= m^2 %bottom side of the cube
74              z1 = rand(1,1); %Influence of the left neighbour
75              if mod(j,m) == 1 %left side of the bottom side
76                  if b == 1 && A(j+m-1) == 1 && z1 < p %consider only for periodic
                        boundary conditions
77                      A(j) = 1;
78                  end
79              elseif A(j-1) == 1 && z1 < p
80                  A(j) = 1;
81              end
82              z2 = rand(1,1); %Influence of the right neighbour
83              if mod(j,m) == 0 %right side of the bottom side
84                  if b == 1 && A(j-m+1) == 1 && z2 < p %consider only for periodic
                        boundary conditions
85                      A(j) = 1;
86                  end
87              elseif A(j+1) == 1 && z2 < p
88                  A(j) = 1;
89              end
90              z3 = rand(1,1); %Influence of the front neighbour
91              if j <= m %front side of the bottom side
92                  if b == 1 && A(j-m+m^2) == 1 && z3 < p %consider only for periodic
                        boundary conditions
93                      A(j) = 1;
94                  end
95              elseif A(j-m) == 1 && z3 < p
96                  A(j) = 1;
97              end
98              z4 = rand(1,1); %Influence of the back neighbour
99              if j >= m^2-m+1 %back side of the bottom side
100                 if b == 1 && A(j+m-m^2) == 1 && z4 < p %consider only for periodic
                        boundary conditions
101                     A(j) = 1;
102                 end
103             elseif A(j+m) == 1 && z4 < p
104                 A(j) = 1;
105             end
106             z5 = rand(1,1); %Influence of the bottom neighbour
107             if b == 1 && A(j-m^2+m^3) == 1 && z5 < p %consider only for periodic
                    boundary conditions
108                 A(j) = 1;
109             end
110             z6 = rand(1,1); %Influence of the top neighbour
111             if A(j+m^2) == 1 && z6 < p
112                 A(j) = 1;
113             end
114
115         elseif j > m^3-m^2 %top side of the cube, because of 'elseif' edges are
                only considered once even if they occur twice in the loops
116             z1 = rand(1,1); %Influence of the left neighbour
117             if mod(j,m) == 1 %left side of the top side
118                 if b == 1 && A(j+m-1) == 1 && z1 < p %consider only for periodic
                        boundary conditions
119                     A(j) = 1;
```

```
120                 end
121             elseif A(j-1) == 1 && z1 < p
122                 A(j) = 1;
123             end
124             z2 = rand(1,1); %Influence of the right neighbour
125             if mod(j,m) == 0 %right side of the top side
126                 if b == 1 && A(j-m+1) == 1 && z2 < p %consider only for periodic
                        boundary conditions
127                     A(j) = 1;
128                 end
129             elseif A(j+1) == 1 && z2 < p
130                 A(j) = 1;
131             end
132             z3 = rand(1,1); %Influence of the front neighbour
133             if j <= m^3-m^2+m %front side of the top side, alredy j > m^3-m^2
134                 if b == 1 && A(j-m+m^2) == 1 && z3 < p %consider only for periodic
                        boundary conditions
135                     A(j) = 1;
136                 end
137             elseif A(j-m) == 1 && z3 < p
138                 A(j) = 1;
139             end
140             z4 = rand(1,1); %Influence of the back neighbour
141             if j > m^3-m %back side of the top side
142                 if b == 1 && A(j+m-m^2) == 1 && z4 < p %consider only for periodic
                        boundary conditions
143                     A(j) = 1;
144                 end
145             elseif A(j+m) == 1 && z4 < p
146                 A(j) = 1;
147             end
148             z5 = rand(1,1); %Influence of the bottom neighbour
149             if A(j-m^2) == 1 && z5 < p
150                 A(j) = 1;
151             end
152             z6 = rand(1,1); %Influence of the top neighbour
153             if b == 1 && A(mod(j+m^2,m^3)) == 1 && z6 < p %consider only for
                    periodic boundary conditions
154                 A(j) = 1;
155             end
156
157         elseif mod(j,m) == 1 %left side of the cube
158             z1 = rand(1,1); %Influence of the left neighbour
159             if b == 1 && A(j+m-1) == 1 && z1 < p %consider only for periodic
                    boundary conditions
160                 A(j) = 1;
161             end
162             z2 = rand(1,1); %Influence of the right neighbour
163             if A(j+1) == 1 && z2 < p
164                 A(j) = 1;
165             end
166             z3 = rand(1,1); %Influence of the front neighbour
167             if mod(j,m^2) == 1 %front side of the left side, alredy mod(j,m) == 1
168                 if b == 1 && A(j+m^2-m) == 1 && z3 < p %consider only for periodic
                        boundary conditions
169                     A(j) = 1;
170                 end
171             elseif A(j-m) == 1 && z3 < p
172                 A(j) = 1;
173             end
174             z4 = rand(1,1); %Influence of the back neighbour
175             if mod(j,m^2) == m^2-m+1 %back side of the left side
176                 if b == 1 && A(j+m-m^2) == 1 && z4 < p %consider only for periodic
                        boundary conditions
177                     A(j) = 1;
```

```
178                 end
179             elseif A(j+m) == 1 && z4 < p
180                 A(j) = 1;
181             end
182             z5 = rand(1,1); %Influence of the bottom neighbour
183             if j <= m^2 %bottom side of the left side
184                 if b == 1 && A(j+m^3-m^2) == 1 && z5 < p %consider only for
                        periodic boundary conditions
185                     A(j) = 1;
186                 end
187             elseif A(j-m^2) == 1 && z5 < p
188                 A(j) = 1;
189             end
190             z6 = rand(1,1); %Influence of the top neighbour
191             if j > m^3-m^2 %top side of the left side
192                 if b == 1 && A(mod(j+m^2),m^3) == 1 && z6 < p %consider only for
                        periodic boundary conditions
193                     A(j) = 1;
194                 end
195             elseif A(j+m^2) == 1 && z6 < p
196                 A(j) = 1;
197             end
198
199         elseif mod(j,m) == 0 %right side of the cube
200             z1 = rand(1,1); %Influence of the left neighbour
201             if A(j-1) == 1 && z1 < p
202                 A(j) = 1;
203             end
204             z2 = rand(1,1); %Influence of the right neighbour
205             if b == 1 && A(j-m+1) == 1 && z2 < p
206                 A(j) = 1;
207             end
208             z3 = rand(1,1); %Influence of the front neighbour
209             if mod(j,m^2) == m %front side of the right side, alredy mod(j,m) == 1
210                 if b == 1 && A(j+m^2-m) == 1 && z3 < p %consider only for periodic
                        boundary conditions
211                     A(j) = 1;
212                 end
213             elseif A(j-m) == 1 && z3 < p
214                 A(j) = 1;
215             end
216             z4 = rand(1,1); %Influence of the back neighbour
217             if mod(j,m^2) == 0 %back side of the right side
218                 if b == 1 && A(j+m-m^2) == 1 && z4 < p %consider only for periodic
                        boundary conditions
219                     A(j) = 1;
220                 end
221             elseif A(j+m) == 1 && z4 < p
222                 A(j) = 1;
223             end
224             z5 = rand(1,1); %Influence of the bottom neighbour
225             if j <= m^2 %bottom side of the right side
226                 if b == 1 && A(j+m^3-m^2) == 1 && z5 < p %consider only for
                        periodic boundary conditions
227                     A(j) = 1;
228                 end
229             elseif A(j-m^2) == 1 && z5 < p
230                 A(j) = 1;
231             end
232             z6 = rand(1,1); %Influence of the top neighbour
233             if j > m^3-m^2 %top side of the right side
234                 if b == 1 && A(mod(j+m^2),m^3) == 1 && z6 < p %consider only for
                        periodic boundary conditions
235                     A(j) = 1;
236                 end
```

```
237             elseif A(j+m^2) == 1 && z6 < p
238                 A(j) = 1;
239             end
240
241         elseif 1 <= mod(j,m^2) && mod(j,m^2) <= m %front side of the cube
242             z1 = rand(1,1); %Influence of the left neighbour
243             if mod(j,m) == 1 %left side of the front side
244                 if b == 1 && A(j+m-1) == 1 && z1 < p %consider only for periodic
                        boundary conditions
245                     A(j) = 1;
246                 end
247             elseif A(j-1) == 1 && z1 < p
248                 A(j) = 1;
249             end
250             z2 = rand(1,1); %Influence of the right neighbour
251             if mod(j,m) == 0 %right side of the front side
252                 if b == 1 && A(j-m+1) == 1 && z2 < p %consider only for periodic
                        boundary conditions
253                     A(j) = 1;
254                 end
255             elseif A(j+1) == 1 && z2 < p
256                 A(j) = 1;
257             end
258             z3 = rand(1,1); %Influence of the front neighbour
259             if b == 1 && A(j+m^2-m) == 1 && z3 < p
260                 A(j) = 1;
261             end
262             z4 = rand(1,1); %Influence of the back neighbour
263             if A(j+m) == 1 && z4 < p
264                 A(j) = 1;
265             end
266             z5 = rand(1,1); %Influence of the bottom neighbour
267             if j <= m^2 %bottom side of the front side
268                 if b == 1 && A(j+m^3-m^2) == 1 && z5 < p %consider only for
                        periodic boundary conditions
269                     A(j) = 1;
270                 end
271             elseif A(j-m^2) == 1 && z5 < p
272                 A(j) = 1;
273             end
274             z6 = rand(1,1); %Influence of the top neighbour
275             if j > m^3-m^2 %top side of the front side
276                 if b == 1 && A(mod(j+m^2),m^3) == 1 && z6 < p %consider only for
                        periodic boundary conditions
277                     A(j) = 1;
278                 end
279             elseif A(j+m^2) == 1 && z6 < p
280                 A(j) = 1;
281             end
282
283         elseif m^2-m+1 <= mod(j,m^2) && mod(j,m^2) <= m^2 %back side of the cube
284             z1 = rand(1,1); %Influence of the left neighbour
285             if mod(j,m) == 1 %left side of the back side
286                 if b == 1 && A(j+m-1) == 1 && z1 < p %consider only for periodic
                        boundary conditions
287                     A(j) = 1;
288                 end
289             elseif A(j-1) == 1 && z1 < p
290                 A(j) = 1;
291             end
292             z2 = rand(1,1); %Influence of the right neighbour
293             if mod(j,m) == 0 %right side of the back side
294                 if b == 1 && A(j-m+1) == 1 && z2 < p %consider only for periodic
                        boundary conditions
295                     A(j) = 1;
```

```
296                 end
297             elseif A(j+1) == 1 && z2 < p
298                 A(j) = 1;
299             end
300             z3 = rand(1,1); %Influence of the front neighbour
301             if A(j-m) == 1 && z3 < p
302                 A(j) = 1;
303             end
304             z4 = rand(1,1); %Influence of the back neighbour
305             if b == 1 && A(j+m-m^2) == 1 && z4 < p
306                 A(j) = 1;
307             end
308             z5 = rand(1,1); %Influence of the bottom neighbour
309             if j <= m^2 %bottom side of the back side
310                 if b == 1 && A(j+m^3-m^2) == 1 && z5 < p %consider only for
                        periodic boundary conditions
311                     A(j) = 1;
312                 end
313             elseif A(j-m^2) == 1 && z5 < p
314                 A(j) = 1;
315             end
316             z6 = rand(1,1); %Influence of the top neighbour
317             if j > m^3-m^2 %top side of the back side
318                 if b == 1 && A(mod(j+m^2),m^3) == 1 && z6 < p %consider only for
                        periodic boundary conditions
319                     A(j) = 1;
320                 end
321             elseif A(j+m^2) == 1 && z6 < p
322                 A(j) = 1;
323             end
324
325         else %no bounary point, has 6 neighbours
326             z1 = rand(1,1);
327             if A(j-1) == 1 && z1 < p %Influence of the left neighbour
328                 A(j) = 1;
329             end
330             z2 = rand(1,1);
331             if A(j+1) == 1 && z2 < p %Influence of the right neighbour
332                 A(j) = 1;
333             end
334             z3 = rand(1,1);
335             if A(j-m) == 1 && z3 < p %Influence of the front neighbour
336                 A(j) = 1;
337             end
338             z4 = rand(1,1);
339             if A(j+m) == 1 && z4 < p %Influence of the back neighbour
340                 A(j) = 1;
341             end
342             z5 = rand(1,1);
343             if A(j-m^2) == 1 && z5 < p %Influence of the bottom neighbour
344                 A(j) = 1;
345             end
346             z6 = rand(1,1);
347             if A(j+m^2) == 1 && z6 < p %Influence of the top neighbour
348                 A(j) = 1;
349             end
350         end
351     end
352
353     for i = 1 : M
354         if mod(t,2) == 1
355             j = a1(i); %sites existing at time t odd
356         else
357             j = a2(i); %sites existing at time t even
358         end
```

```
359             A(j) = 0; %sites existing at time t-1 do not exist at time t
360         end
361
362         rho(1,t+1) = sum(sum(sum(A)))/M; %particle density to time t
363
364         x = []; %storage vector for x coordinates of active sites at time t
365         y = []; %storage vector for y coordinates of active sites at time t
366         z = []; %storage vector for z coordinates of active sites at time t
367
368         k = 1;
369         for i = 1 : m
370             for j = 1:m
371                 for l = 1:m
372                     if A(i,j,l) == 1
373                         x(k) = i; %x coordinates of active sites to time t
374                         y(k) = j; %y coordinates of active sites to time t
375                         z(k) = l; %z coordinates of active sites to time t
376                         k = k+1;
377                     end
378                 end
379             end
380         end
381
382         scatter3(x,y,z,'filled') %plot all active sites in a 3D coordinate system
383         axis([0 m+1 0 m+1 0 m+1])
384         pause(0.1) %show each configuration for 0.1 seconds
385
386     end
387
388         plot(0:T,rho)
389
390     end
```

C.2. Approximation of the Critical Probabilities

A first way to approximate the critical probabilities was shown in Figures 4.4(a) to 4.4(c). They arise from the following Matlab code. Depending on the dimensions d, we have to change the estimated interval including the critical probability in lines 7 to 8 and call the function DP1, DP2 or DP3 in line 20.

```
1  function pc = findpc(N,K,T)
2
3  %N: lattice size
4  %K: Number of Simulations
5  %T: time until we simulate
6
7  pmin = 0.633; %first estimates for the interval including pc, other values for
       directed percolation in two and three dimensions
8  pmax = 0.638;
9  np = 11; %number of different values of p
10 p = linspace(pmin,pmax,np); %different values for p
11 Q = zeros(1,np); %counts for every p how many sites survive until time T on
       average
12 q = zeros(1,K); %counts for one p how many sites survive until time T in each of
       the K simulations
13
14 i = 1; %counter
15 e = 1; %fully occupied lattice
16 b = 1; %periodic boundary conditions
17
18 for l = linspace(pmin,pmax,np)
19     for k = 1:K
```

```
20          rho = DP1(N,l,T,e,b); %insert here DP2 or DP3 for directed percolation in
                two or three dimensions
21          q(1,k) = rho(1,T); %fraction of sites which exist at time T
22      end
23      Q(1,i) = sum(q)/K; %average over all simulations
24      i = i+1; %i is counter for l
25  end
26
27  pc = p(find(Q>0,1));
28  plot(p,Q)
29  xlabel('p')
30  ylabel('fraction of surviving sites')
31
32  end
```

The second way to approximate the critical probabilities was shown in Figures 4.5(a) to 4.5(f). They arise from the following Matlab code. Depending on the dimensions d, we have to change the estimated interval including the critical probability in lines 7 to 8, call the function DP1, DP2 or DP3 in line 19 and change the legend entries in line 31.

```
1   function findpcneu(N,K,T)
2
3   %N: lattice size
4   %K: Number of Simulations
5   %T: time until we simulate
6
7   pmin = 0.6437; %first estimates for the interval including pc, other values for
        directed percolation in two and three dimensions
8   pmax = 0.6457;
9   np = 3; %number of different values of p
10
11  e = 1; %fully occupied lattice
12  b = 1; %periodic boundary conditions
13  j = 1; %counter for the different values of p
14  G = zeros(np,T+1); %storage matrix for the average particle density with
        probability parameter p at time t
15
16  for p = linspace(pmin,pmax,np)
17      ges = zeros(1,T+1); %storage vector for the sum over all simulations of the
            particle density at time t
18      for i=1:K %all  simulations
19          rho = DP1(N,p,T,e,b); %insert here DP2 or DP3 for directed percolation in
                two or three dimensions
20          ges = ges + rho;
21      end
22      G(j,:) = ges./K; %average over all simulations for the probability parameter p
23      j = j+1;
24  end
25
26  for k = 1:np
27      loglog(0:T,G(k,:))
28      hold on;
29      xlabel('t')
30      ylabel('\rho(t)')
31      legend('0.6437','0.6447','0.6457') %insert other values for directed
            percolation in two and three dimensions
32  end
33
34  end
```

C.3. Approximation of the Critical Exponents

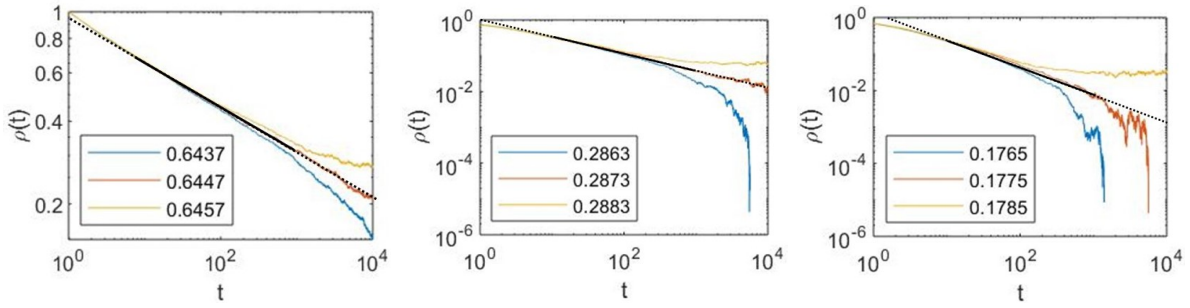
Approximation of the Critical Exponent α

According to Section 4.2., the critical exponent $\alpha(d)$ is represented as the negative slope of Figures C.2(a) to C.2(c). To avoid inaccuracies at the beginning and died-out processes in the active phase in $3+1$ dimensions (Figure C.2(c)), we measure the slope of the line from $T_1 = 10^1$ to $T_2 = 10^3$ and obtain the following values:

$$\alpha(1) = -\frac{\log(0.6547) - \log(0.3104)}{\log(10^1) - \log(10^3)} \approx 0.162, \tag{C.1}$$

$$\alpha(2) = -\frac{\log(0.3376) - \log(0.03687)}{\log(10^1) - \log(10^3)} \approx 0.481, \tag{C.2}$$

$$\alpha(3) = -\frac{\log(0.2348) - \log(0.007073)}{\log(10^1) - \log(10^3)} \approx 0.761. \tag{C.3}$$



(a) $d = 1$, $N = 2048$, $K = 100$ (b) $d = 2$, $N = 32$, $K = 100$ (c) $d = 3$, $N = 8$, $K = 100$

Figure C.2.: Fraction of surviving sites over $K = 100$ simulations of directed percolation in d dimensions with N sites until time $T = 10000$ depending on the probability parameter p with approximation line in black from time $T_1 = 10^1$ to $T_2 = 10^3$.

Approximation of the Critical Exponent β

To approximate the critical exponent β, the stationary density was plotted against the distance from criticality $\Delta = p - p_c$ in Figure 4.6 in Section 4.2. The linear plot 4.6(a) and the double-logarithmic plot 4.6(b) arise from the following Matlab code.

```
function stationary

pc1 = 0.6447; %crtitical value in one dimension
pc2 = 0.2873; %crtitical value in two dimensions
pc3 = 0.1775; %crtitical value in three dimensions

N1 = 2048; %Input N of DP1
N2 = 32; %Input N of DP2
N3 = 8; %Input N of DP3

e = 1; %fully o ccupied lattice
b = 1; %periodic boundary conditions
r = 10; %number of values of Delta
T = 10000; %time until we simulate
dT = 5000; %number of points for the calculation of the stationary solution
K = 100; %number of simulations

y1 = zeros(K,r); %storage matrix for all simulations and values Delta for DP1
y2 = zeros(K,r); %storage matrix for all simulations and values Delta for DP2
y3 = zeros(K,r); %storage matrix for all simulations and values Delta for DP3
```

```
Y1 = zeros(1,r); %storage vector for the average over all simulations for DP1
Y2 = zeros(1,r); %storage vector for the average over all simulations for DP2
Y3 = zeros(1,r); %storage vector for the average over all simulations for DP3

for k=1:K
    j = 1;
    for i = linspace(-4,-1,r) %logarithmically spaced values for Delta
        rho1 = DP1(N1,pc1+10^i,T,e,b);
        y1(k,j) = sum(rho1(1,(T-dT+1):T))/dT; %average over the last dT values of
            the particle density
        rho2 = DP2(N2,pc2+10^i,T,e,b);
        y2(k,j) = sum(rho2(1,(T-dT+1):T))/dT; %average over the last dT values of
            the particle density
        rho3 = DP3(N3,pc3+10^i,T,e,b);
        y3(k,j) = sum(rho3(1,(T-dT+1):T))/dT; %average over the last dT values of
            the particle density
        j = j+1;
    end
end

for i = 1:r
    z1 = y1(:,i);
    if sum(z1)>0
        Y1(i) = sum(z1)./(length(z1(z1>0))); %average over all non-zero entries (
            because of finite size effects there is always the probability to die
            out)
    else
        Y1(i) = 0;
    end
    z2 = y2(:,i);
    if sum(z2)>0
        Y2(i) = sum(z2)./(length(z2(z2>0))); %average over all non-zero entries (
            because of finite size effects there is always the probability to die
            out)
    else
        Y2(i) = 0;
    end
    z3 = y3(:,i);
    if sum(z3)>0
        Y3(i) = sum(z3)./(length(z3(z3>0))); %average over all non-zero entries (
            because of finite size effects there is always the probability to die
            out)
    else
        Y3(i) = 0;
    end
end

x = 10.^(linspace(-4,-1,r));
plot(x,Y1)
hold on;
plot(x,Y2)
hold on;
plot(x,Y3)
xlabel('p-p_c');
ylabel('\rho^{stat}')
legend('1D','2D','3D') %plot the three vectors Y1, Y2 and Y3 in a common linear
    plot

figure(2); %new figure
loglog(x,Y1)
hold on;
loglog(x,Y2)
hold on;
loglog(x,Y3)
xlabel('p-p_c');
```

```
ylabel('\rho^{stat}')
legend('1D','2D','3D') %plot the three vectors Y1, Y2 and Y3 in a common double-
    logarithmic plot

end
```

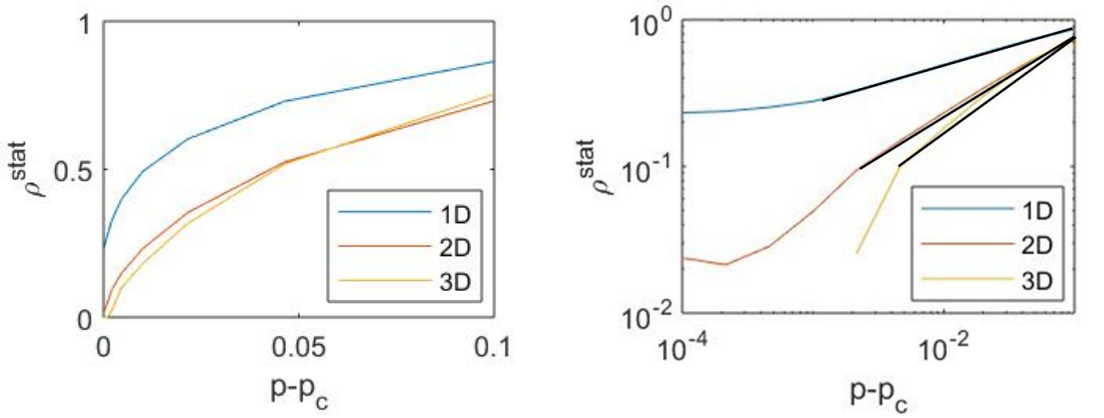
According to Section 4.2., the critical exponent $\beta(d)$ is represented as the slope of the double-logarithmic plot of the stationary density ρ^{stat}. The closer p is p_c, the longer is the time to reach the stationary density [15]. Furthermore, in $3+1$ dimensions it happens that even in the active phase, the process dies out and the absorbing state is reached, such that the logarithm of the particle density is $-\infty$ and not represented in the double-logarithmic plot. Consequently, we determine β as the slope of the parts indicated in Figure C.3. We obtain the following values:

$$\beta(1) = \frac{\log(0.2776) - \log(0.8643)}{\log(0.001) - \log(0.1)} \approx 0.247, \tag{C.4}$$

$$\beta(2) = \frac{\log(0.0941) - \log(0.7313)}{\log(0.002154) - \log(0.1)} \approx 0.534, \tag{C.5}$$

$$\beta(3) = \frac{\log(0.0999) - \log(0.7542)}{\log(0.004642) - \log(0.1)} \approx 0.658. \tag{C.6}$$

These values can be improved by larger systems, more simulations and using linear regression instead of the black parts indicated in Figure C.3.



(a) Linear plot of ρ_p^{stat} depending on $p - p_c$

(b) Double-logarithmic plot of ρ_p^{stat} depending on $p-p_c$ with approximation lines

Figure C.3.: Stationary density ρ_p^{stat} depending on the difference $p-p_c$ for directed pond percolation in $1+1$, $2+1$ and $3+1$ dimensions with 2048 particles and $K = 100$ simulations each. Because of fluctuations, the stationary density was averaged from $T_0 = 5000$ to $T = 10000$.

C.4. Eigenvalues of the Q-matrix of the Contact Process

In Figure 3.10 the eigenvalues of the Q matrices Q^{free} and Q^{periodic} are shown. The following Matlab code returns for $b = 1$ the matrix Q^{periodic} and for other values of b the matrix Q^{free}.

```
function Q = Qmatrix(lambda,N,b)

%lambda: rate parameter of the contact process
%N: lattice size
%b: boundary conditions, 1=periodic, otherwise free

```

```
K = [0, 0, 0, 0;
     0.5, -0.5*(1+lambda), 0, 0.5*lambda;
     0.5, 0, -0.5*(1+lambda), 0.5*lambda;
     0, 0.5, 0.5, -1]; %local Q-matrix Q_i
Q = zeros(2^N,2^N); %storage for the Q matrix

for i = 1:(N-1)
    L = kron(eye(2^(i-1)),K);
    M = kron(L,eye(2^(N-1-i)));
    Q = Q+M; %calculation according to equation (3.24)
end

if b == 1 %for periodic boundary conditions the matrix Q* is added, see equation
    (3.25)
    P = kron(eye(2^(N-1)),K);
    l = zeros(2^N,1);
    i = 1:(2^(N-1));
    j = (2^(N-1)+1):(2^(N));
    l(i) = 2*i-1;
    l(j) = 2*j;
    Q = Q+P(l,l); %Q*=P(l,l) choose rows and columns according to Proposition B.9.
end

end
```

Figures 3.10(a) and 3.10(b) arise from the following Matlab code, which calls the function Qmatrix from above.

```
function Eigenvalues(N)

for lambda = linspace(0,50,10)
    Q = Qmatrix(lambda,N);
    L = Q.'; %transpose as in Matlab eigenvalues are defined as the solutions of L
        *v = lambda*v (instead of pi*Q = eta*pi)
    e = real(eig(L)); %real part of the eigenvalues
    l = lambda*ones(2^(N),1);
    hold on;
    q = scatter(l(:),e(:),2,'filled'); %plot for each value of lambda all
        eigenvalues
    q.MarkerFaceColor = 'k';
end

lambdac = 3.29786;
p = plot(lambdac.*ones(100,1),linspace(-3,0,100),':'); %mark lambdac in the plot
p.Color = 'k';
p.LineWidth = 2;
axis([0 5 -3 0])
xlabel('\lambda')
ylabel('Re(\eta_{n})')

end
```

Bibliography

[1] K. Allhoff and B. Eckhardt. Directed percolation model for turbulence transition in shear flows. *IOP Publishing, Fluid Dynamics Research*, 44(031201), May 2012.

[2] C. Bezuidenhuot and G. Grimmett. The critical contact process dies out. *The Annals of Probability*, 18(4):1462–1482, 1990.

[3] P. Brémaud. *Markov Chains: Gibbs Fields, Monte Carlo Simulation, and Queues*, volume 31 of *Texts in Applied Mathematics*. Springer, 1999.

[4] S. M. Dammer and H. Hinrichsen. Spreading with immunization in high dimensions. *Journal of Statistical Mechanics: Theory and Experiment, An IOP and SISSA Journal*, July 2004.

[5] R. Durrett. *Essentials of Stochastic Processes*. Springer Texts in Statistics. Springer, second edition, 2012.

[6] O. Forster. *Analysis 1, Differential- und Integralrechnung einer Veränderlichen*, volume 12 of *Grundkurs Mathematik*. Springer Spektrum, 2016.

[7] P. Grassberger and A. de la Torre. Reggeon field theory (schlöl's first model) on a lattice: Monte carlo calculations of critical behaviour. *Annals of Physics*, 122:373–396, Nov. 1979.

[8] G. Grimmett. *Percolation*, volume 321 of *A Series of Comprehensive Studies in Mathematics*. Springer-Verlag Berlin Heidelberg GmbH, second edition, 1999.

[9] G. Grimmett. *Probability on Graphs, Random Processes on Graphs and Lattices*. Number 1 in Institute of Mathematical Statistical Textbooks. Cambridge University Press, 2010.

[10] G. Grimmett and P. Hiemer. Directed percolation and random walk. *arXiv:math/0108062v1 [math.PR]*, Aug. 2001.

[11] J. Guckenheimer and P. Holmes. *Nonlinear Oscillations, Dynamical Systems, and Bifurcations of Vector Fields*, volume 42 of *Applied Mathematical Sciences*. Springer Schience+Business Media, LLC, 2015.

[12] M. Habib, C. McDiarmid, J. Ramirez-Alfonsin, and B. Reed. *Probabilistic Methods for Algorithmic Discrete Mathematics*. Number 16 in Algorithms and Combinatorics. Springer, 1998.

[13] T. Hara and G. Slade. Mean-field critical behaviour for percolation in high dimensions. *Communications in Mathematical Physics, Springer-Verlag*, 128:333–391, 1990.

[14] F. Hiai and D. Petz. *Introduction to Matrix Analysis and Applications*. Universitext. Springer and Hindustan Book Agency, 2014.

[15] H. Hinrichsen. Non-equilibrium criticial phenomena and phase transitions into absorbing states. *Advances in Physics*, 49(7):815–958, 2000.

[16] I. Jensen. Temporally disordered bond percolation on the directed square lattice. *Physical Review Letters*, 77(25):4, Dec. 1996.

[17] W. Kinzel. Phase transitions of cellular automata. *Zeitschrift für Physik B, Condensed Matter, Springer-Verlag*, 58:229–244, Aug. 1984.

[18] A. Klenke. *Probability Theory, A Comprehensive Course.* Universitext. Springer-Verlag London, 2008.

[19] R. Livi and P. Politi. *Nonequilibrium statistical physics.* Cambridge University Press, 2017.

[20] A. Messer and H. Hirichsen. Crossover from directed percolation to mean field behaviour in the diffusive contact process. *Journal of Statistical Mechanics: Theory and Experiment - An IOP and SISSA journal*, page ArXiv ePrint: 0802.2789, 2008.

[21] T. M.Liggett. *Interacting Particle Systems.* Number 276 in Grundlehren der mathematischen WIssenschaften - A Series of Comprehensive Studies in Mathematics. Springer-Verlag New York Berlin Heidelberg Tokyo, 1985.

[22] J. R. Norris. *Markov Chains.* Cambridge Series in Statistical and Probabilistic Mathematics. Cambridge University Press, 2005.

[23] A. Sakai. Hyperscaling inqequalities for the contact process and oriented percolation. *Journal of Dtatistical Physics*, 106(1/2):201–211, Jan. 2002.

[24] M. Sipos and N. Goldenfeld. Directed percolation describes lifetime and growth of turbulent puffs and slugs. *Rapid Communications, Physical Review*, E84(035304(R)), Sept. 2011.

[25] A. Y. Tretyakov and N. Inui. Critical behaviour for mixed site-bond directed percolation. *Journal of Physics A: Mathematical and General*, 28:3985 ff, 1995.

[26] G. F. Zebende and T. J. P. Penna. The domany-kinzel cellular automaton phase diagram. *Journal of Statistical Physics*, 74(5/6):1273 ff, 1994.